CML 90-2

DISSIPATION OF MECHANICAL WORK AND TEMPERATURE RISE IN AS4/PEEK THERMOPLASTIC COMPOSITE

I. Georgiou and C. T. Sun
School of Aeronautics and Astronautics
Purdue University
West Lafayette, In 47907

October 1990

A technical report submitted to
NASA Langley Research Center
Hampton, Virginia

ABSTRACT

The dissipated mechanical work per cycle of sinusoidal stress in the thermoplastic composite material AS4/PEEK has been measured as a function of stress amplitude for fixed frequency and fiber orientation. The experimental result shows that the dissipated work per cycle is proportional to the square of the stress amplitude. Using the concept of the equivalent isotropic material, it is shown that the relaxation modulus satisfies a proportionality condition. Also, the rate of temperature rise due to sinusoidal stresses has been measured as a function of stress amplitude. The result shows that the rate of temperature rise is not proportional to the square of the stress amplitude.

1. Introduction

The result of a continuous effort to enhance both mechanical and thermal properties, AS4/PEEK is a new thermoplastic composite material. The purpose of this research is to investigate the dissipative character of this material system. Moreover, the possibility of substituting an equivalent isotopic material is examined. The results of the investigation are presented in this report.

2. Experimental Procedure

The experimental procedure used to investigate the dissipative character of the material system AS4/PEEK is described in this section. An organic composite material, AS4/PEEK consists of continuous straight AS4 graphite fibers (64 % volume content) emdodied in a thermoplastic matrix (polyether-ether-ketone). Because the fibers are arranged unidirectionally, AS4/PEEK is macroscopically an orthotropic material. Its axes of material symmetry are parallel to the fiber direction and perpendicular to it. Therefore, its mechanical and thermal properties are described by orthotopic tensors.

Uniaxial specimens 279.40 mm. long, 25.4 mm. wide and 1.27 mm. thick, were cut from a 304.8 x 304.8 mm^2 $[0]_{10}$ laminate provided by ICI Fiberite. Fiber glass tabs 38.10 mm. long, 25.40 mm. wide and 1.27 mm. thick, reinforced the specimen ends. These fiber glass tabs not only prevent the specimen ends from fracturing during cyclic loading but also do not disjoin when grip pressure is released. Unlike fiber glass tabs, metallic tabs both disjoin

when grip pressure is released and because of their rigidity often do not protect the specimen ends when grip pressure is applied.

To measure strain response caused by uniaxial cyclic stress, constantan strain gages for fatigue (EA-13-125AC-350) made by Micro-Measurements were used. Glued at the middle of the specimen (203.20mm gage length) where an approximate state of homogeneous strain prevails, these gages could measure strain caused by sinusoidal stress frequency up to 70 Hz. Figure 1 depicts the specimen geometry and the electronic instruments that were used to measure the strain response due to both monotonic and uniaxial sinusoidal tension-tension stresses.

2.1 Rate Dependence-Monotonic Stress History

The σ–ε curve (graph of $\sigma(\varepsilon)$ corresponding to a monotonic stress of constant rate) can indicate whether the strain response depends on the stress history. The strain response due to the stress history is presented in Fig. 3. The stress history consisting of six monotonic load-unload parts, is shown in Fig. 2. Figure 4 shows the stress vs. strain relation.

Figures 5 through 10 show the σ–ε curves that correspond to the six load-unload monotonic parts of the stress history shown in Fig. 2. We notice that strain is not proportional to stress, that the σ–ε curve forms a loop, and that the strain returns almost to its value just before loading. If the nonlinearity were due to plastic flow, the slope of the σ–ε curve in the neighborhood of the moment where unloading started should be less or at least equal to the slope at the moment where loading started. However, the experimental results

indicate the opposite. This means that immediately after unloading, elastic strain prevails while recovery strain eliminates part of the creep strain. As time progresses, it is seen that the slope of the unloading part of the $\sigma-\varepsilon$ curve decreases. This reveals the fact that the recovery strain is added to the instantaneous elastic strain. The permanent strain that has accumulated after the second monotonic loading is a creep strain.

The above experimental findings indicate that the material has memory; that is, if the material is a non aging linear viscoelastic, then its strain response depends on the history of stress:

$$\varepsilon(t) = \int_0^t J(t-\tau)\dot{\sigma}(\tau)d\tau \qquad (1)$$

where J is a creep compliance, t is time and τ any time before t.

Having found that the material is rate dependent, the investigation was continued to determine the linear viscoelasticity of the material.

2.2 Dissipation of Mechanical Work-Cyclic Loading

The shape of the $\sigma-\varepsilon$ curve corresponding to a specified sinusoidal stress as well as the dependence of dissipated mechanical work per cycle on the stress amplitude can indicate whether a rate sensitive material is linear viscoelastic. Therefore, for fixed frequency cyclic stress, the strain response of uniaxial off-axis specimens as a function of stress amplitude $\Delta\sigma$ was measured.

It was found that irrespective of fiber orientation, frequency (tested range: 5 to 30 Hz), and stress amplitude, the σ–ϵ curve is a smooth ellipse. Therefore, the strain response is sinusoidal but lags behind stress by a phase angle δ, the loss angle.

$$\epsilon(t) = \Delta\epsilon\sin(\omega t - \delta) \tag{2}$$

where $\Delta\epsilon$ is the amplitude of the strain response. Figures 11-24 show the σ–ϵ response when the stress is sinusoidal.

The area enclosed by the σ–ϵ curve represents the dissipated mechanical work per cycle, W_{dc}. It was found that irrespective of type of off-axis specimen and frequency, the dissipated mechanical work per cycle is proportional to the square of the stress amplitude; that is,

$$W_{dc} = A(\theta,\omega)\Delta\sigma^2 \tag{3}$$

Moreover, W_{dc} does not depend on the mean stress, σ_{mean} , Fig. 25.

Since the σ–ϵ curve is a smooth ellipse and W_{dc} is a quadratic function of $\Delta\sigma$, the material system AS4/PEEK is seen to behave like a linear viscoelastic material. This implies that the strain amplitude, $\Delta\epsilon$, is proportional to the stress amplitude, $\Delta\sigma$.

$$\Delta\epsilon = \dot{J}(\omega,\theta)\Delta\sigma \tag{4}$$

where

$$J^*(\omega,\theta) = \left\{ J_1^*(\omega,\theta)^2 + J_2^*(\omega,\theta)^2 \right\}^{\frac{1}{2}} \tag{5}$$

$$J^*(\omega,\theta) = J_1^*(\omega,\theta) + iJ_2^*(\omega,\theta) \tag{6}$$

$J^*(\omega,\theta)$ is the magnitude of the Fourrier transform to the compliance characterizing the

material system AS4/PEEK.

$$J^*(\omega,\theta) \equiv \int_0^\infty J(t)e^{-i\omega t}dt \tag{7}$$

$$\varepsilon(t) = \int_0^t J(t-\tau)\dot{\sigma}(\tau)d\tau \tag{8}$$

2.3 The Effect of Frequency on the Dynamic Modulus

In the theory of linear viscoelasticity, the dynamic modulus is defined by

$$E^* \equiv \frac{\Delta\sigma}{\Delta\varepsilon}e^{i\delta} \tag{9}$$

Therefore, its magnitude is

$$E^* \equiv \left\{E_1^2+E_2^2\right\}^{\frac{1}{2}} \tag{10}$$

Figures 34-42 are plots of $\Delta\sigma$ vs. $\Delta\varepsilon$ response. It is found that $\Delta\sigma$ is proportional to $\Delta\varepsilon$. As shown in Fig. 43, E^* increases slowly with frequency, indicating that the rubbery state of the material extends at least up to 30 Hz.

2.4 The Equivalent Isotropic Material

The possibility of substituting the given orthotropic material with an isotropic one was examined since the dissipated mechanical work per cycle does not depend on the material anisotropy, that is,

$$W_{dc} = A(\omega)\Delta\bar{\sigma}^2 \tag{11}$$

where $\Delta\bar{\sigma}$ is an effective stress that takes into account the anisotropy of the material

according to the following definition.

$$\Delta\bar{\sigma}^{2} \equiv \frac{2}{3} a_{ij}(\omega)\Delta\sigma_i \Delta\sigma_j \qquad i,j=1,2,3 \tag{12}$$

where $a_{ij}(\omega)$ is the restriction of an orthotropic fourth order tensor to a 3-D Euclidean space, and $\Delta\sigma_i$ (i=1,2,3) is a vector representing the amplitudes of the stress components of a plane state of stress:

$$(\Delta\sigma_1, \Delta\sigma_2, \Delta\sigma_3) \equiv (\Delta\sigma_{11}, \Delta\sigma_{22}, \Delta\sigma_{12}) \tag{13}$$

For a uniaxial state of cyclic stress of amplitude $\Delta\sigma$, the components of stresses refer to a coordinate system coincident with the material axes of symmetry

$$\Delta\sigma_1 = \cos^2\theta\Delta\sigma \tag{14-a}$$

$$\Delta\sigma_2 = \sin^2\theta\Delta\sigma \tag{14-b}$$

$$\Delta\sigma_3 = -\sin\theta\cos\theta\Delta\sigma \tag{14-c}$$

The amplitude of the effective stress that corresponds to a uniaxial cyclic stress making an angle θ with the fiber direction takes the form

$$\Delta\bar{\sigma} = h(a_{ij},\theta)\Delta\sigma \tag{15}$$

where

$$h(a_{ij},\theta) \equiv \frac{2}{3}\left[(a_{11}\cos^4\theta + a_{22}\sin^4\theta + 2(a_{12}+a_{66})\sin^2\theta\cos^2\theta)\right]^{1/2} \tag{15-a}$$

where a_{ij} , if it exists, is the solution to the following set of equations.

$$|W_{dc}(\theta_1,\omega) = W_{dc}(\theta_2,\omega)| \tag{16-a}$$

$$|W_{dc}(\theta_2,\omega) = W_{dc}(\theta_3,\omega)| \tag{16-b}$$

$$|W_{dc}(\theta_3,\omega) = W_{dc}(\theta_1,\omega)| \tag{16-c}$$

where

$$|W_{dc}(\theta,\omega)| \equiv \int_0^c W_{dc}(\theta,\omega)d\Delta\sigma \tag{16-d}$$

where c is a constant, and $W_{dc}(\theta,\omega)$ represents the $W_{dc}-\Delta\sigma$ graph for fixed ω and θ. It was found that W_{dc} is proportional to $\Delta\sigma$ for fixed frequency and fiber orientation. Therefore, in terms of $\Delta\sigma$, the above equations become

$$|A(\theta_1,\omega)\Delta\sigma^2| = |A(\theta_2,\omega)\Delta\sigma^2| \tag{17-a}$$

$$|A(\theta_2,\omega)\Delta\sigma^2| = |A(\theta_3,\omega)\Delta\sigma^2| \tag{17-b}$$

$$|A(\theta_3,\omega)\Delta\sigma^2| = |A(\theta_1,\omega)\Delta\sigma^2| \tag{17-c}$$

After transforming $\Delta\sigma$ into an effective stress, the above equations take the final form

$$\left|\frac{A(\theta_1,\omega)}{h^2(a_{ij},\theta_2)} = \frac{A(\theta_2,\omega)}{h^2(a_{ij},\theta_2)}\right| \tag{18-a}$$

$$\left|\frac{A(\theta_2,\omega)}{h^2(a_{ij},\theta_2)} = \frac{A(\theta_3,\omega)}{h^2(a_{ij},\theta_3)}\right| \tag{18-b}$$

$$\left|\frac{A(\theta_3,\omega)}{h^2(a_{ij},\theta_3)} = \frac{A(\theta_1,\omega)}{h^2(a_{ij},\theta_1)}\right| \tag{18-c}$$

A solution to the above equations means that for fixed ω the curves $W_{dc}(\theta_1,\omega)$, $W_{dc}(\theta_2,\omega)$, $W_{dc}(\theta_3,\omega)$ collapse into a master curve $W_{dc}(\omega)$ for some value of $a_{ij}(\omega)$, thus eliminating the θ dependence.

Indeed, for $\omega = 10\pi$, 20π, 30π values of $a_{ij}(\omega)$ (without loss of generality, $a_{22} = 1$) were found for which the experimentally obtained curves $W_{dc}(\theta_1=00^o,\omega)$, $W_{dc}(\theta_2=15^o,\omega)$ and

$W_{dc}(\theta_3=70^\circ,\omega)$ collapse into a master curve, Figs. 44.-46.

Given the fact that an orthotropic material is characterized by the following scalar relation,

$$W_{dc} = A(\omega)\Delta\bar{\sigma}^2 \tag{19}$$

the inverse transformation can be used to turn a given $\Delta\bar{\sigma}$ into a unique uniaxial state of stress $\Delta\sigma$, thus obtaining the dissipated mechanical work per cycle for a specified off-axis uniaxial specimen under a uniaxial state of stress.

$$W_{dc} = A(\omega)h(a_{ij},\theta)\Delta\sigma^2 \tag{20}$$

In Figs. 47-49, the dissipated mechanical work per cycle for the off-axis specimens $\theta = 22.5^\circ, 30^\circ, 45^\circ$ is compared to that predicted by the corresponding scalar relation (master curve). The agreement ranges from good to almost excellent. It is concluded that an equivalent isotropic relation exists.

2.5 A Generalization

It is assumed that the dissipated mechanical work per cycle in an orthotropic material under a homogeneous state of multiaxial cyclic stress is given by the following isotropic relation

$$W_{dc} \equiv A(\omega)\Delta\sigma^2 \tag{21}$$

where the amplitude of the effective stress, $\Delta\bar{\sigma}$, is given by the frequency-independent quadratic relation

$$\overline{\Delta\sigma^2} = \frac{2}{3} a_{ijmn} \Delta\sigma_{ij} \Delta\sigma_{mn} \tag{22}$$

Because of eq. (21), W_{dc} becomes

$$W_{dc} = A(\omega) a_{ijmn} \Delta\sigma_{ij} \Delta\sigma mn \tag{23}$$

From the theory of linear viscoelasticity we have the following relation

$$W_{dc} = -\frac{\omega}{2} E^{(2)}_{ijmn}(\omega) \Delta\sigma_{ij} \Delta\sigma_{mn} \tag{24}$$

where $E^{(2)}_{ijmn}(\omega)$ is the imaginary part of the Fourrier transform of the relaxation modulus, $E_{ijmn}(t)$. Comparing eq. (24) to eq. (23), we obtain the relation

$$a_{ijmn} = -\frac{2}{A(\omega)\omega} E^{(2)}_{ijmn}(\omega) \tag{25}$$

This relation implies that an orthotropic material can be substituted by an equivalent isotropic one provided that the relaxation modulus satisfies the following proportionality condition

$$E_{ijmn}(t) = \phi(t) E^{\circ}_{ijmn} \tag{26}$$

where E°_{ijmn} is a constant tensor.

We conclude that the relaxation modulus of the material system AS4/PEEK satisfies the proportionality relation (26). The viscoelasticity of the matrix PEEK is described by the function $\phi(t)$. The anisotropy caused by the embodied unidirectional graphite fibers AS4 is described by the orthotropic tensor E°_{ijmn}.

3. Temperature Rise in Cyclic Loading

In this section the experimental procure used to measure the temperature rise during sinusoidal loading is described. Covering the specimen with insulating tiles and wrapping them with insulating fiber glass insulated the specimen so effectively that a 3°C temperature difference could be constantly maintained between the specimen and the environment. Figure 50 shows the schematic of the insulation.

To measure the temperature rise during cyclic loading, we used two devices: a thermocouple and a strain gage-like thermosensor. The thermocouple consists of copper and constantan wires, giving .0405 Millivolts/ °C. The thermogage is a sensing grid of ultra-pure nickel (50Ω resistance) and can sense temperature changes as low as .018°C.

After the temperature of the insulated specimen had reached a constant value for about 30 minutes, the specimen was subjected to a sinusoidal stress for about 20 seconds, and the temperature rise was recorded. Figures 51-57 show the temperature rise in a 45° specimen loaded at 15 Hz. Notice that the temperature varies linearly during the 20 second duration of the cyclic load. Because the heat loss due to conduction is much smaller than the heat production due to mechanical power dissipation, the slope of this straight line is considered to be the rate of temperature rise.

Figures 58 and 59 indicate that the rate of temperature rise measured by a thermogage is approximately equal to that measured by a thermocouple. Therefore, the thermogage was used to measure temperature changes because it is simple to attach to the specimen.

It is found that, irrespective of frequency and fiber orientation, the rate of temperature rise, $\Delta\dot{T}$, has the following form as a function of stress amplitude, $\Delta\sigma$.

$$\Delta\dot{\sigma} = A\Delta\sigma^2 + B\Delta\sigma^6 \tag{27}$$

where A, B are constants obtained by best curve fitting the experimental data.

Let Q be the heating due to mechanical power dissipation. If we assume that

$$Q = C_v\Delta\dot{T} \tag{28}$$

where C_v is the coefficient of thermal capacity, then $\Delta\dot{T}$ should b proportional to $\Delta\sigma^2$ because W_{dc} is proportional to Q and $\Delta\sigma^2$. However, as the present experiment has revealed (eq. 27), this is not the case with the material system AS4/PEEK.

We propose tentatively that the coefficient of thermal capacity is not constant but a function of stress amplitude, $\Delta\sigma$.

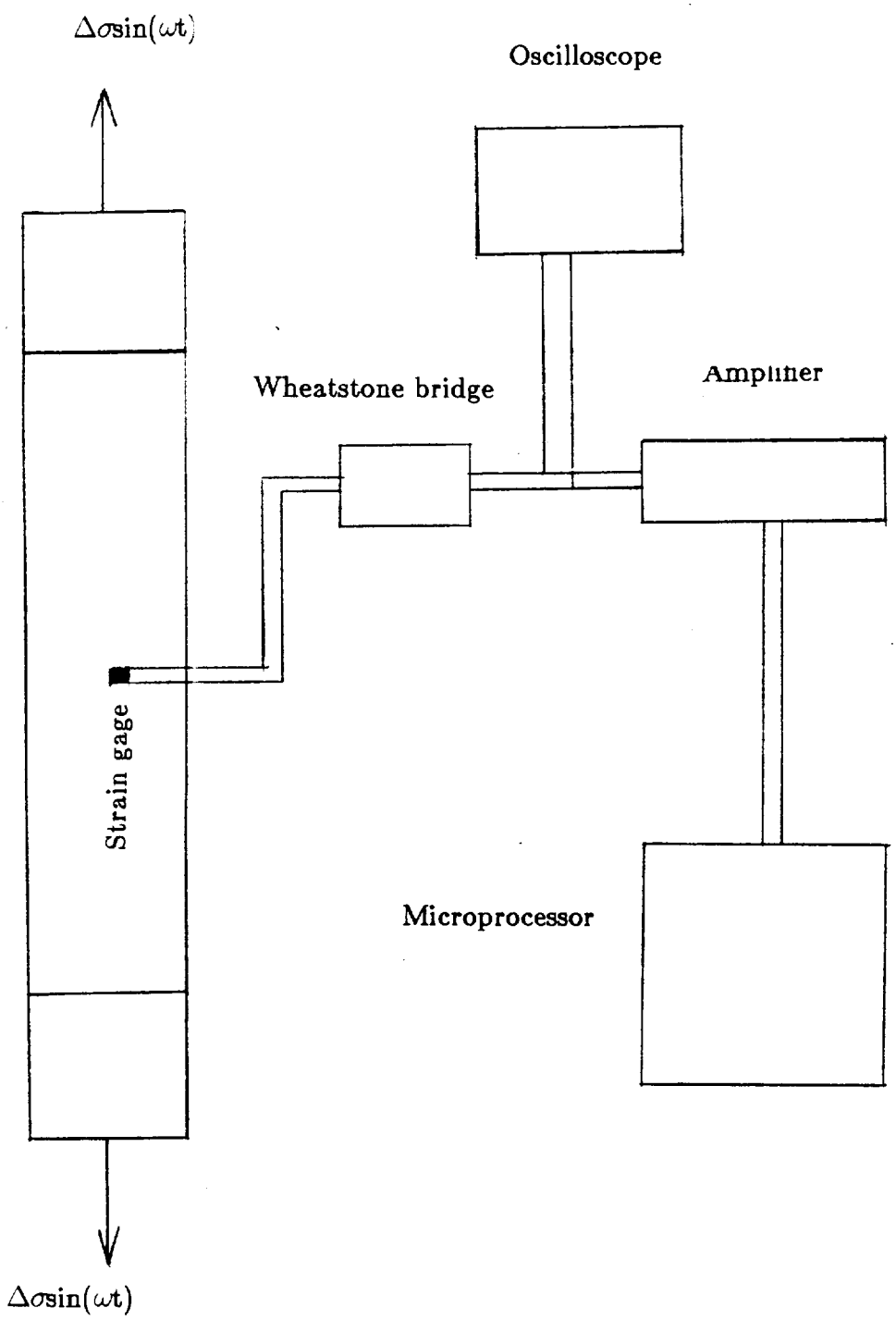

Fig. 1 Specimen geometry and experimental configuration

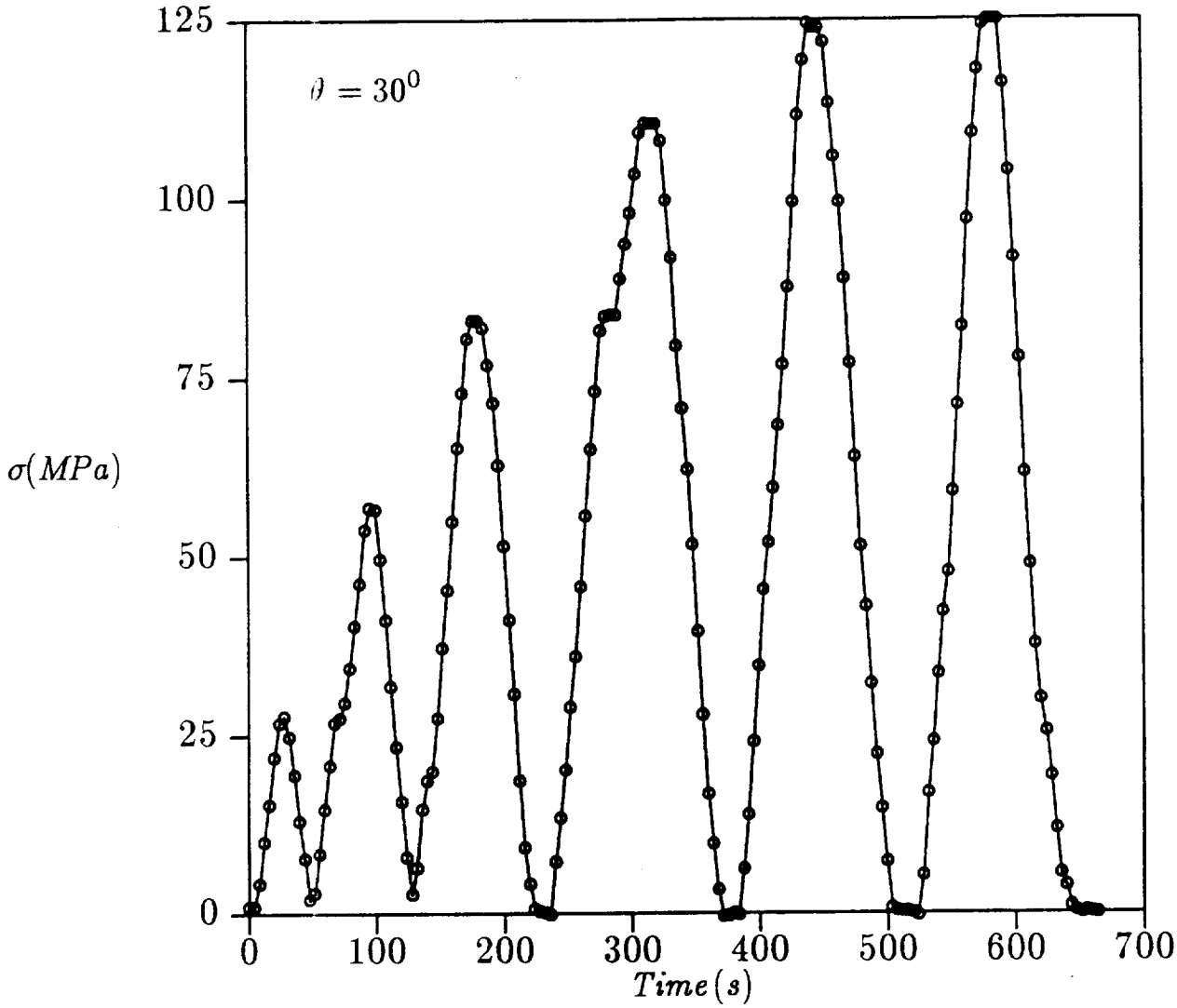

Fig. 2 Prescribed stress history(slope: 0.145 ($\frac{\text{MPa}}{\text{s}}$)).

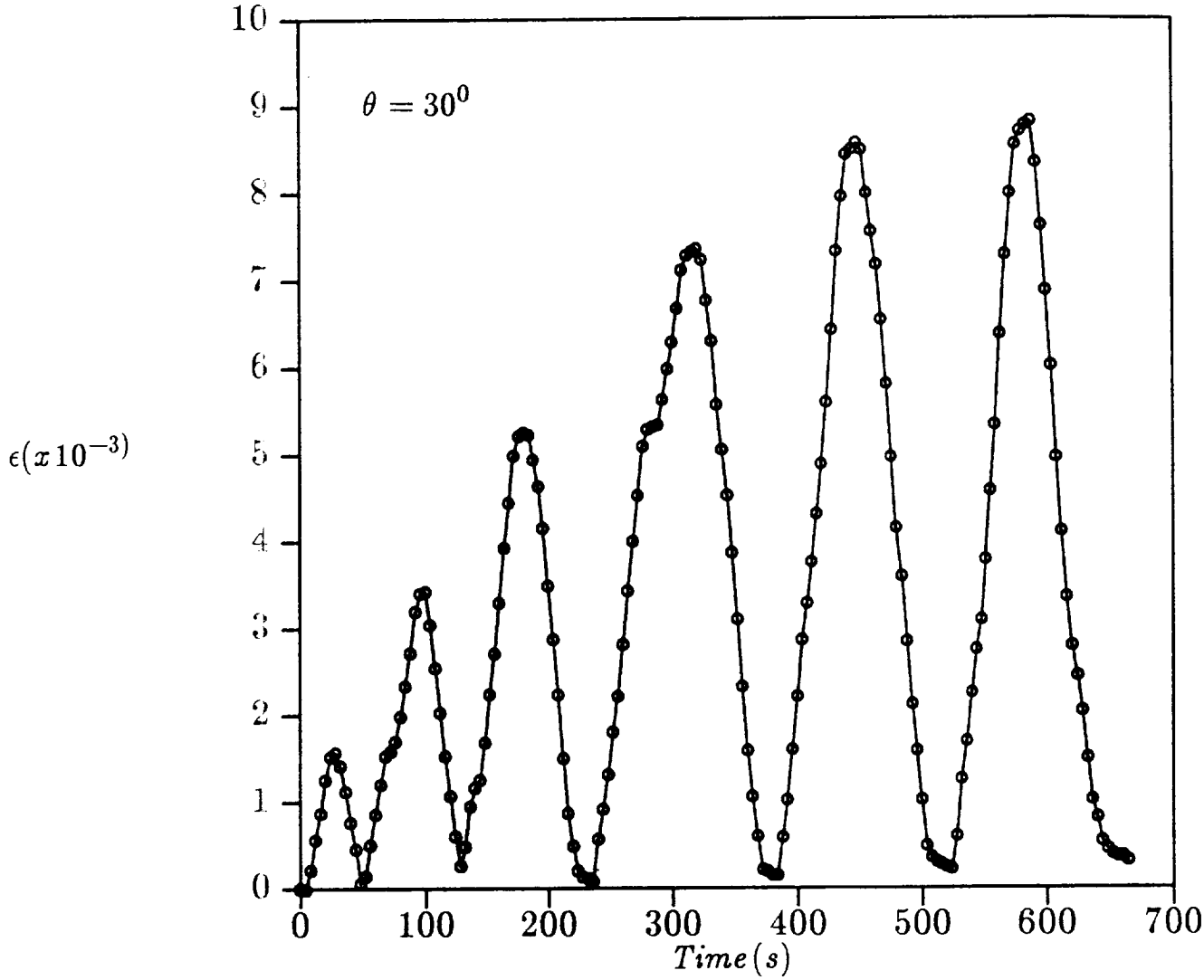

Fig. 3 Strain response history(slope: .0095 ($\frac{1}{s}$).

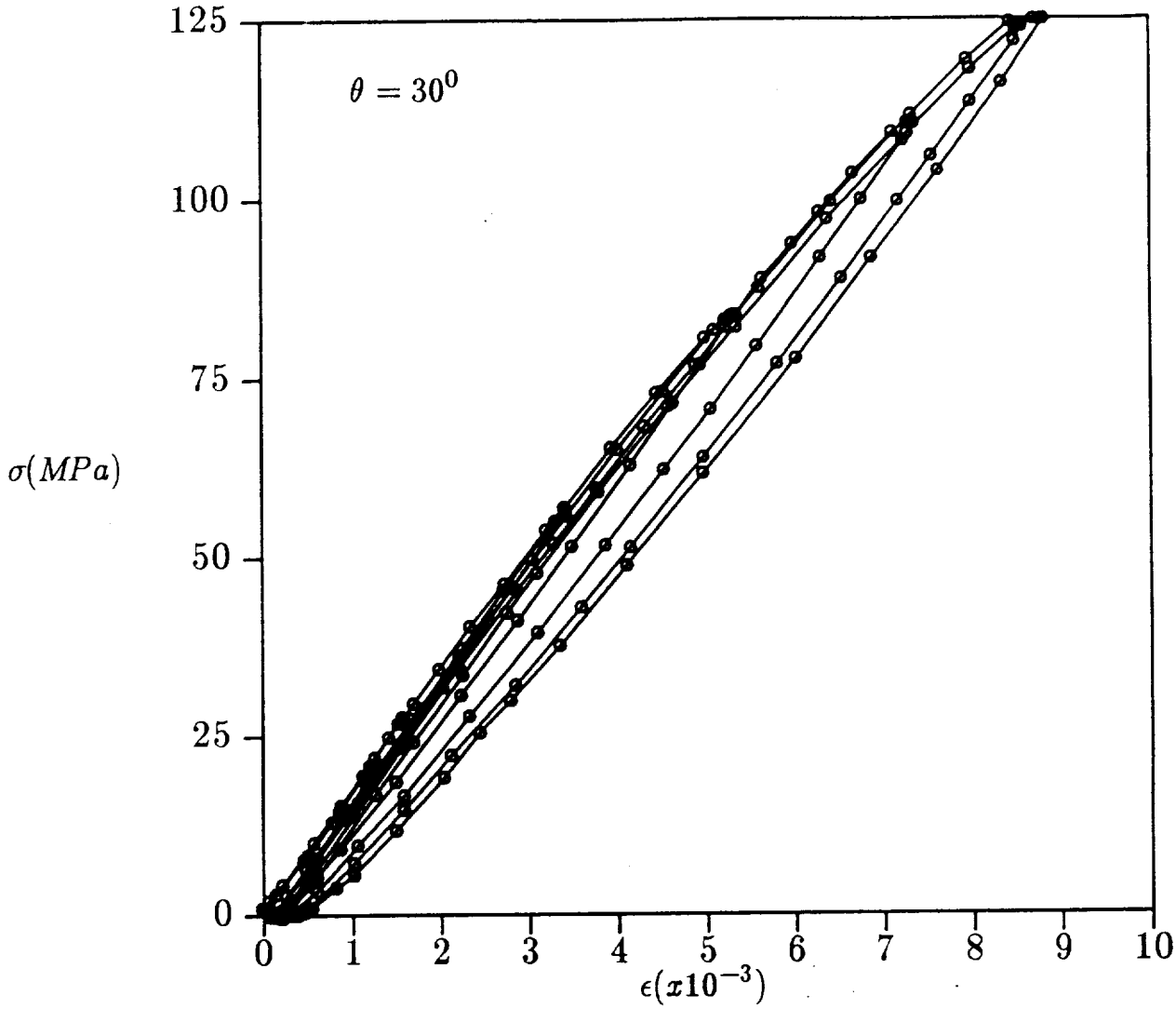

Fig. 4 Stress vs. strain(stress history shown in Fig. 2).

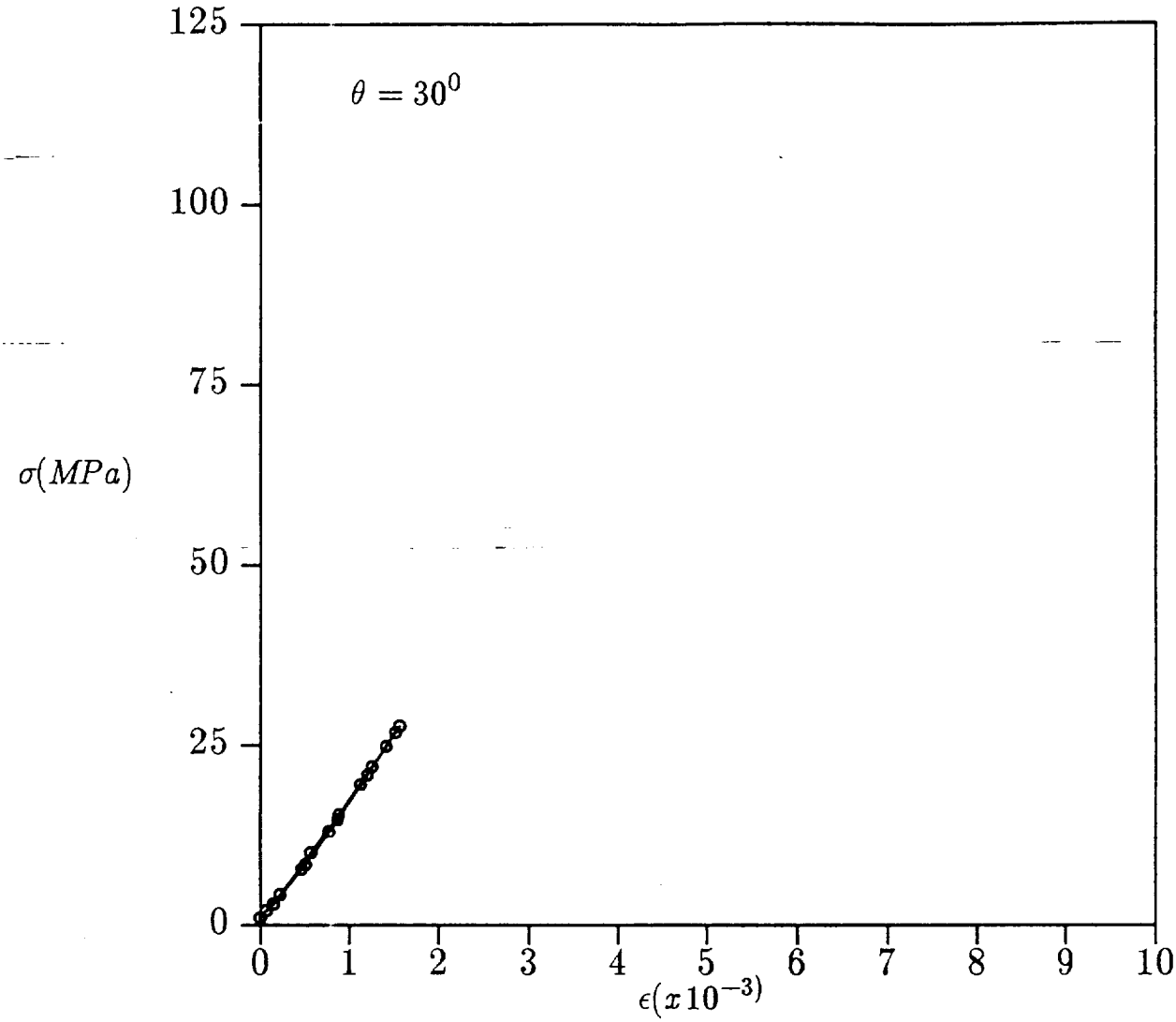

Fig. 5 Stress vs. strain response(part A of stress history shown in Fig. 2).

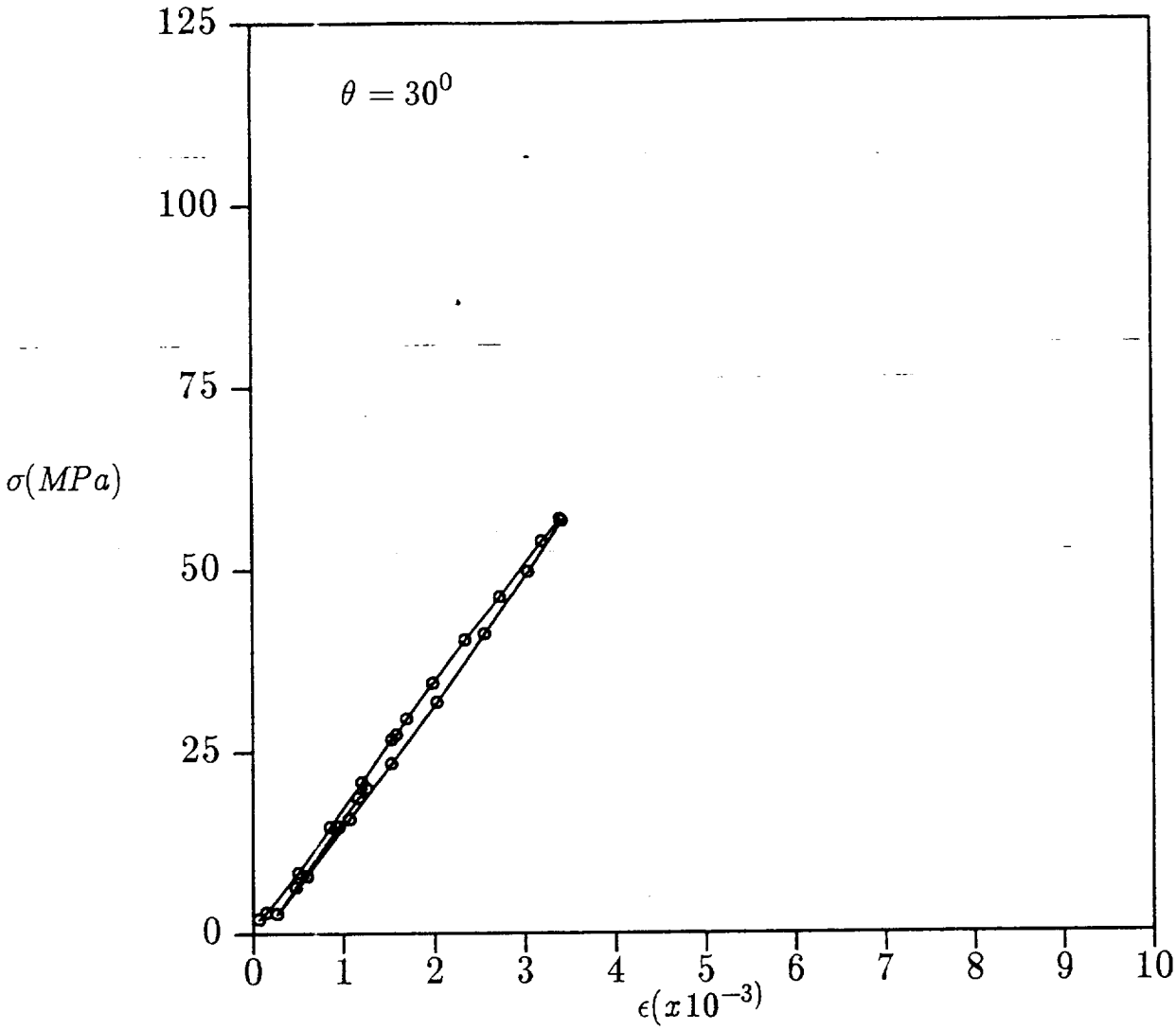

Fig. 6 Stress vs. strain response(part B of stress history shown in Fig. 2).

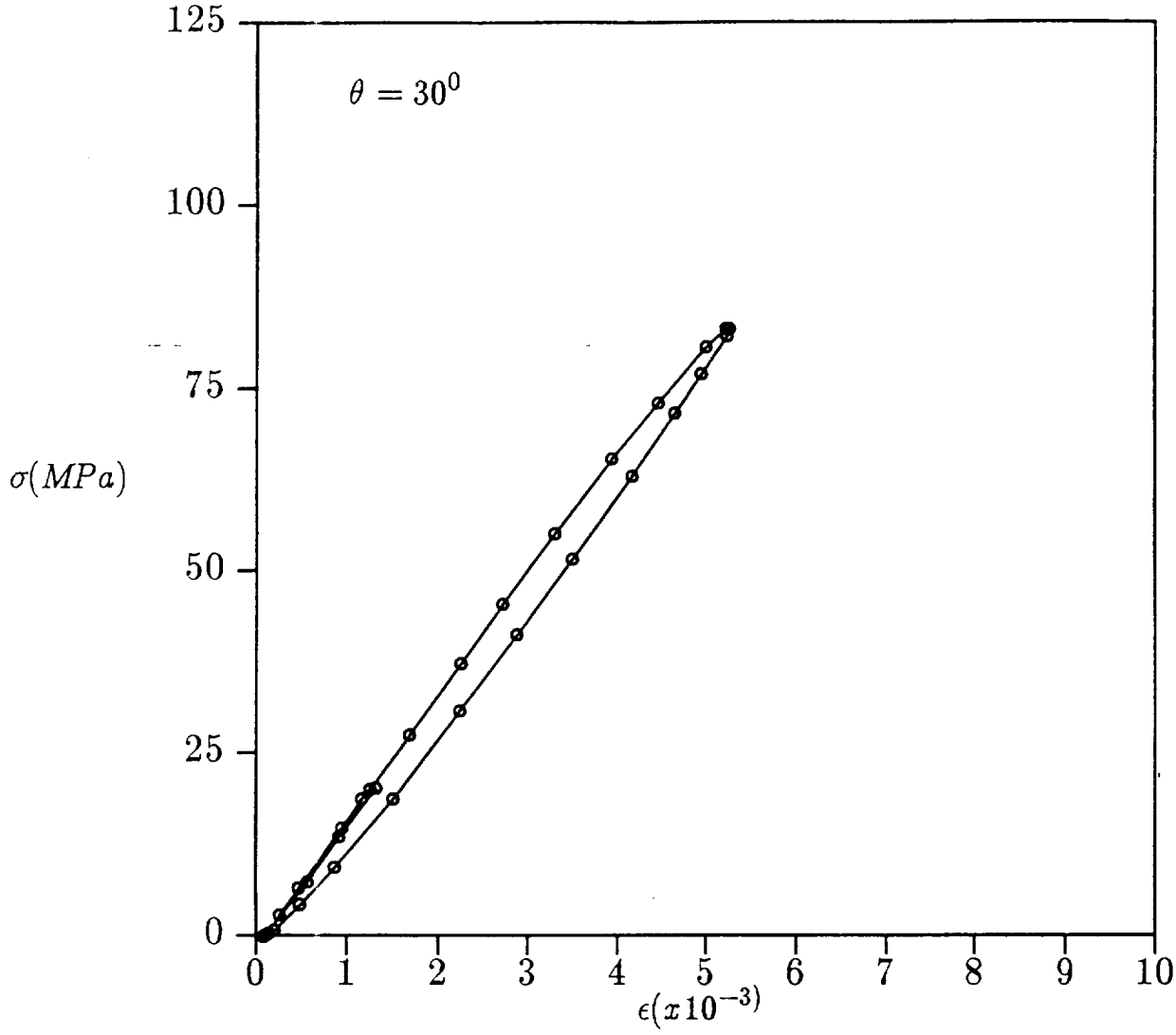

Fig. 7 Stress vs. strain response(part C of stress history shown in Fig. 2).

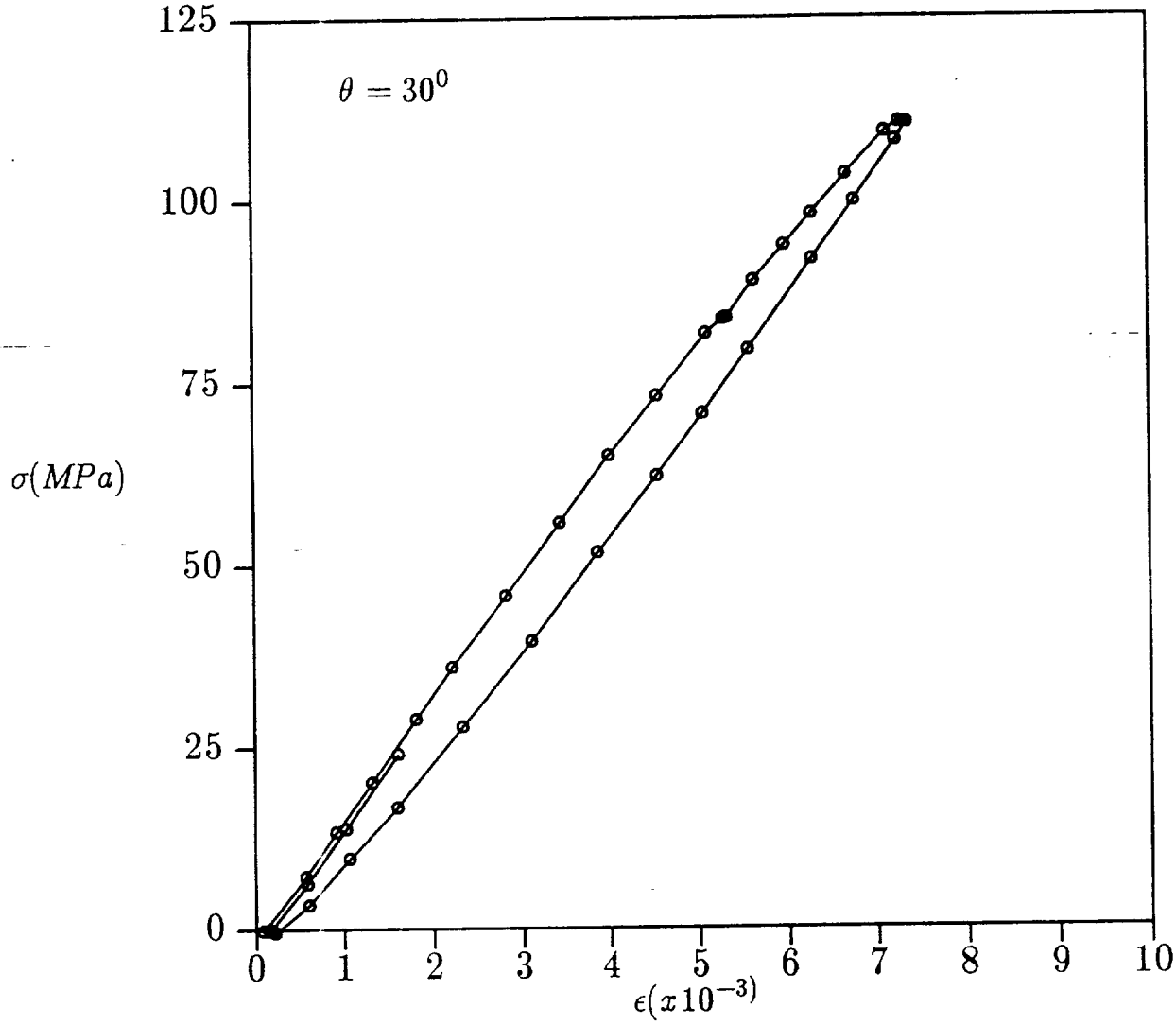

Fig. 8 Stress vs. strain response(part D of stress history shown in Fig. 2).

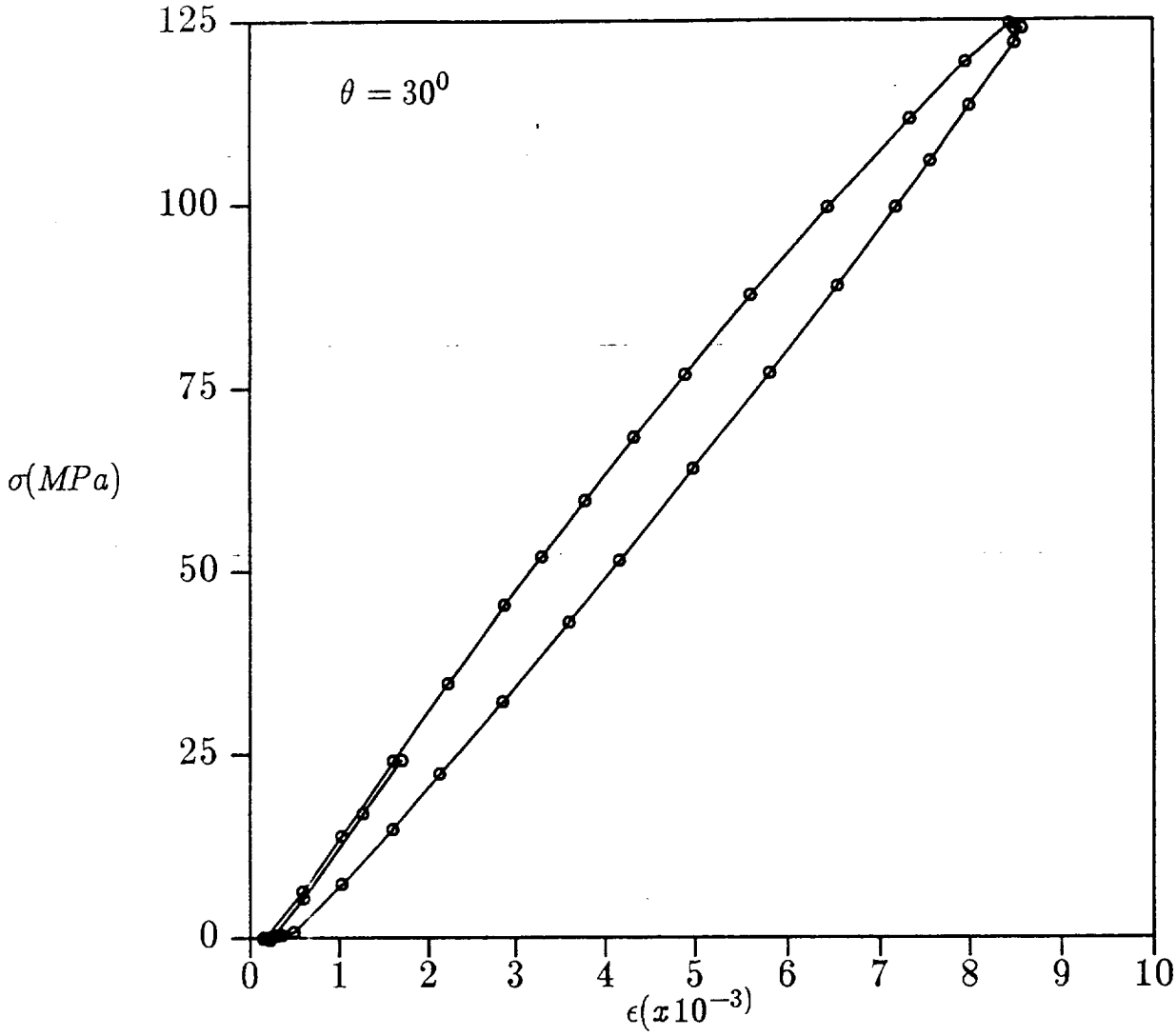

Fig. 9 Stress vs. strain response(part E of stress history shown in Fig. 2).

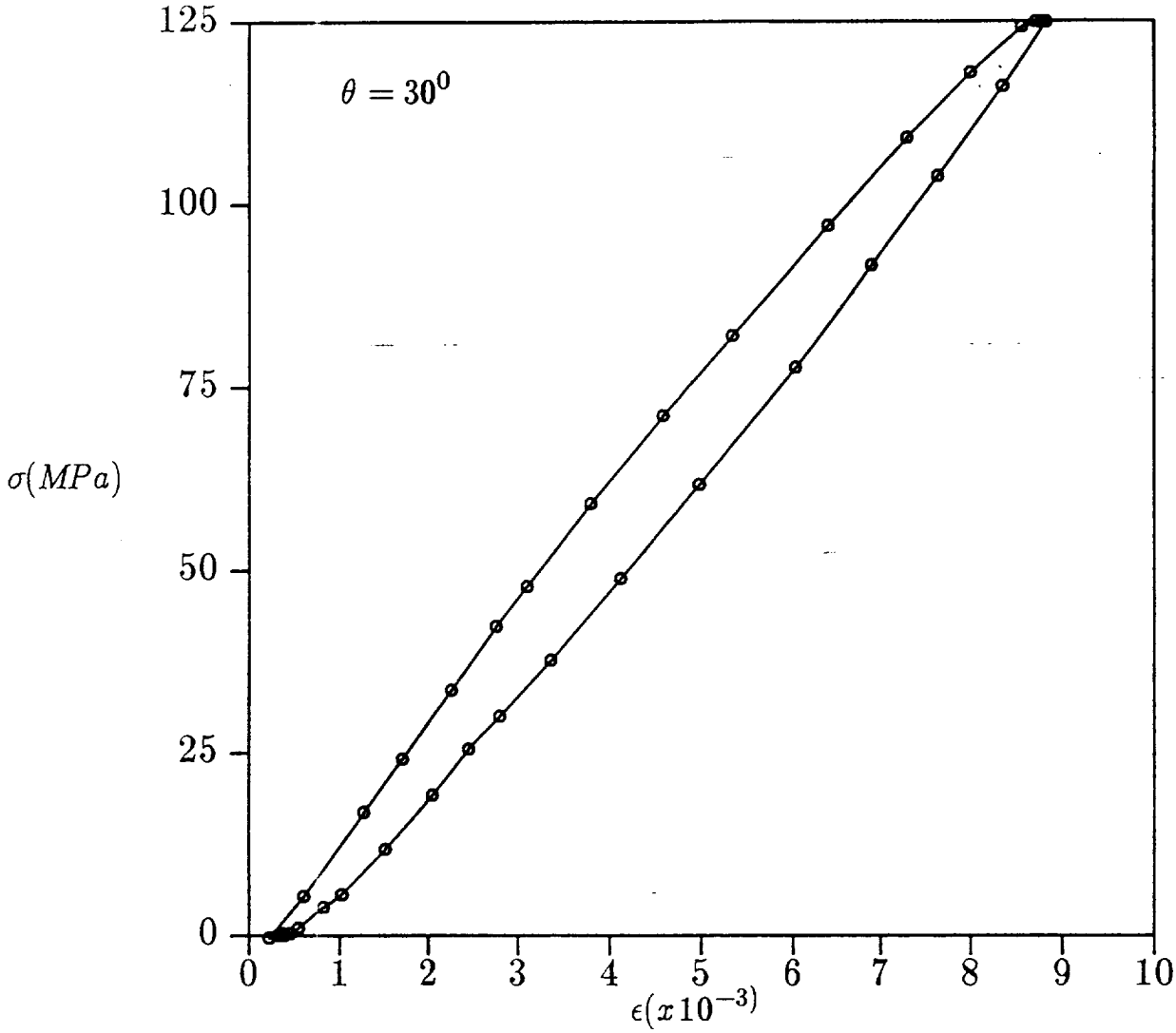

Fig. 10 Stress vs. strain response(part F of stress history shown in Fig. 2).

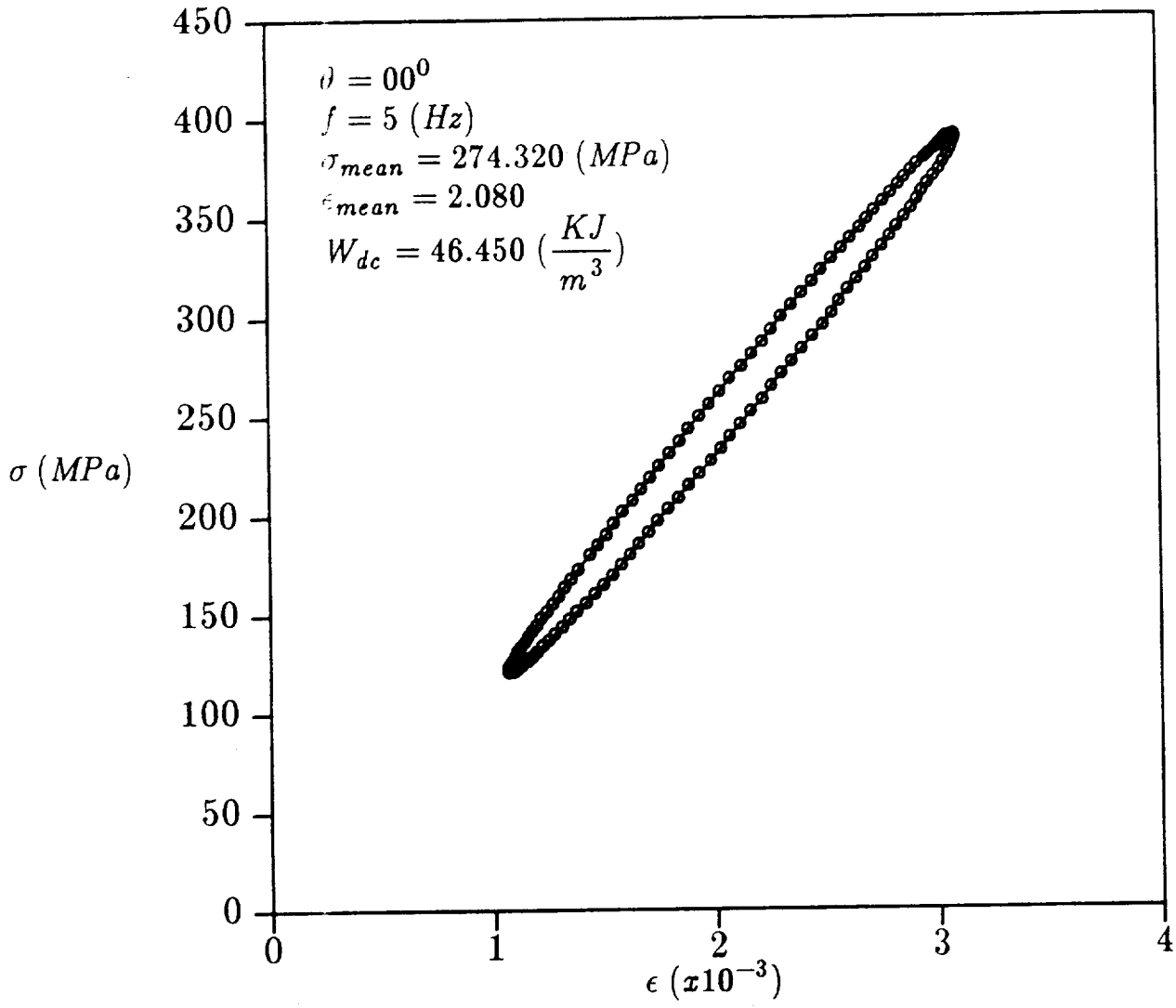

Fig. 11 Stress vs. strain response(one cycle of sinusoidal stress).

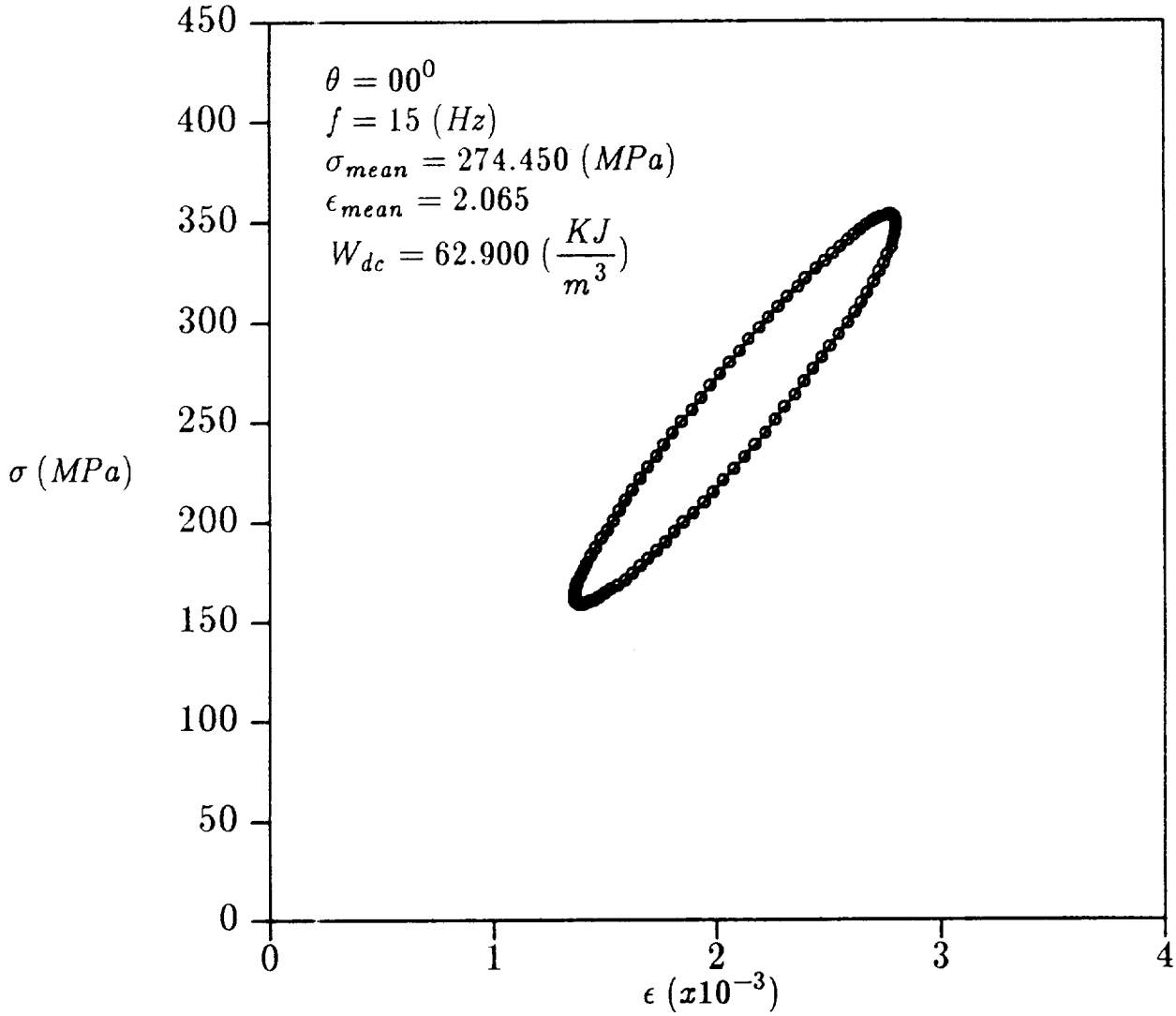

Fig. 12 Stress vs. strain response(one cycle of sinusoidal stress).

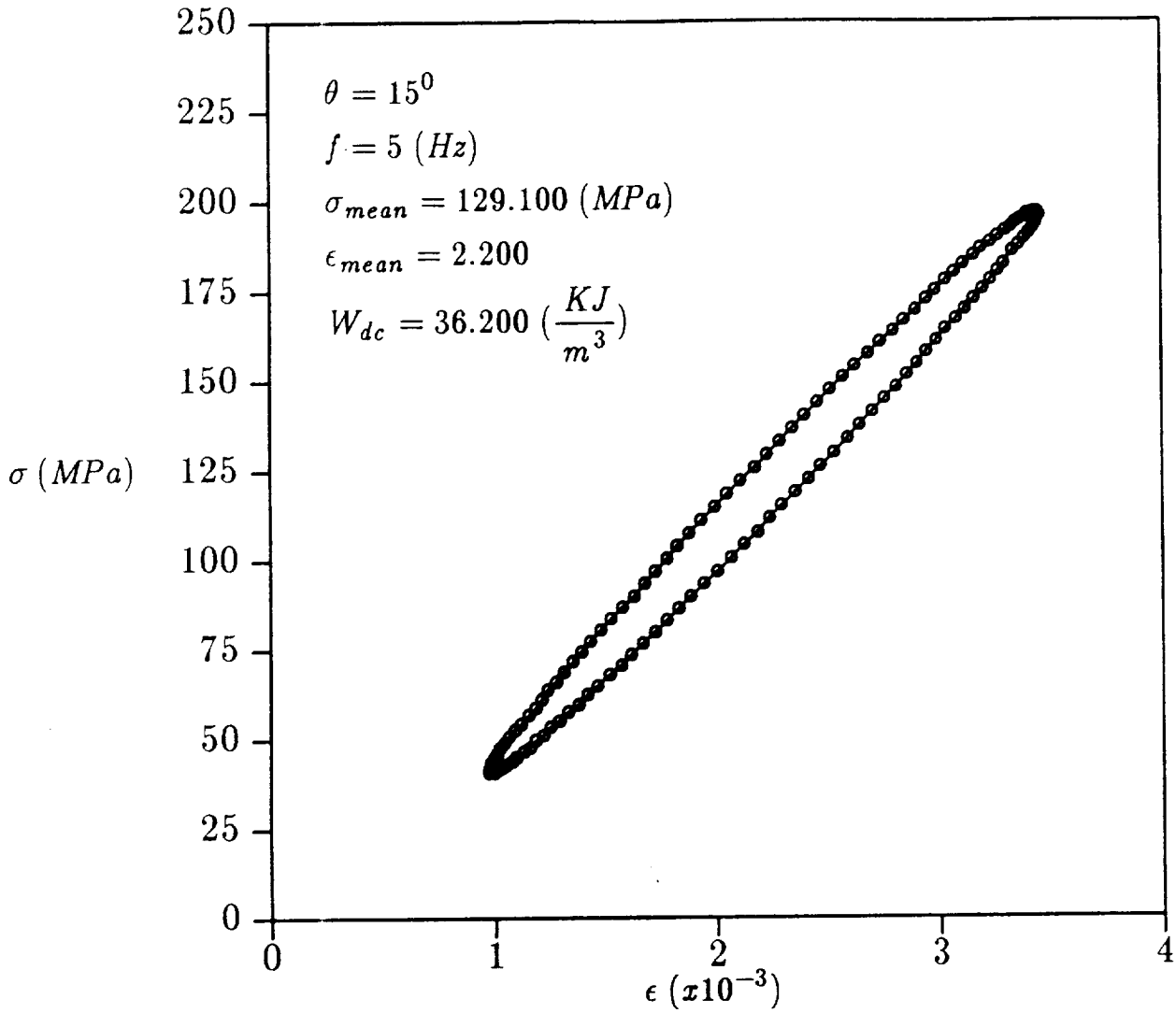

Fig. 13 Stress vs. strain response(one cycle of sinusoidal stress).

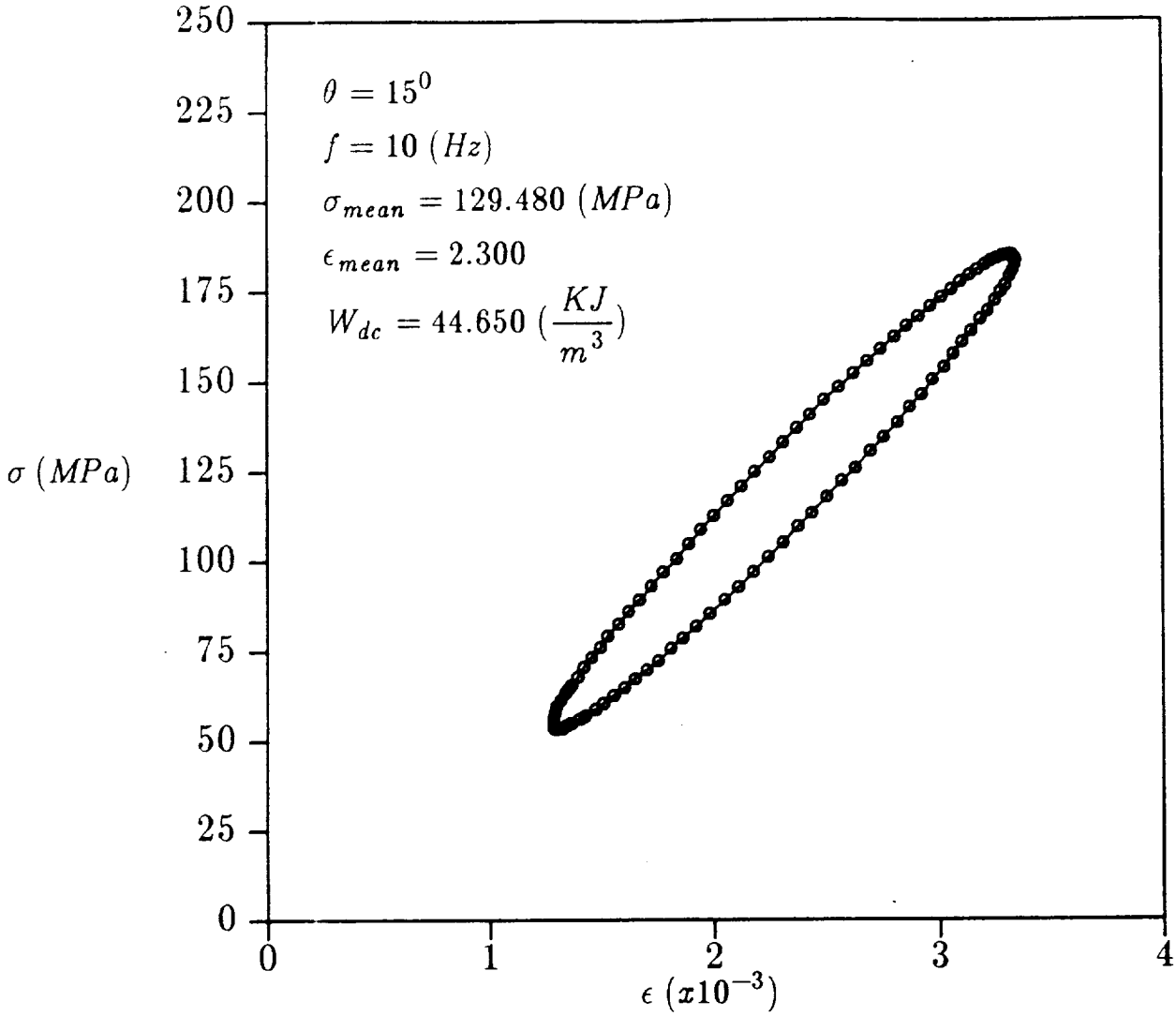

Fig. 14 Stress vs. strain response(one cycle of sinusoidal stress).

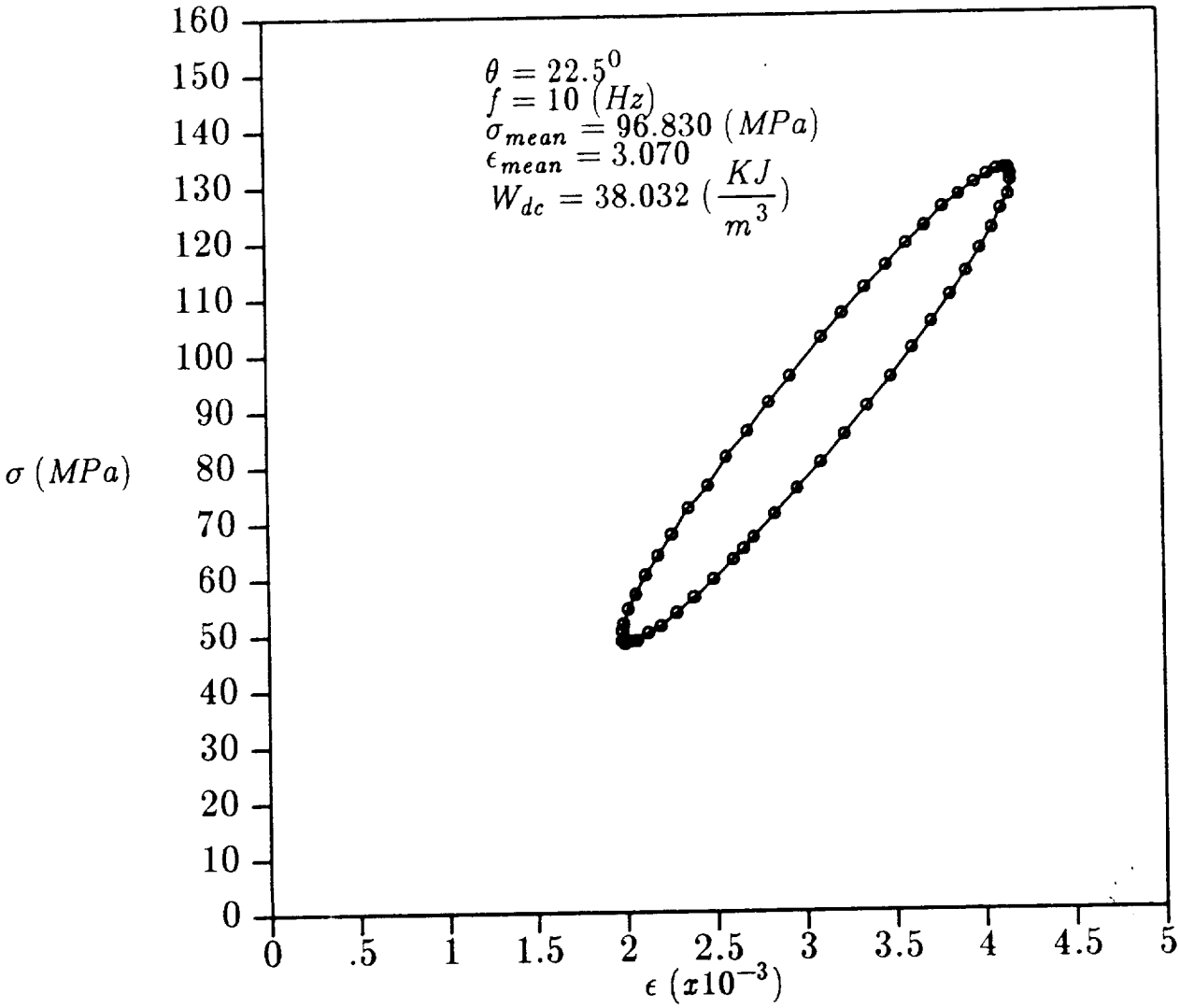

Fig. 15 Stress vs. strain response(one cycle of sinusoidal stress).

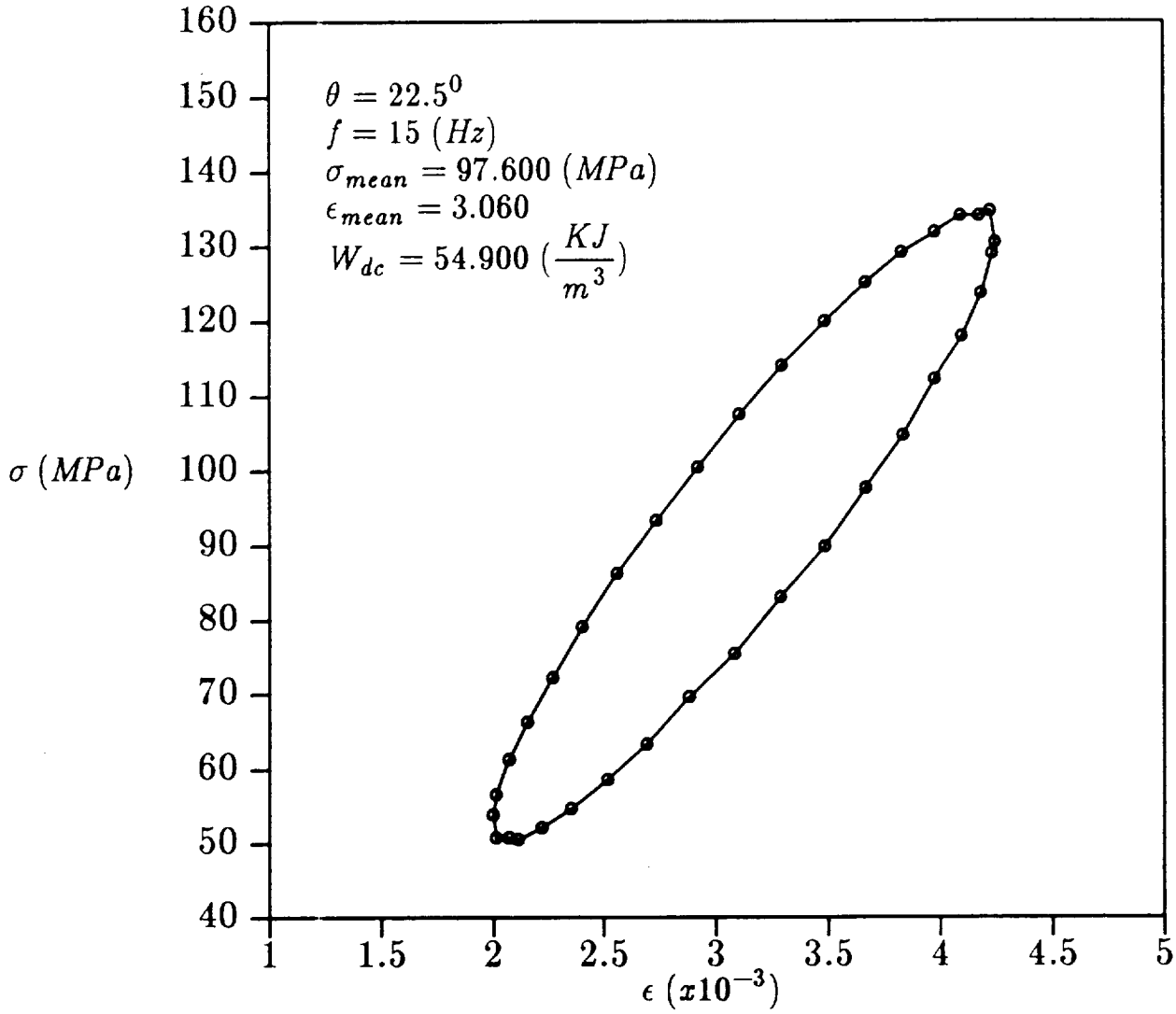

Fig. 16 Stress vs. strain response(one cycle of sinusoidal stress).

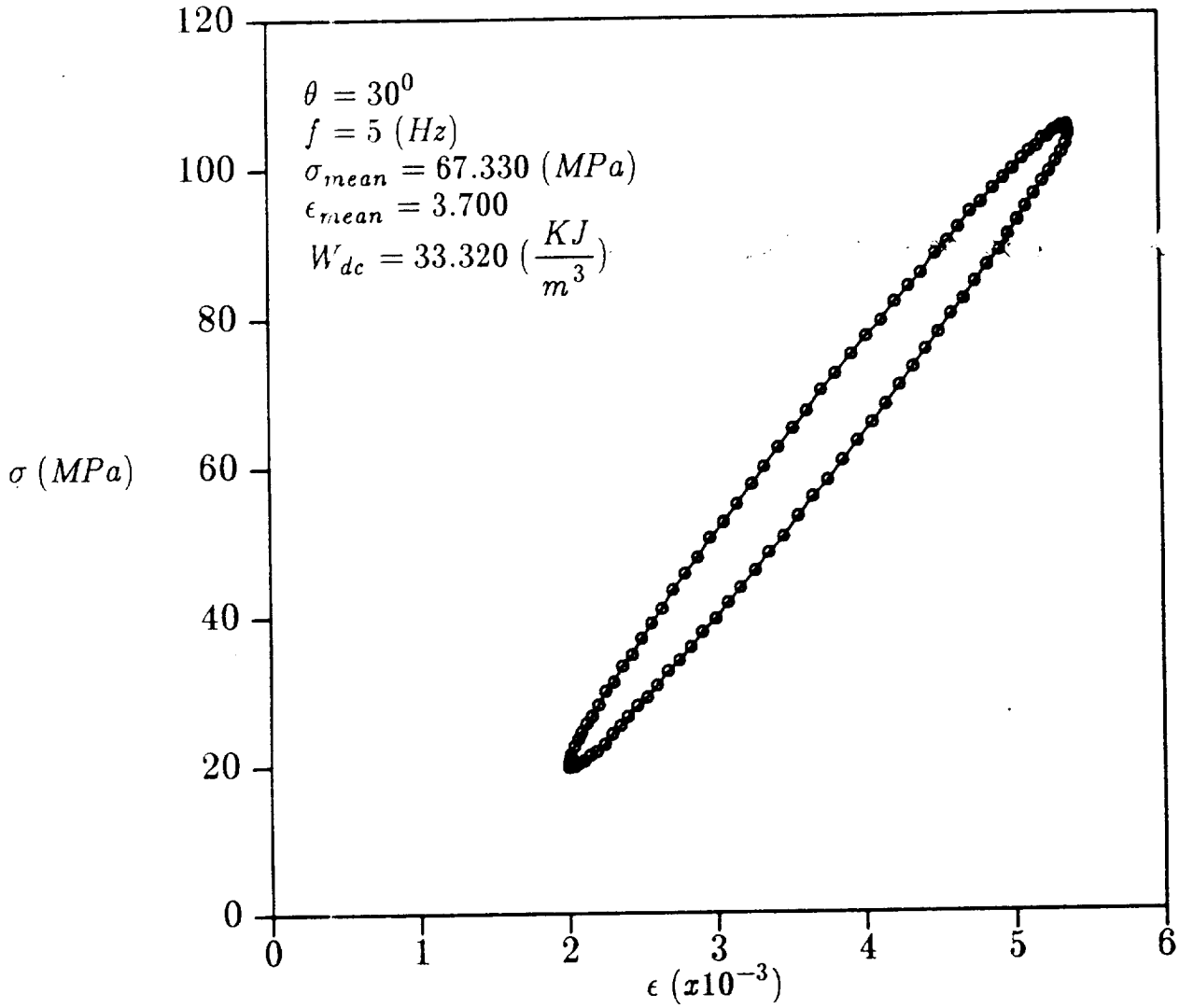

Fig. 7 Stress vs. strain response(one cycle of sinusoidal stress).

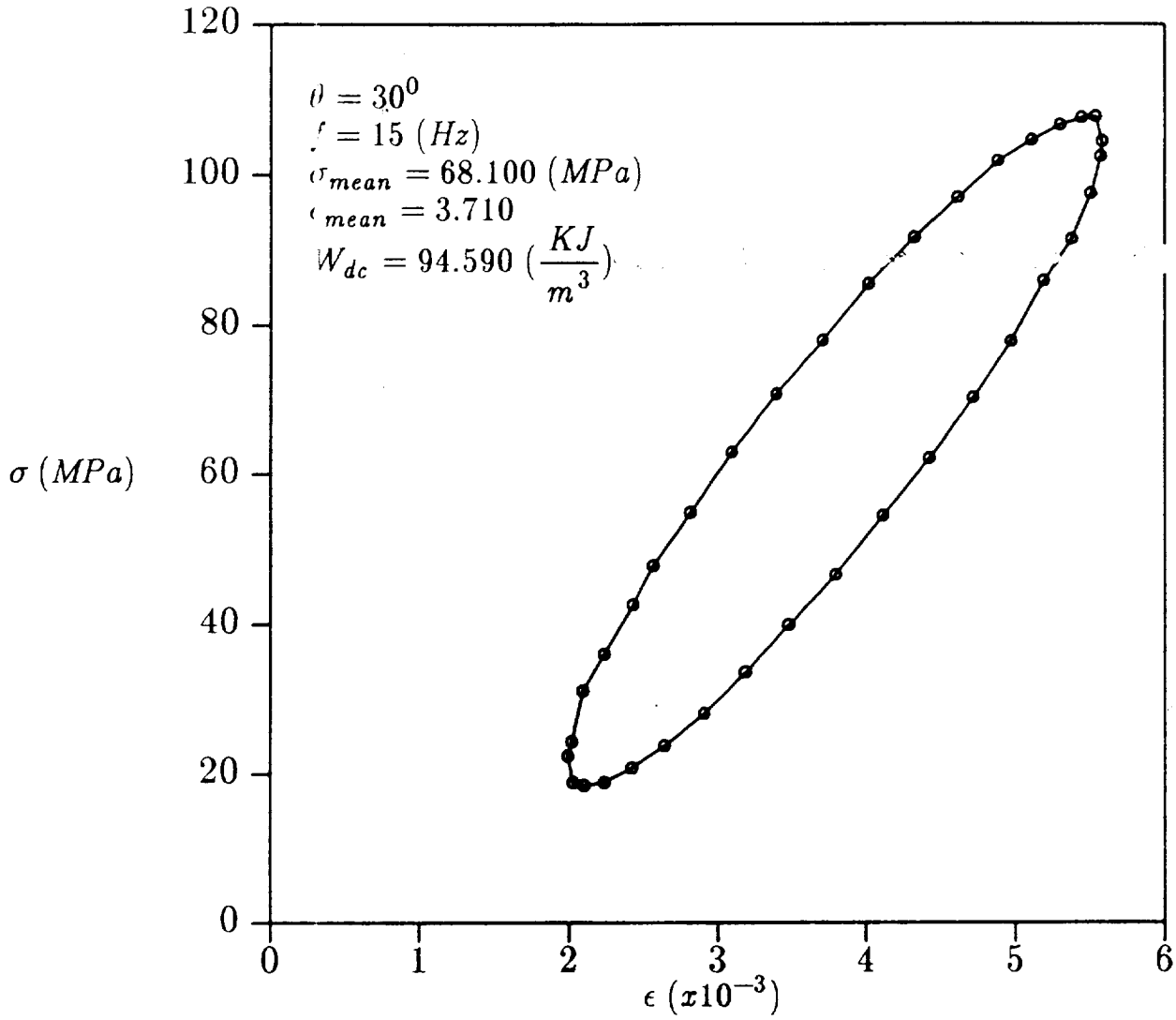

Fig. 18 Stress vs. strain response(one cycle of sinusoidal stress).

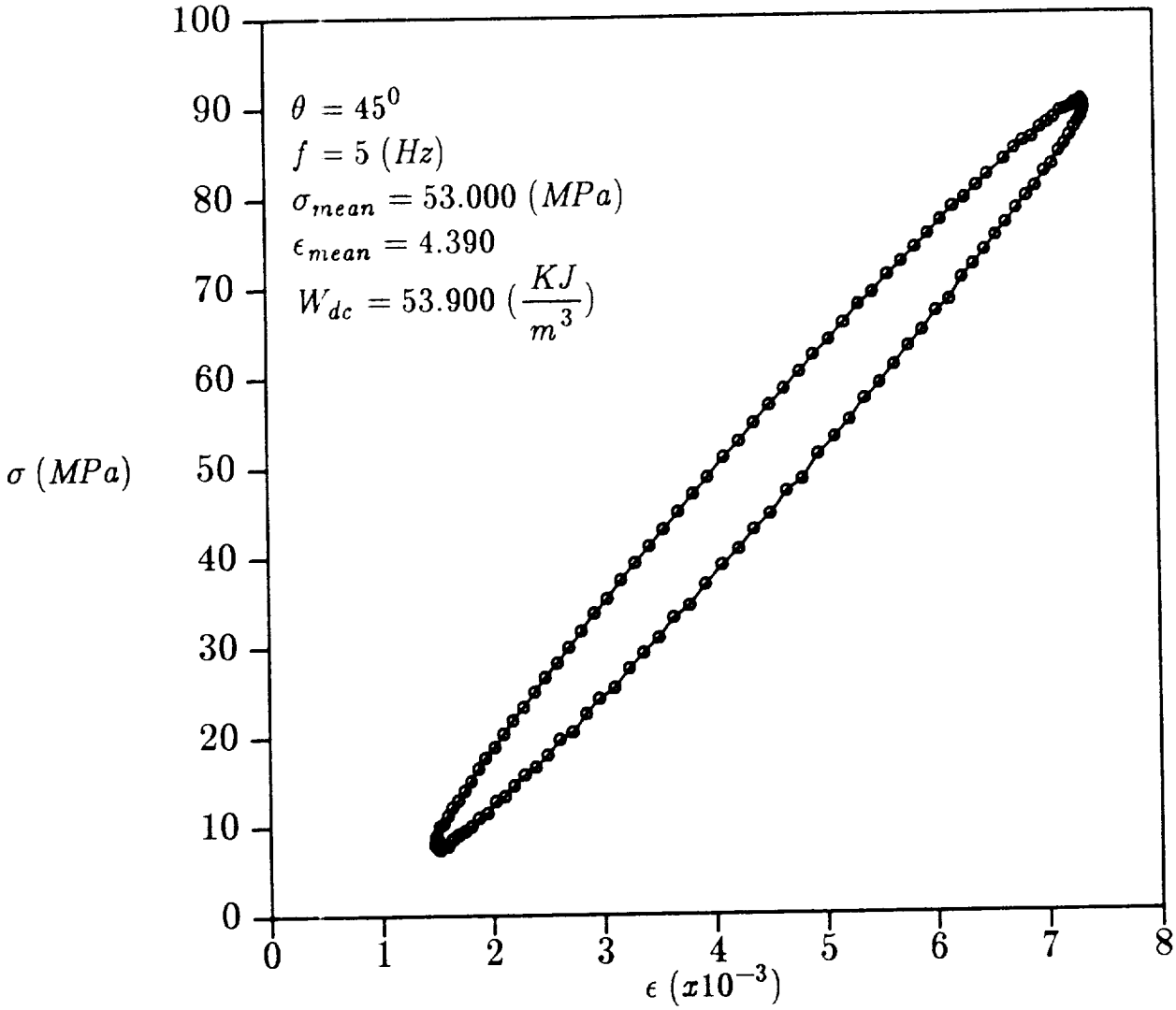

Fig. 19 Stress vs. strain response(one cycle of sinusoidal stress).

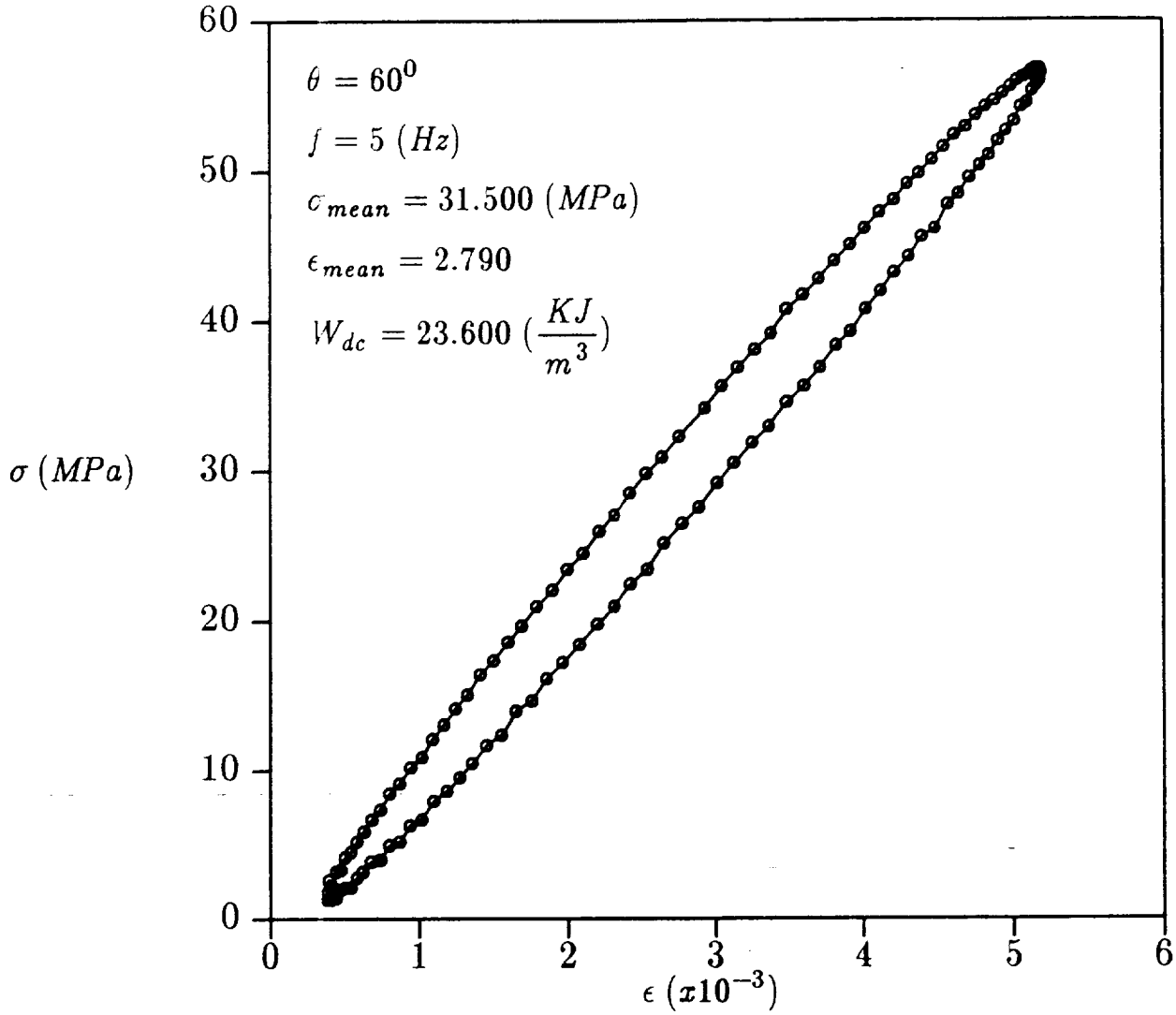

Fig 20 Stress vs. strain response(one cycle of sinusoidal stress).

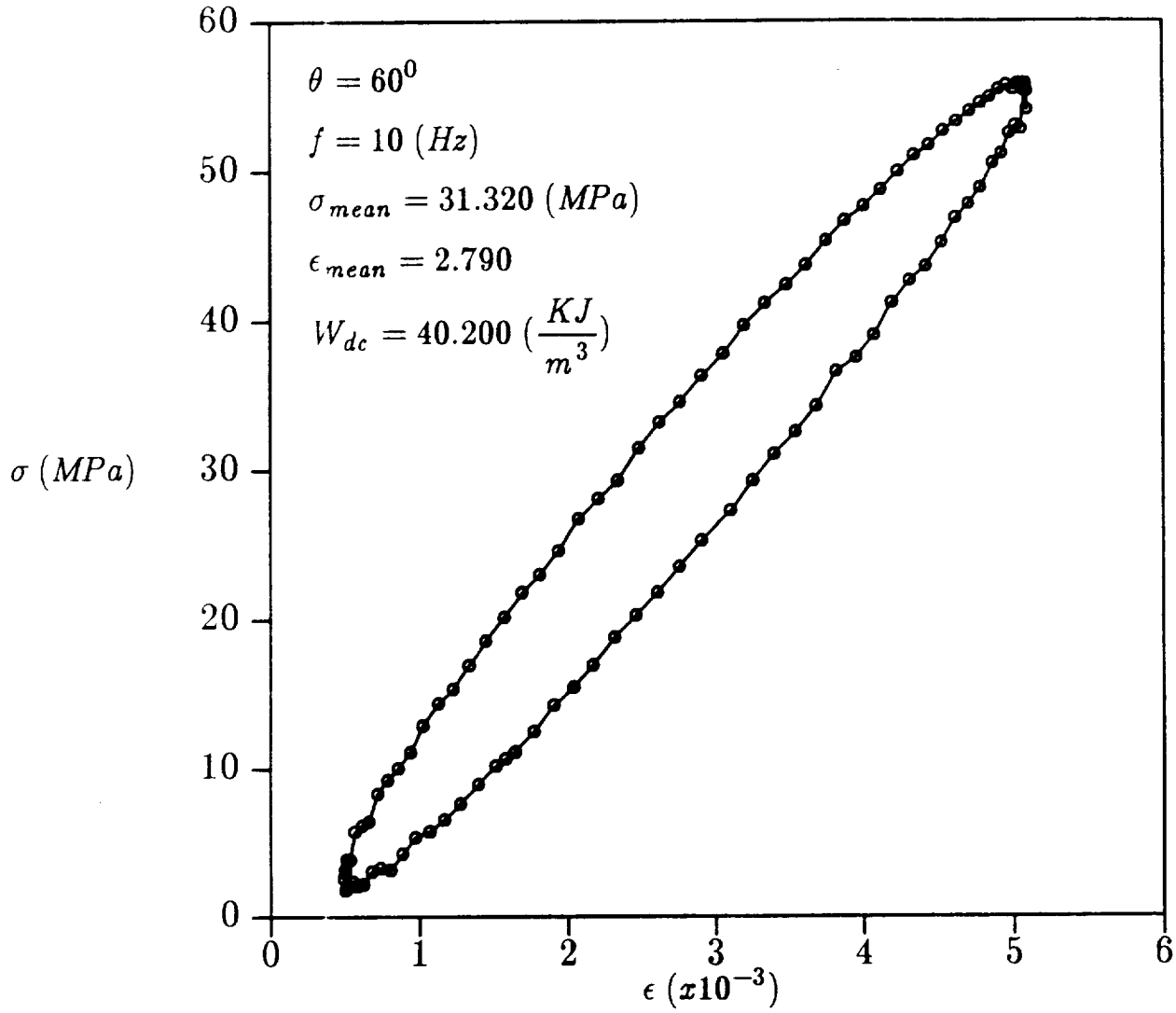

Fig. 21 Stress vs. strain response(one cycle of sinusoidal stress).

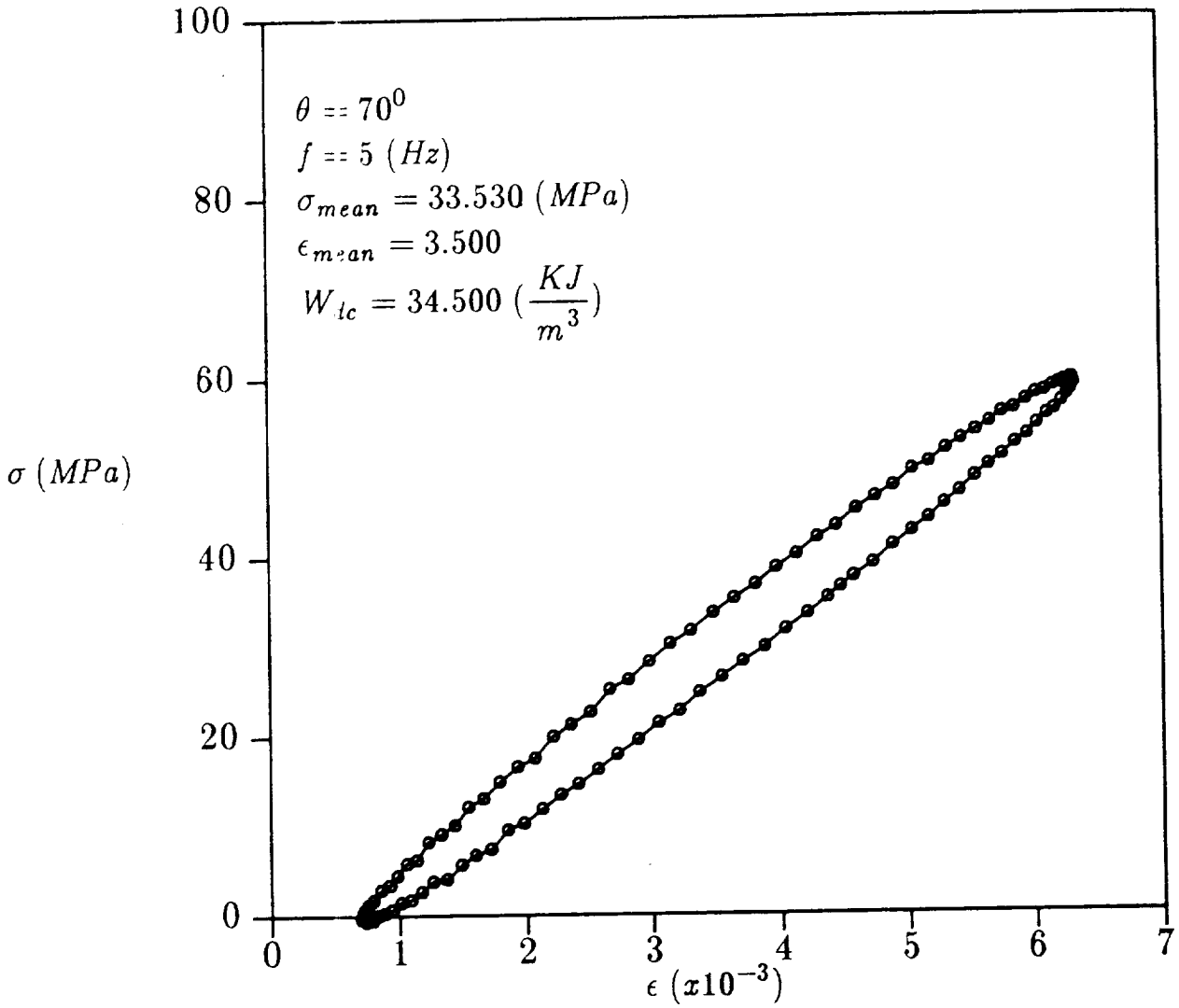

Fig. 22 Stress vs. strain response(one cycle of sinusoidal stress).

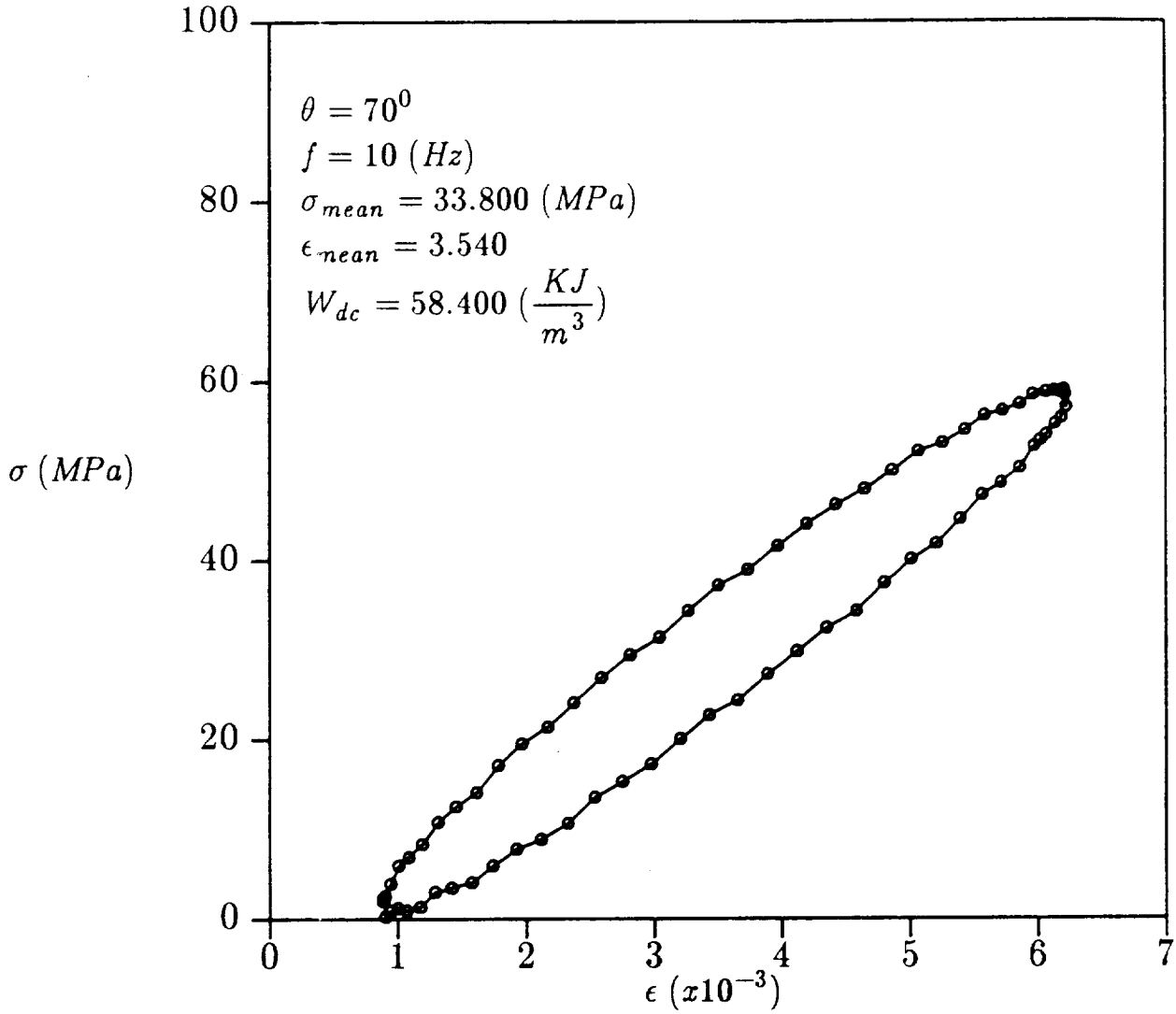

Fig. 22 Stress vs. strain response(one cycle of sinusoidal stress).

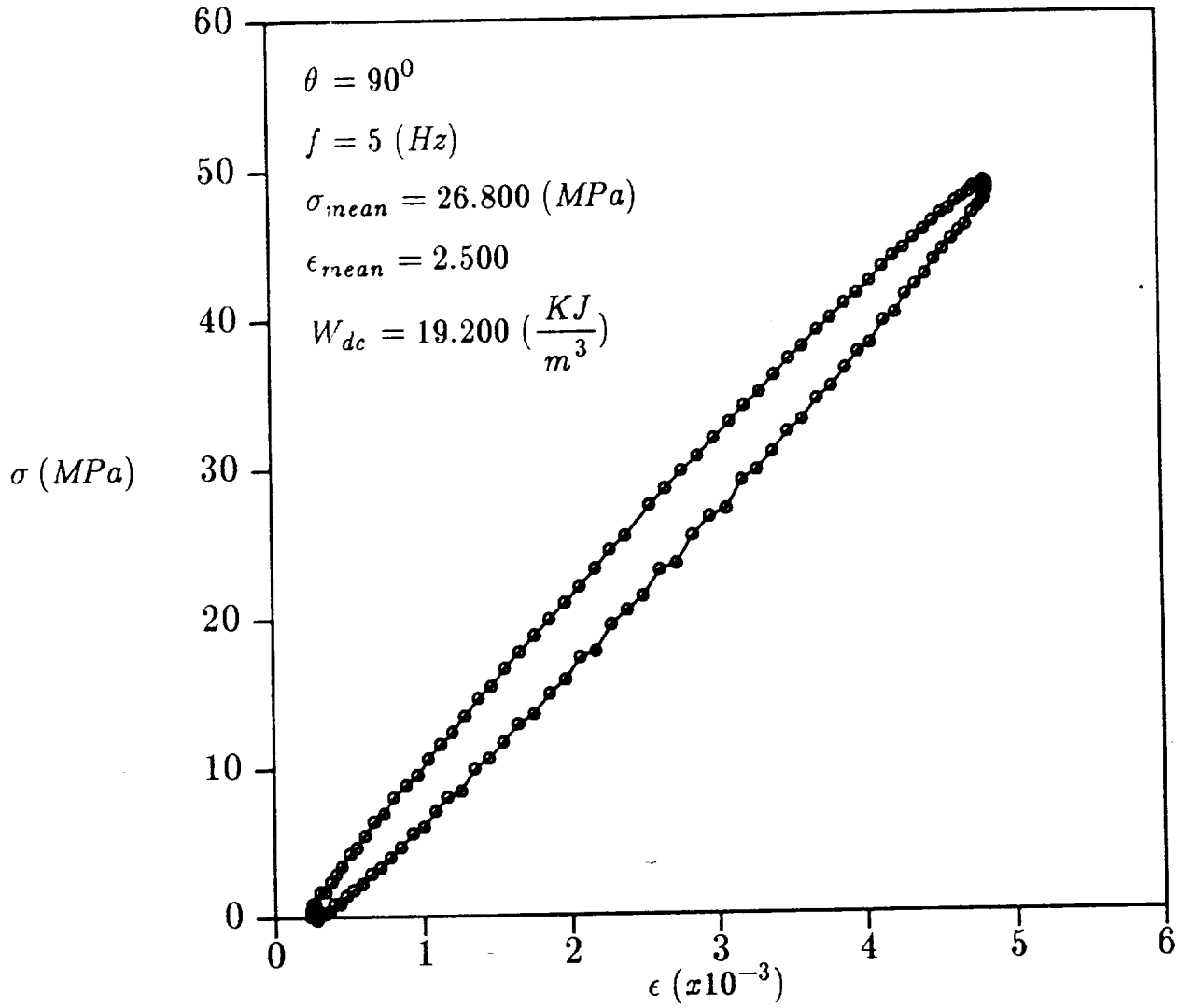

Fig. 24 Stress vs. strain response(one cycle of sinusoidal stress).

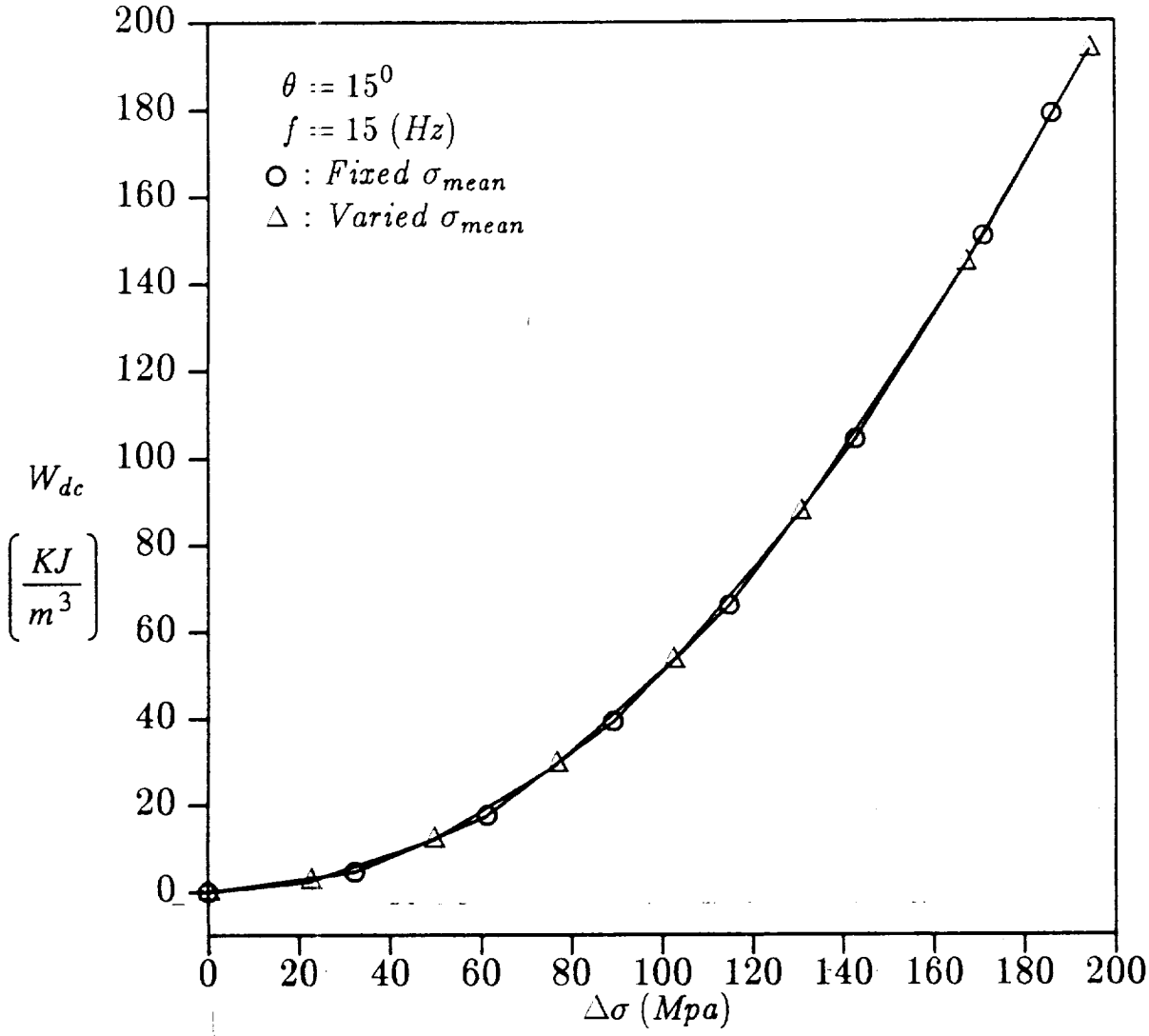

Fig. 25 Dissipated mechanical work per cycle vs. stress amplitude(solid curve: best curve fit).

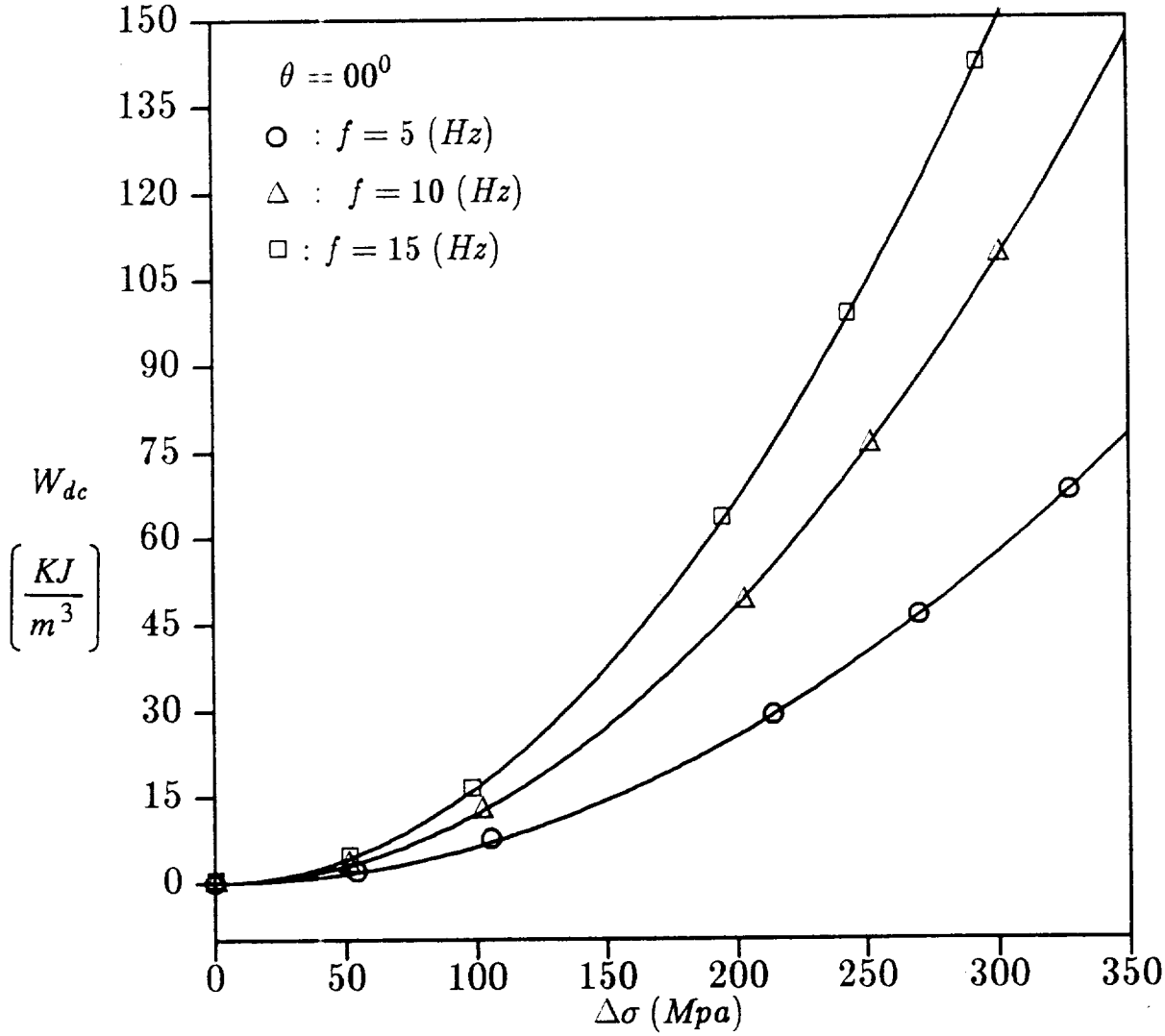

Fig. 26 Dissipated mechanical work per cycle vs. stress amplitude(solid curve: best curve fit).

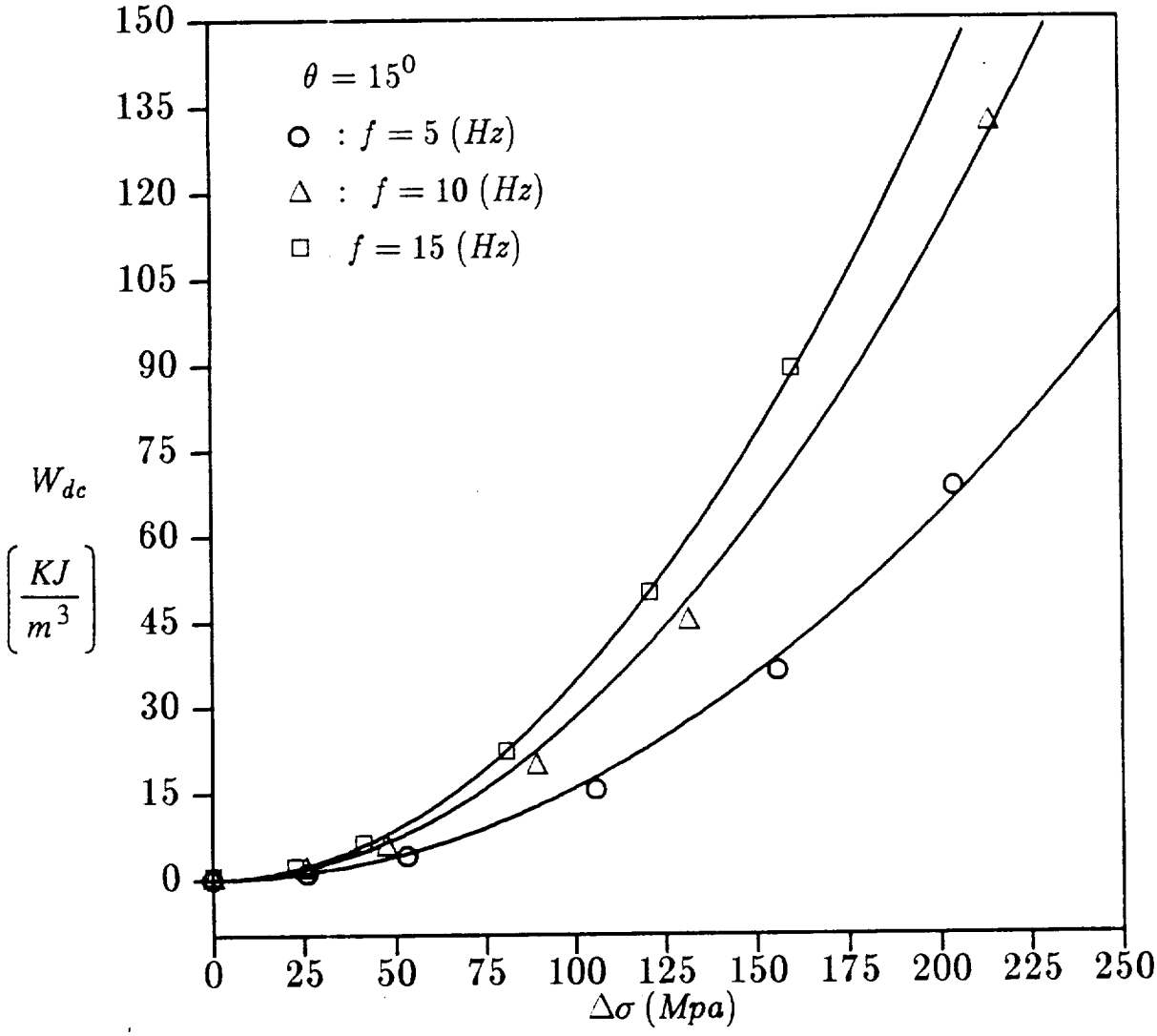

Fig. 27 Dissipated mechanical work per cycle vs.
stress amplitude(solid curve: best curve fit).

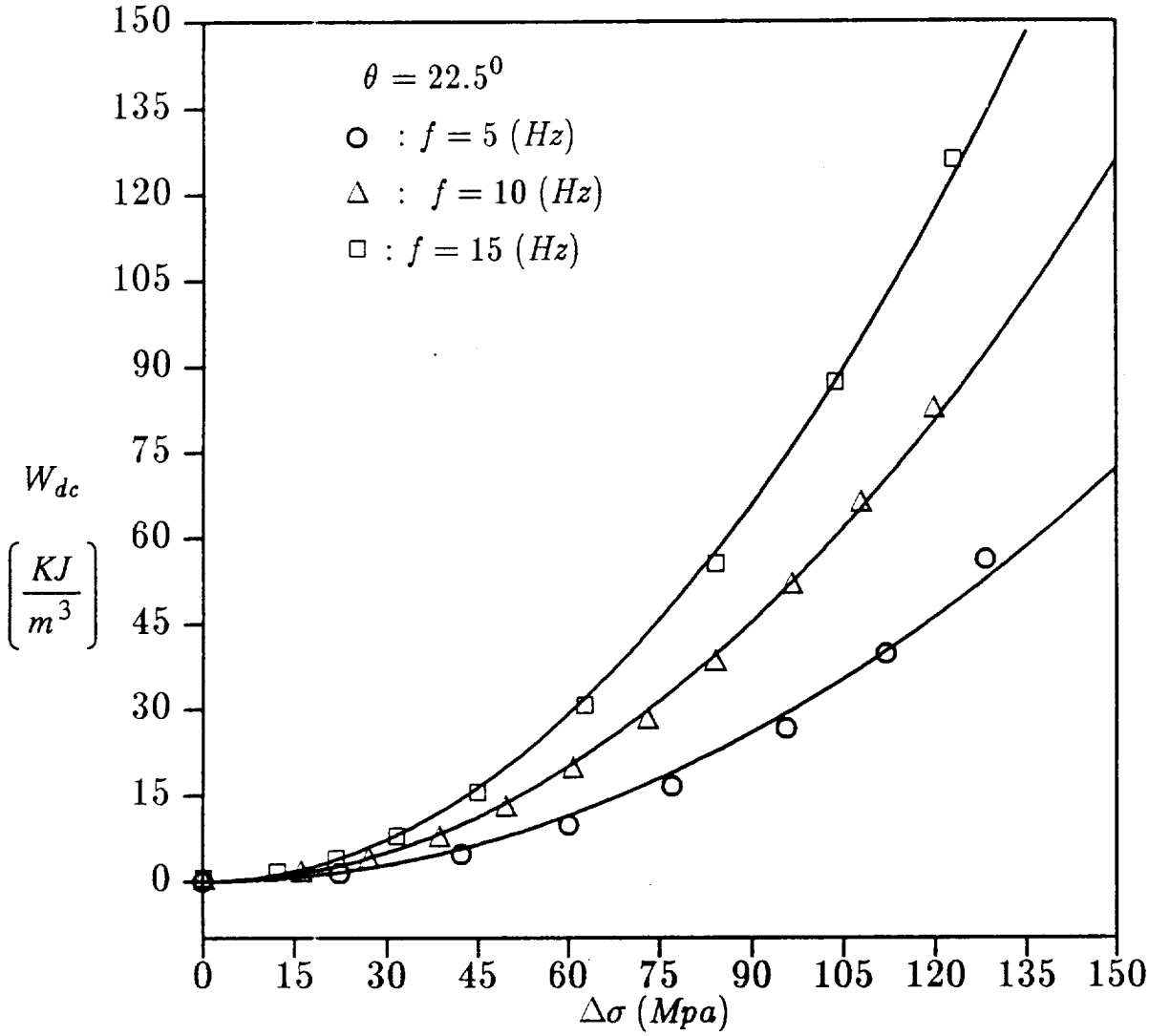

Fig. 28 Dissipated mechanical work per cycle vs. stress amplitude(solid curve: best curve fit).

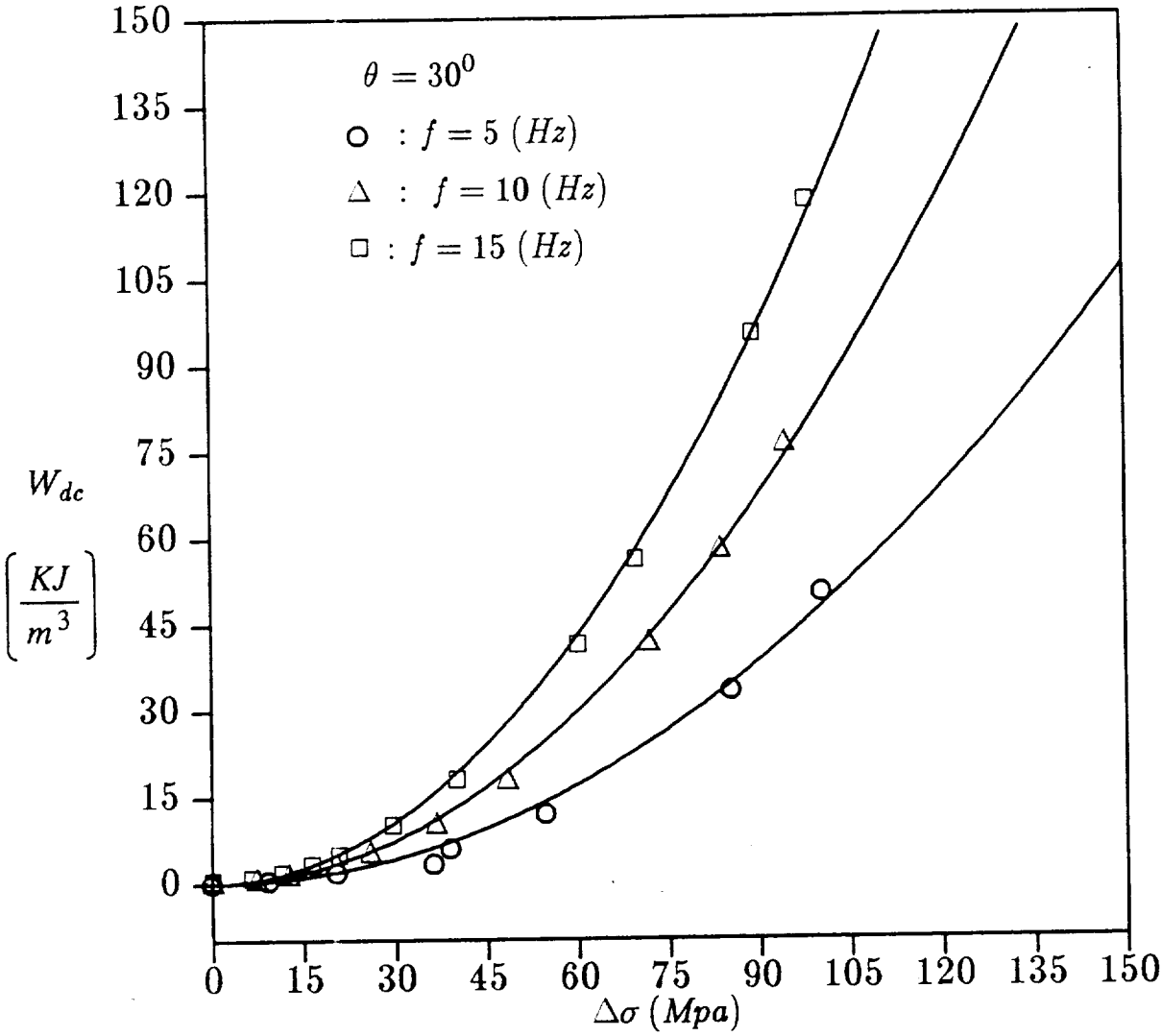

Fig. 29 Dissipated mechanical work per cycle vs. stress amplitude(solid curve: best curve fit).

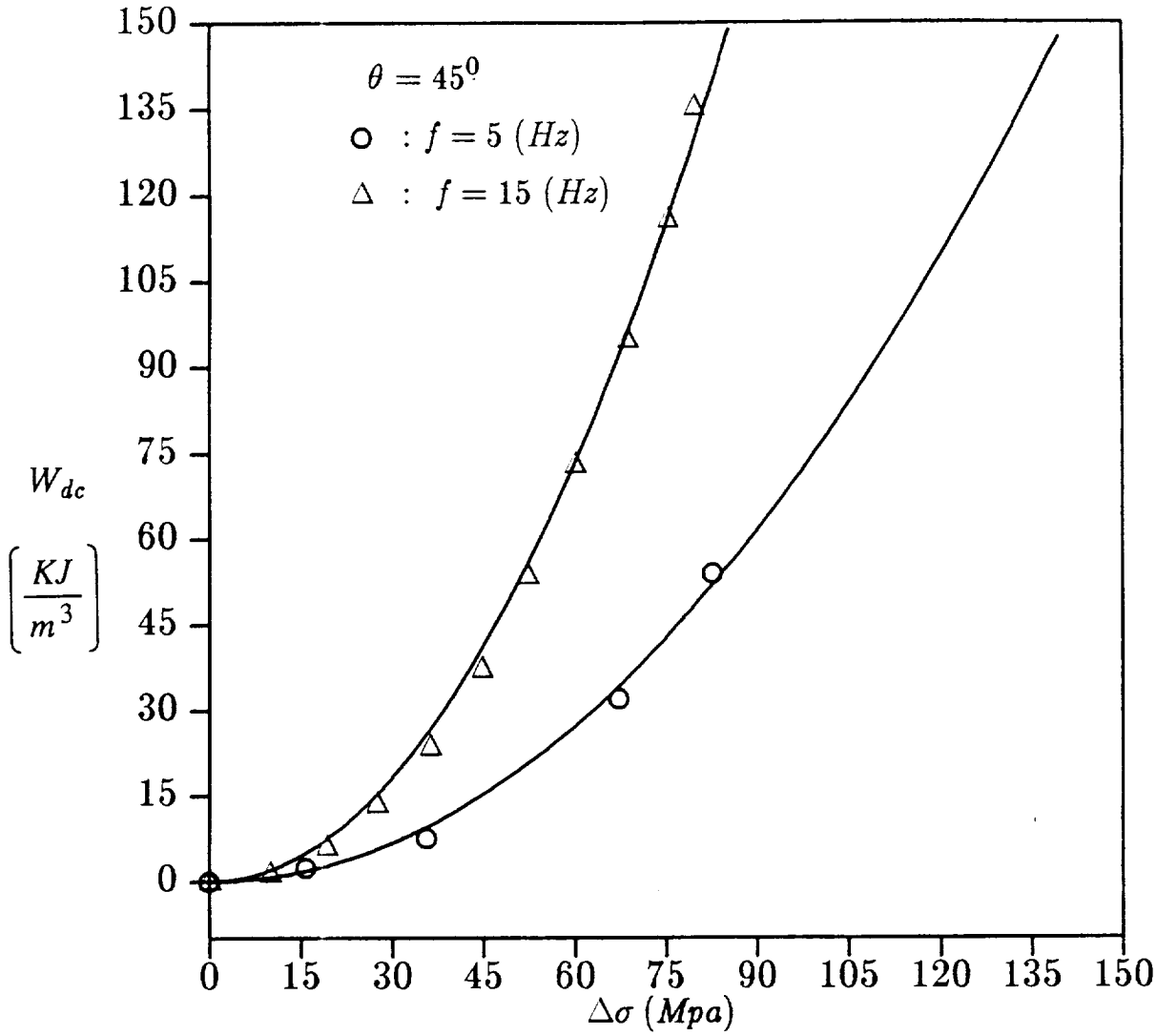

Fig. 30 Dissipated mechanical work per cycle vs. stress amplitude(solid curve: best curve fit).

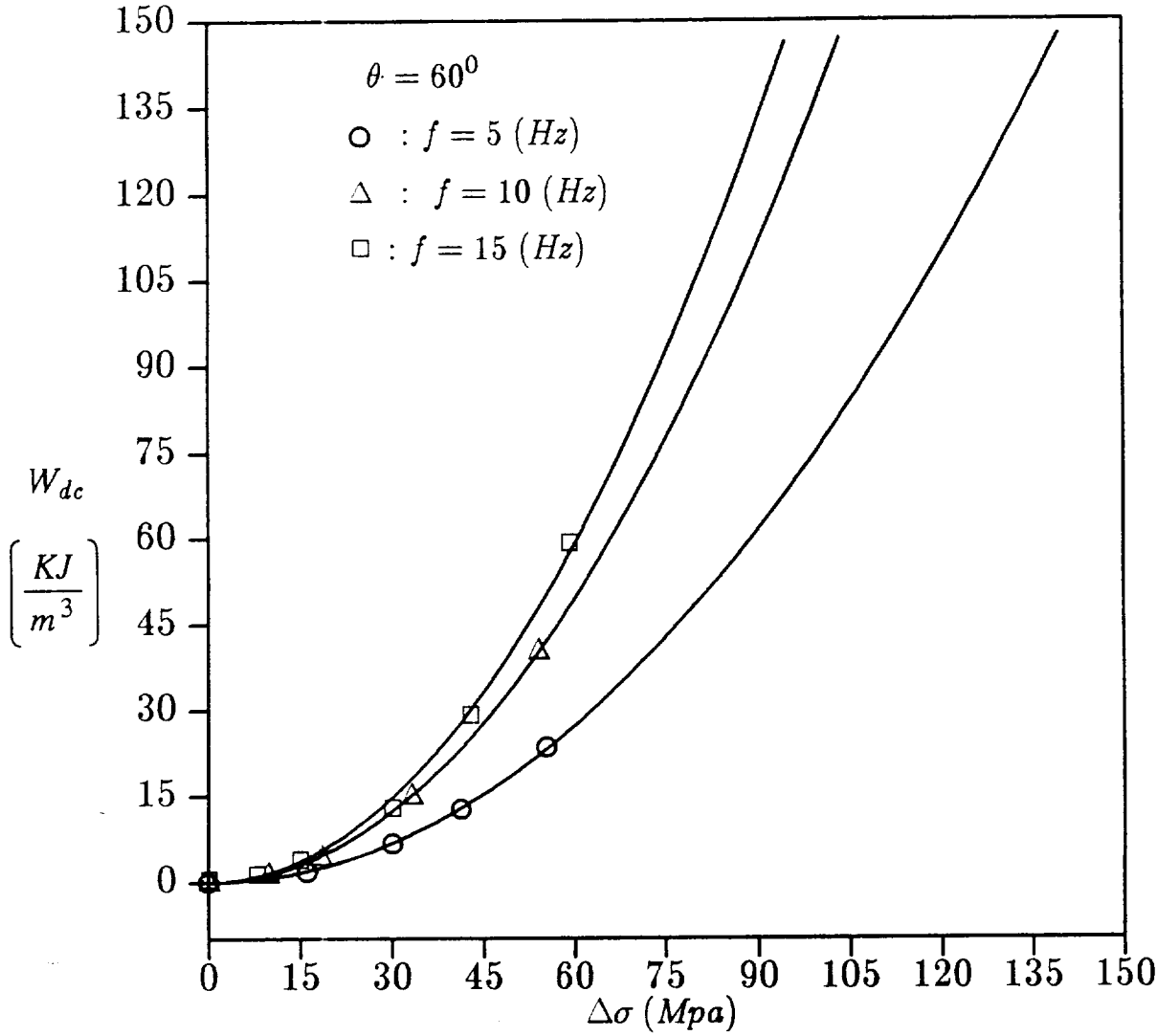

Fig. 31 Dissipated mechanical work per cycle vs. stress amplitude(solid curve: best curve fit).

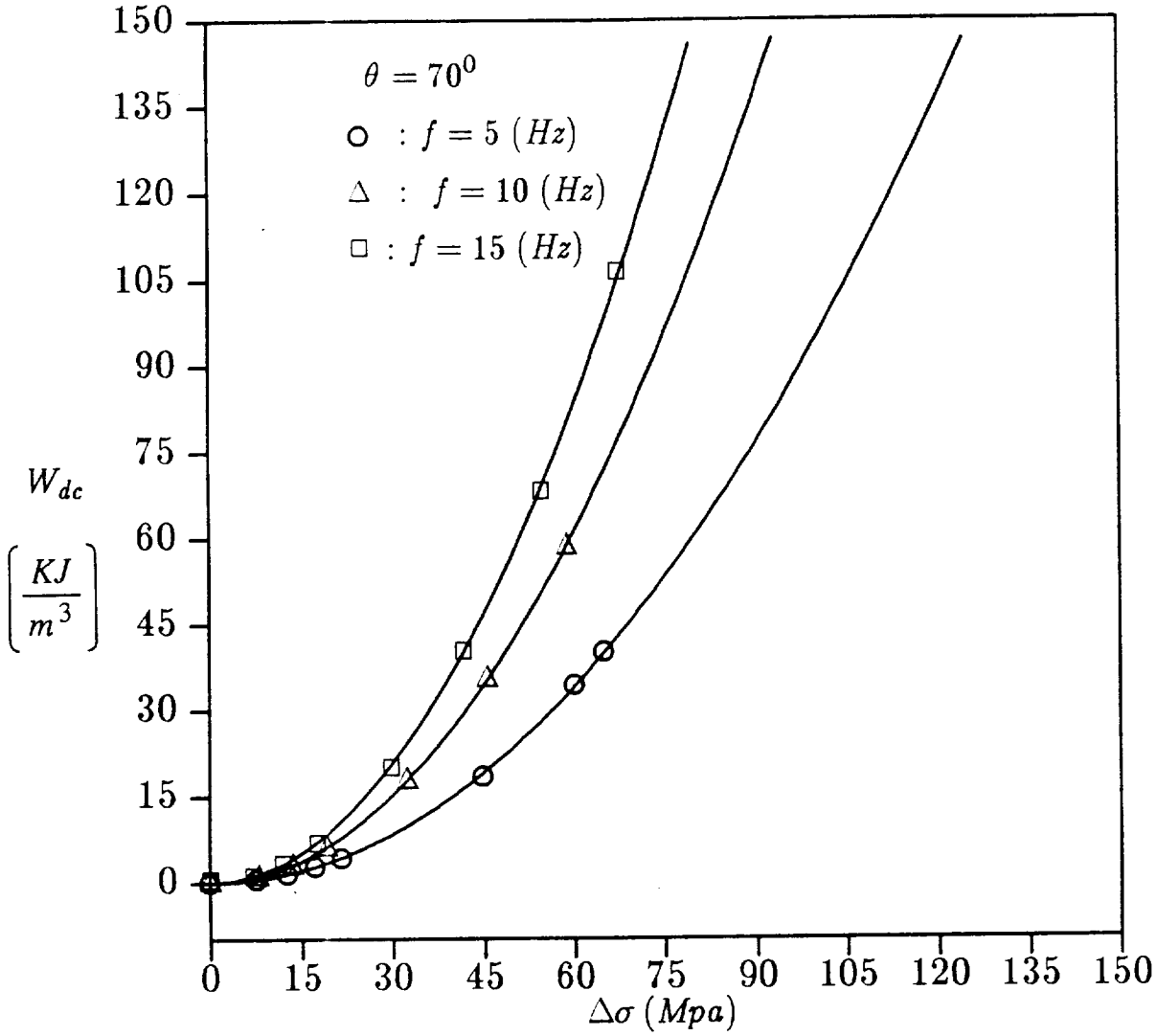

Fig. 32 Dissipated mechanical work per cycle vs. stress amplitude(solid curve: best curve fit).

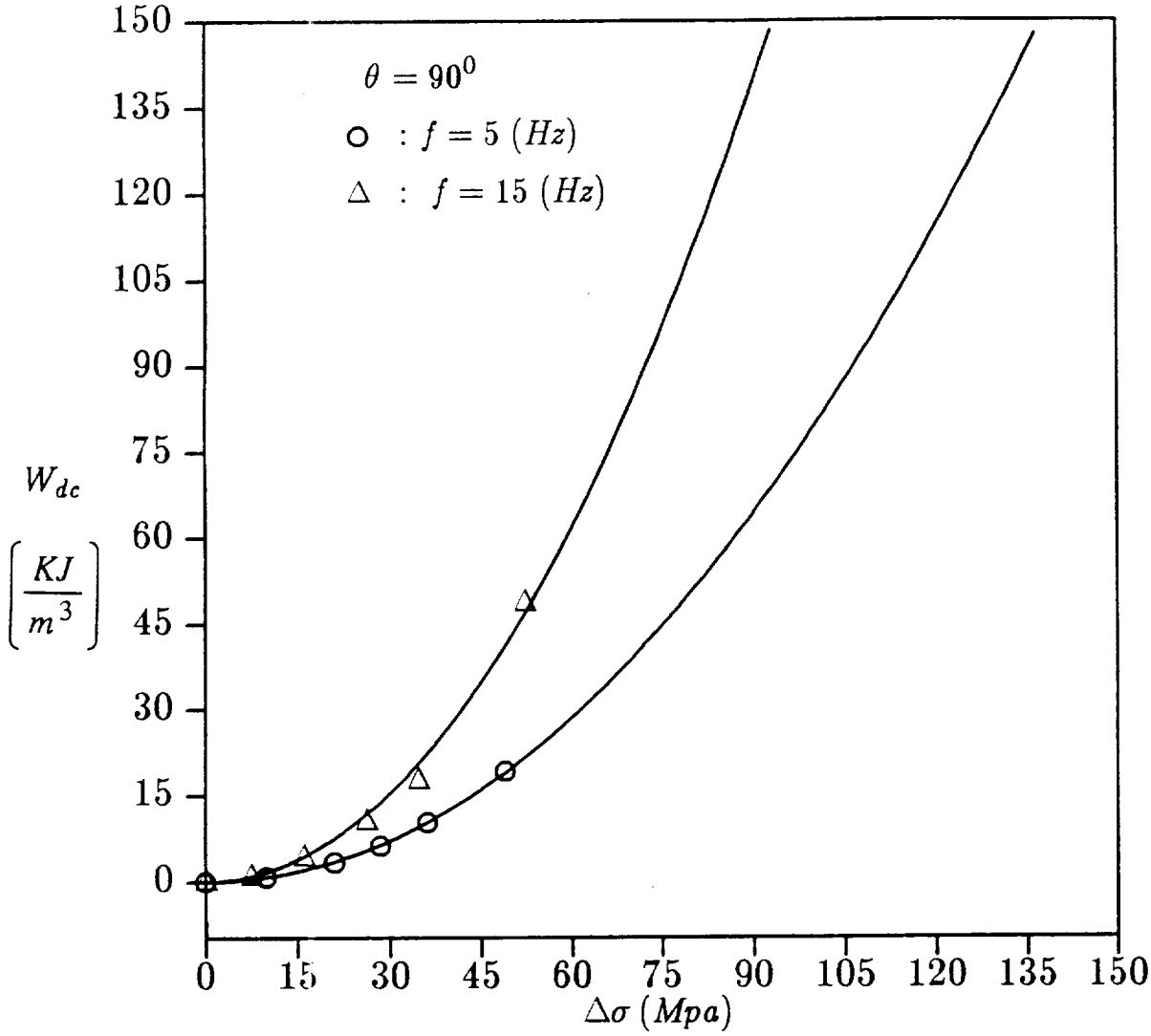

Fig. 33 Dissipated mechanical work per cycle vs. stress amplitude(solid curve: best curve fit).

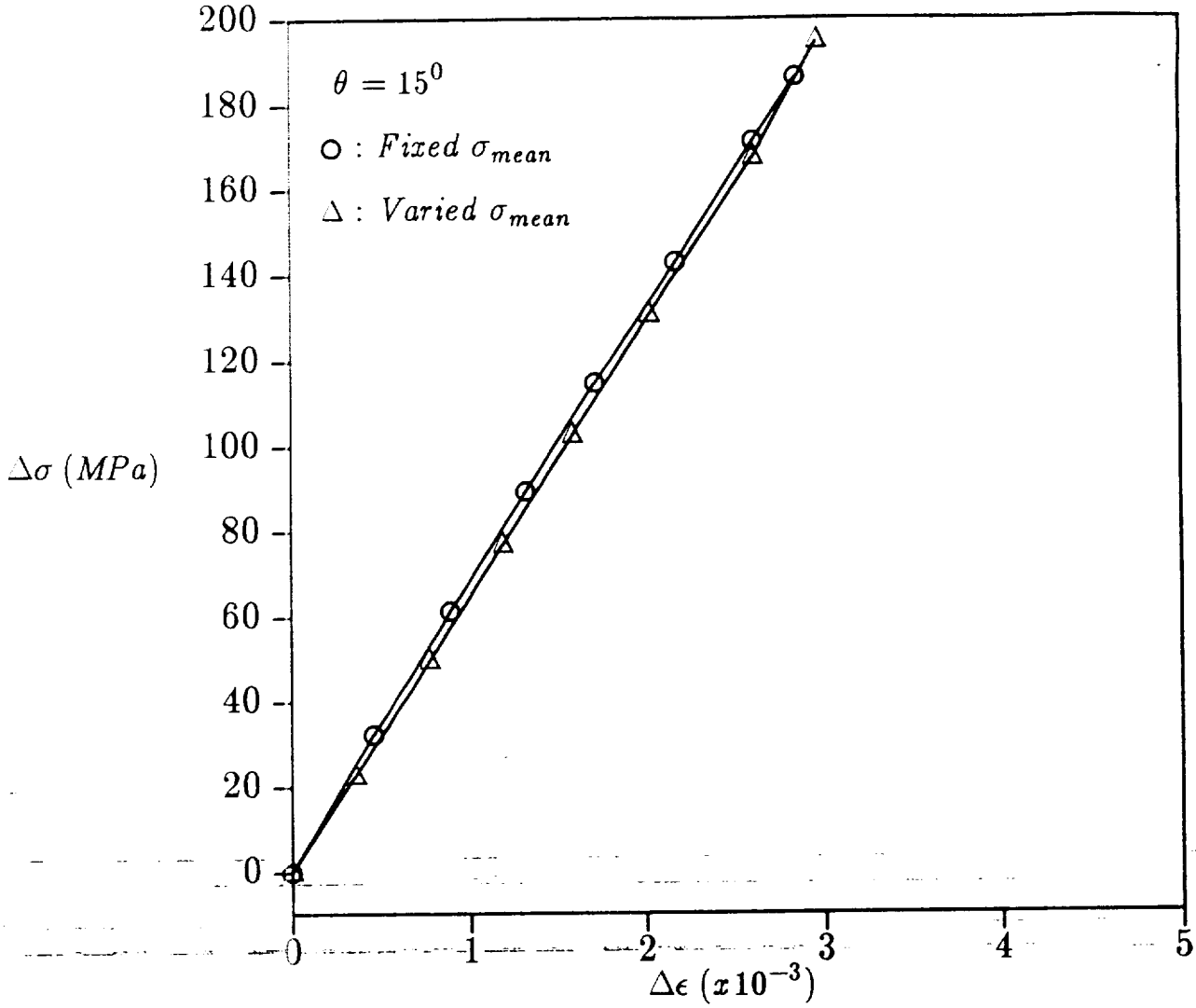

Fig. 34 Stress amplitude vs. strain amplitude response(f = 15 Hz).

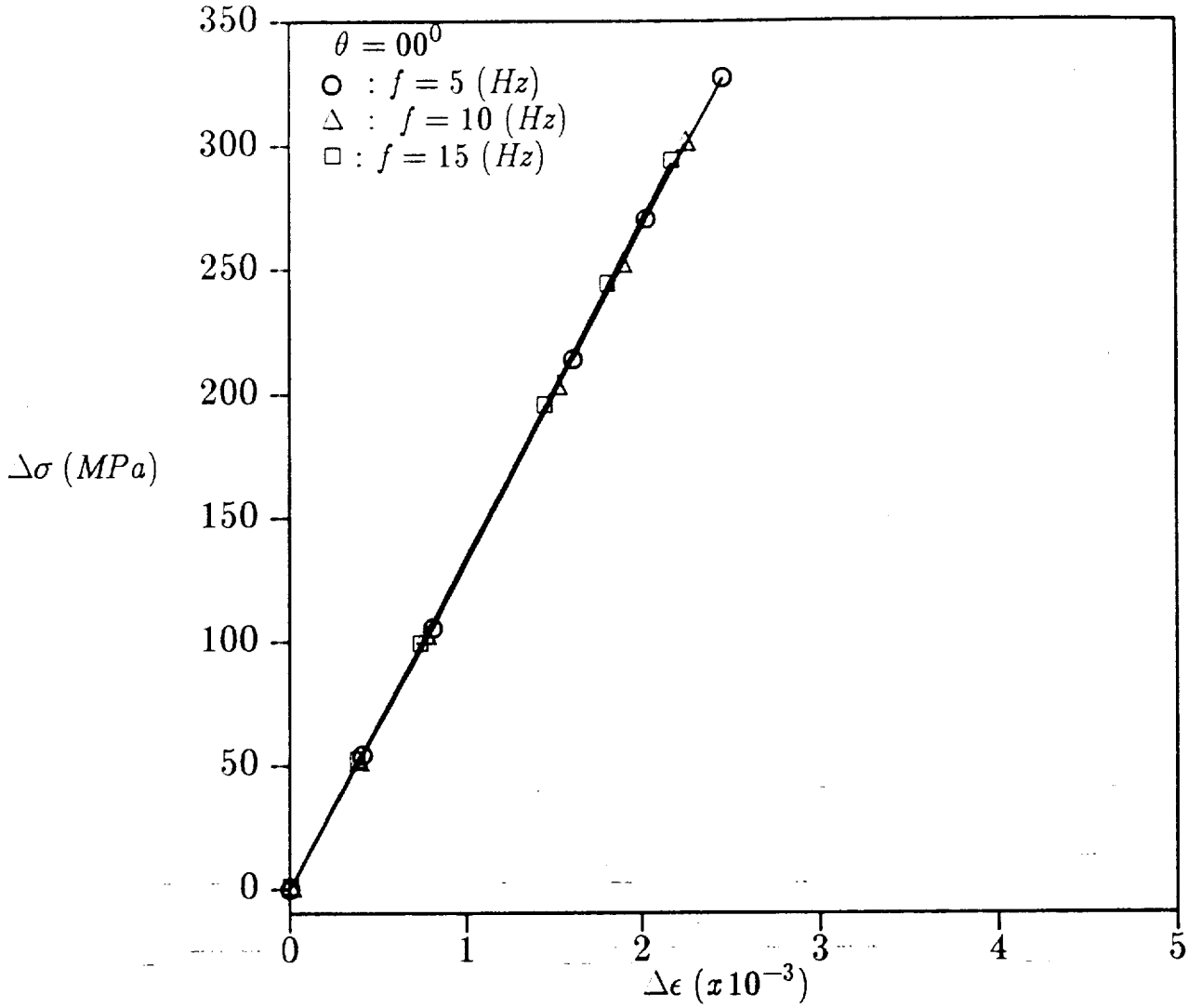

Fig. 35 Stress amplitude vs. strain amplitude response.

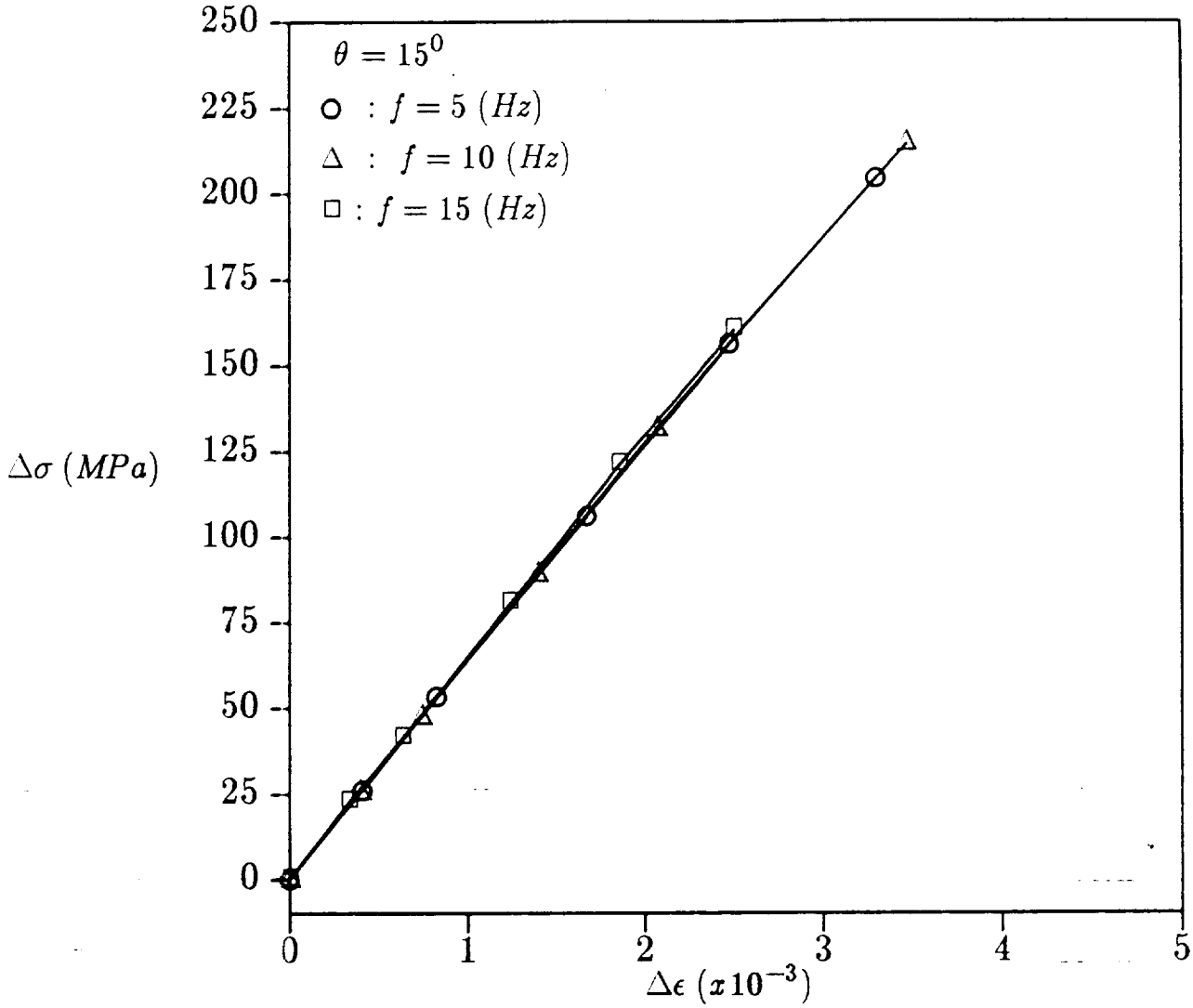

Fig. 36 Stress amplitude vs. strain amplitude response.

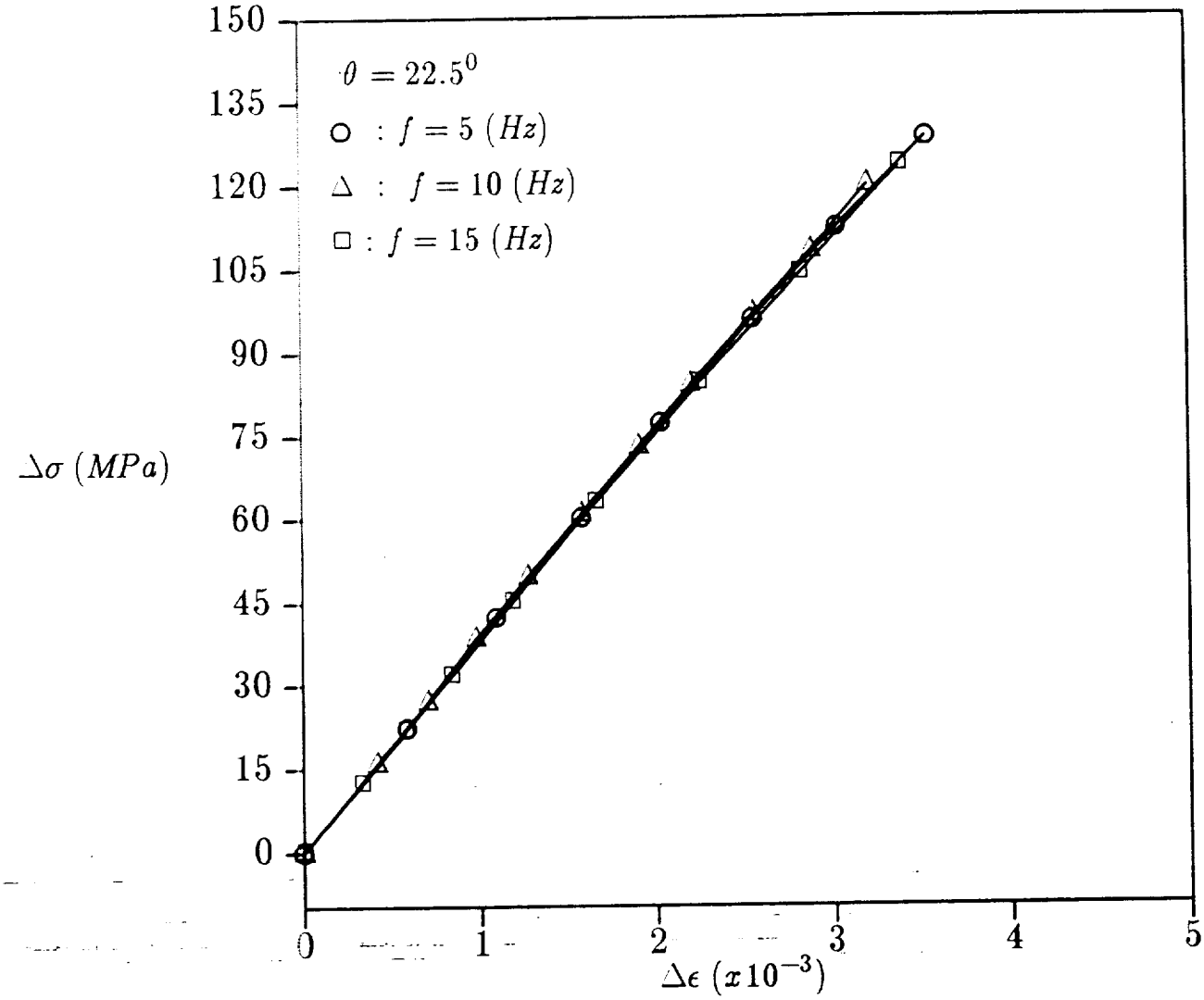

Fig. 37 Stress amplitude vs. strain amplitude response.

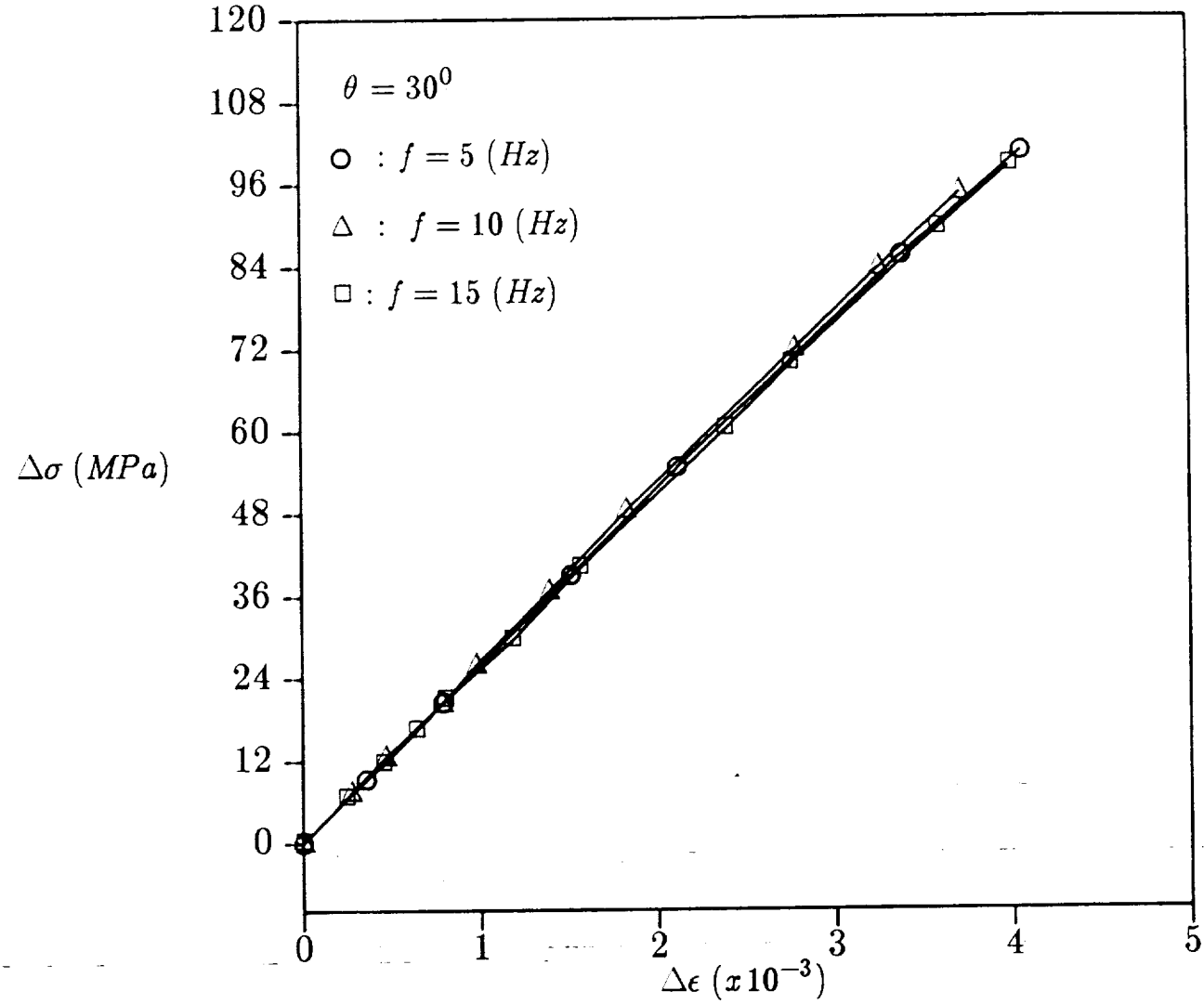

Fig. 38 Stress amplitude vs. strain amplitude response.

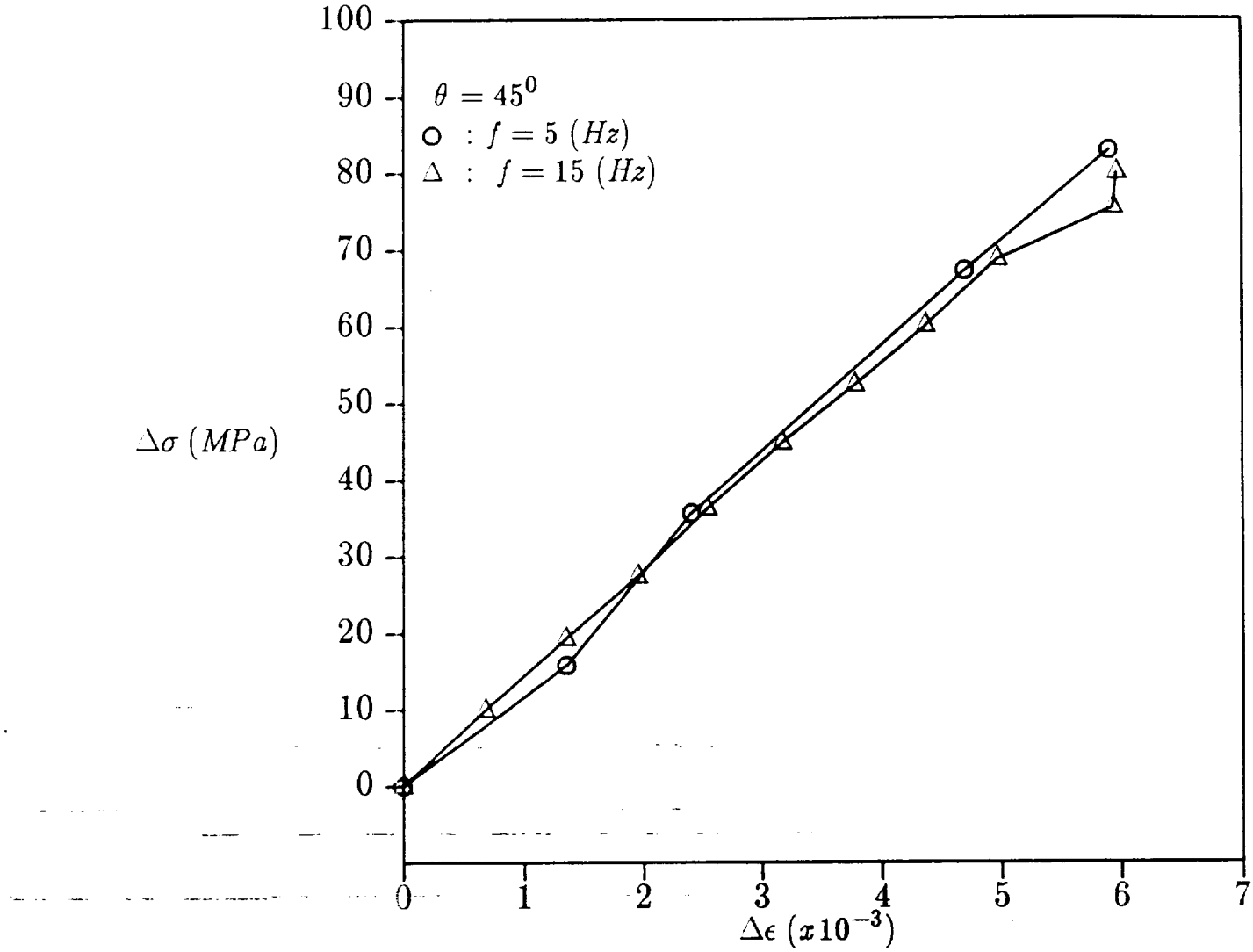

Fig. 39 Stress amplitude vs. strain amplitude response.

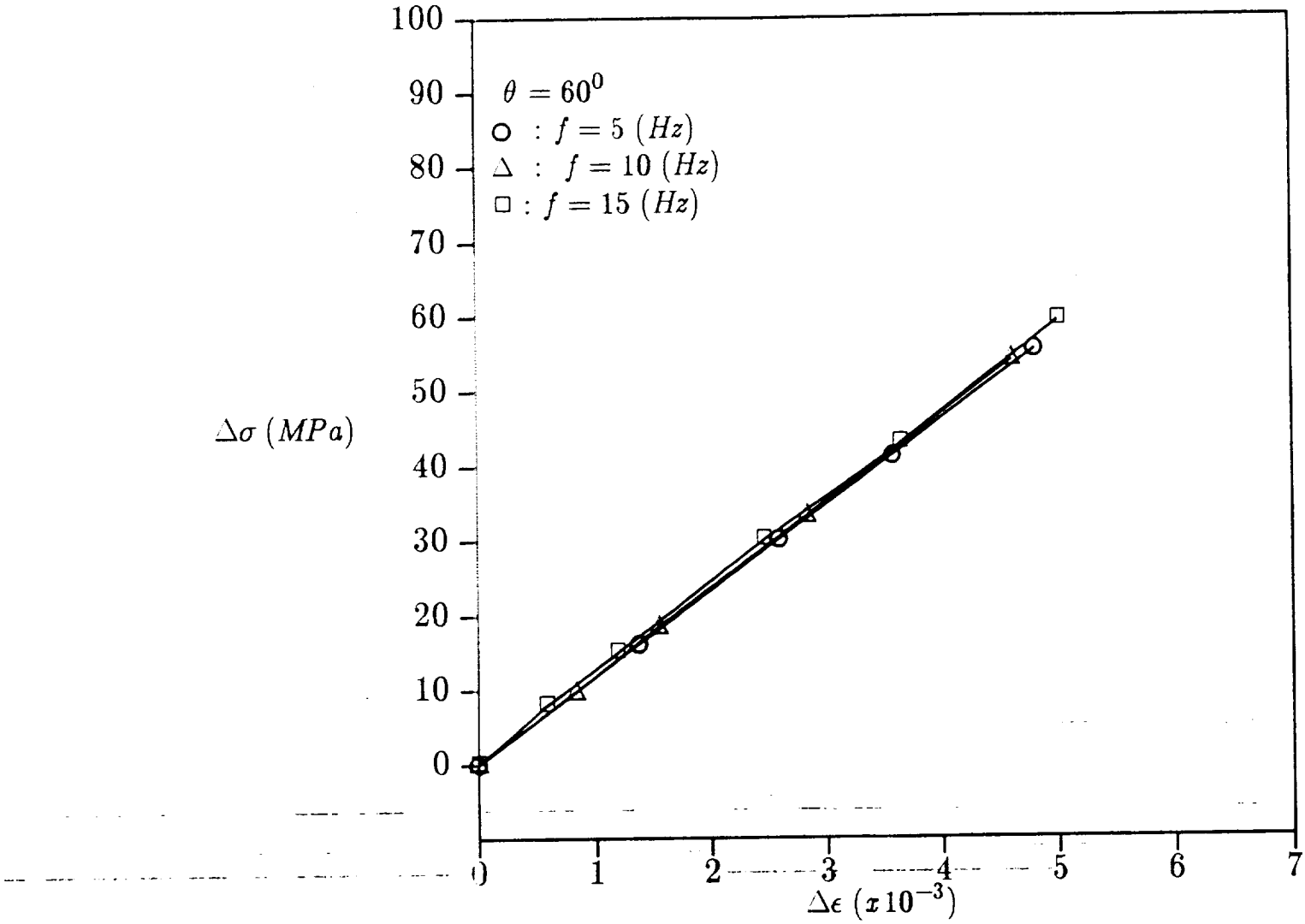

Fig. 40 Stress amplitude vs. strain amplitude response.

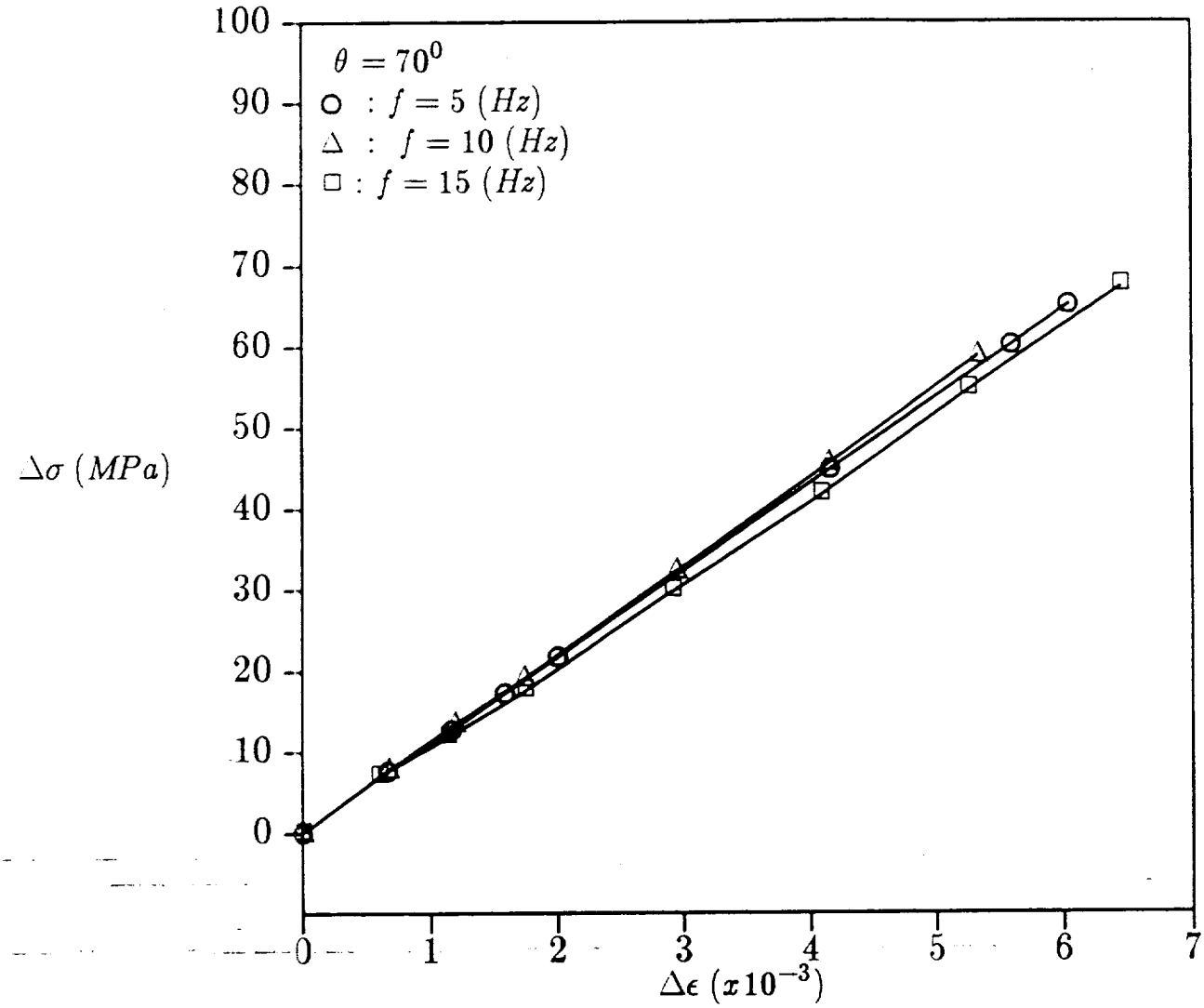

Fig. 41 Stress amplitude vs. strain amplitude response.

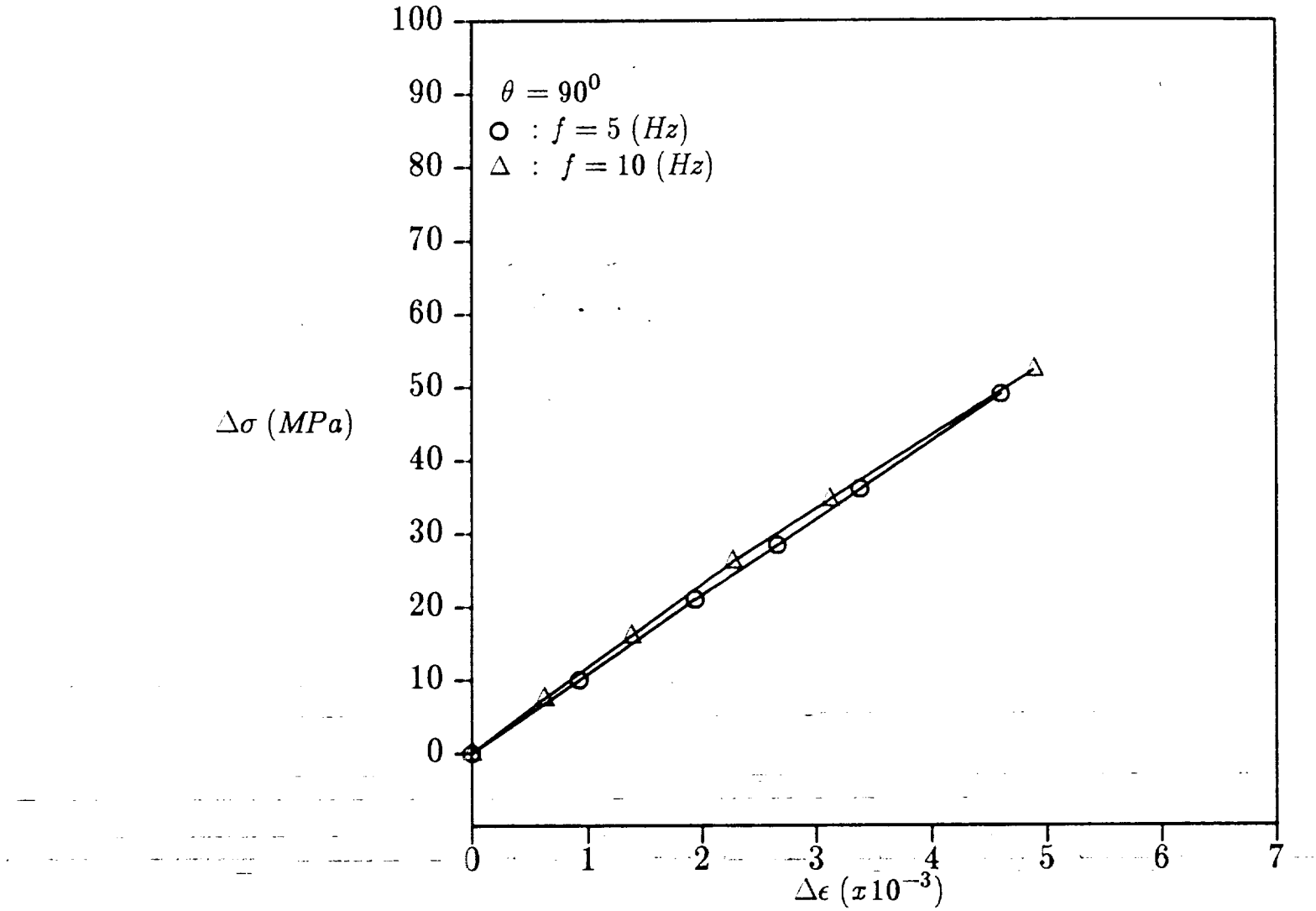

Fig. 42 Stress amplitude vs. strain amplitude response.

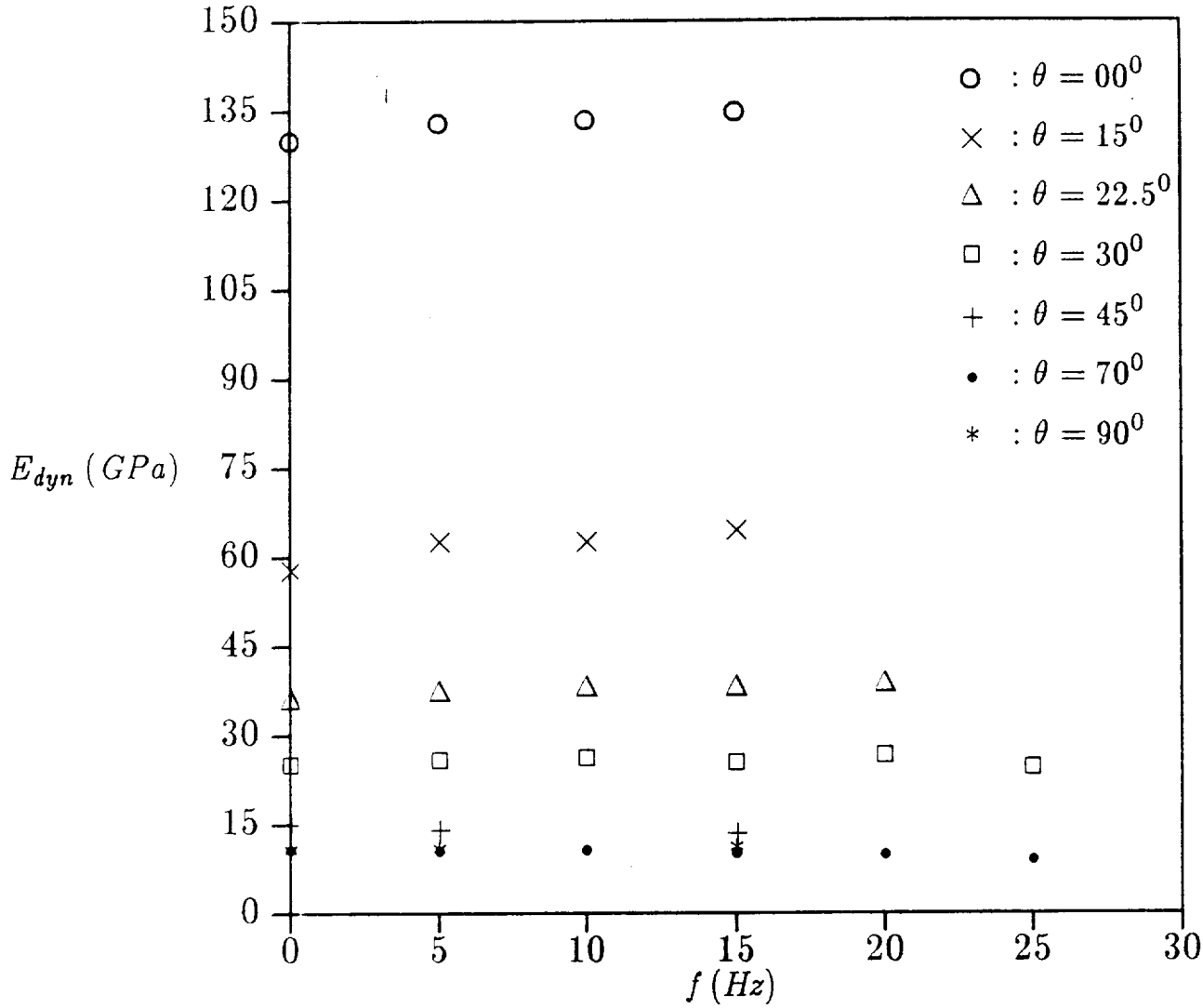

Fig. 43 Magnitude of dynamic modulus vs. frequency.

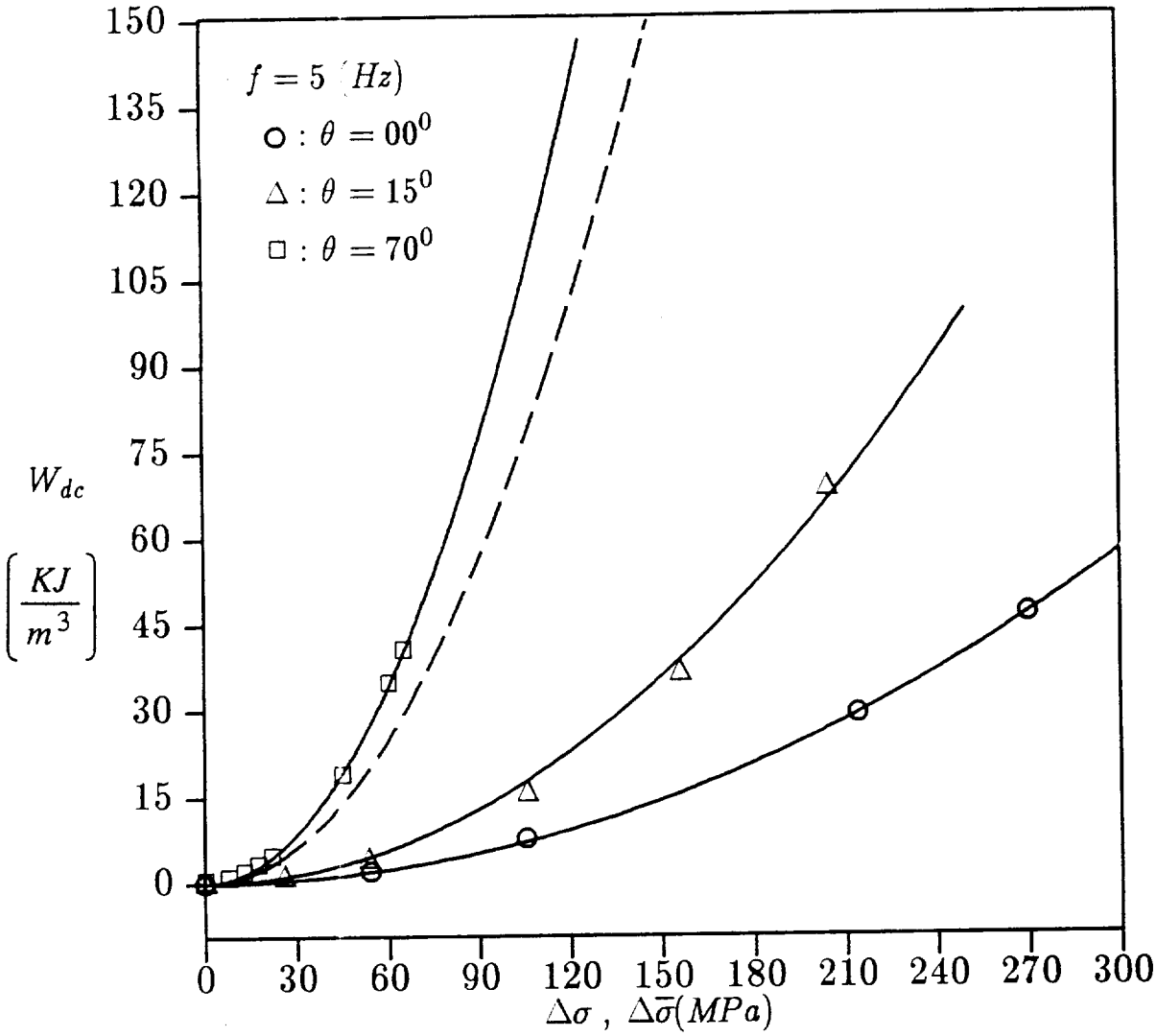

Fig. 44 Dissipated mechanical work per cycle vs. effective stress amplitude and best fit curves used to obtain master curve(- - -)

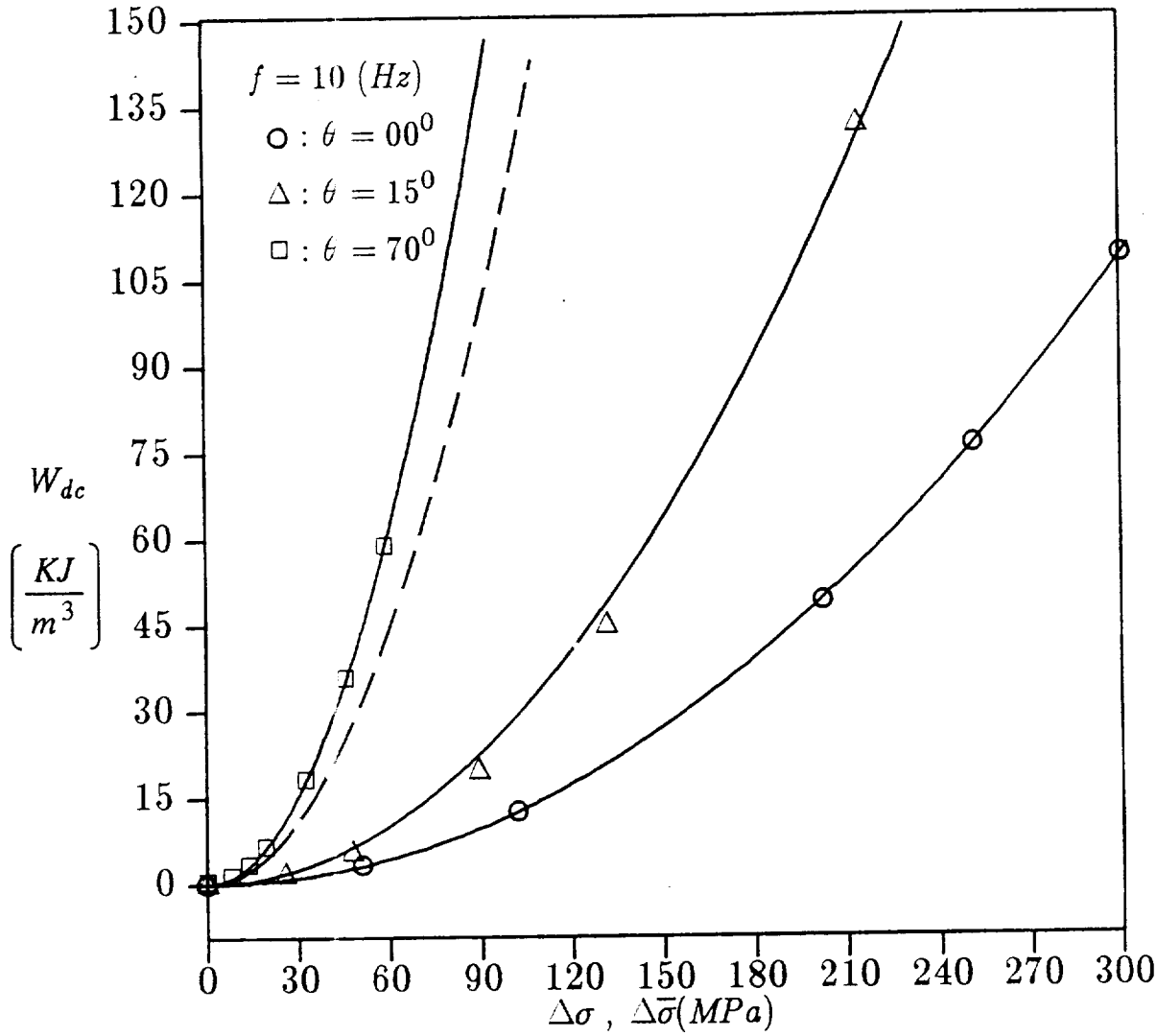

Fig. 45 Dissipated mechanical work per cycle vs. effective stress amplitude and best fit curves used to obtain master curve.(- - -).

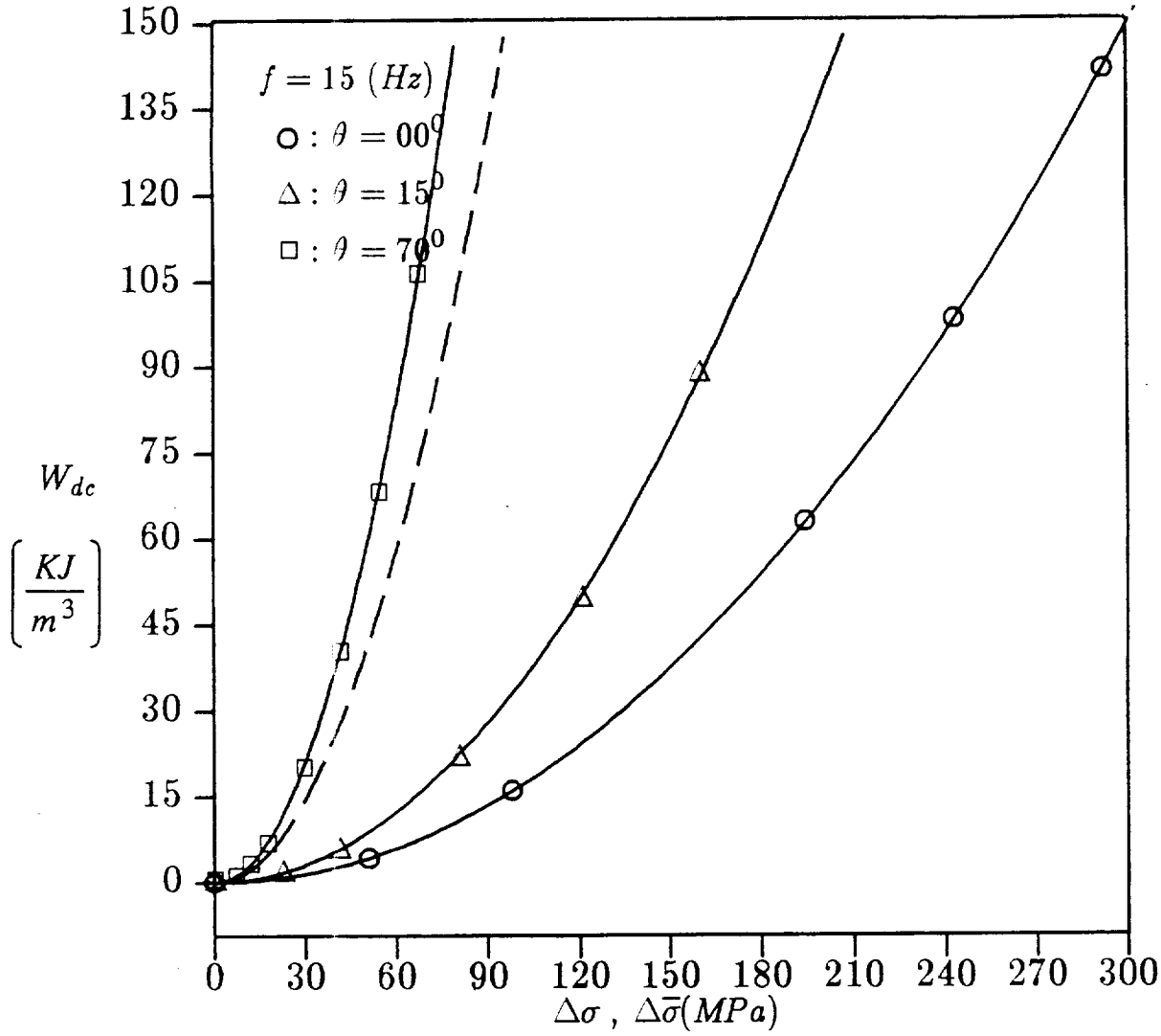

Fig. 46 Dissipated mechanical work per cycle vs. effective stress amplitude and best fit curves used to obtain master curve(– – –).

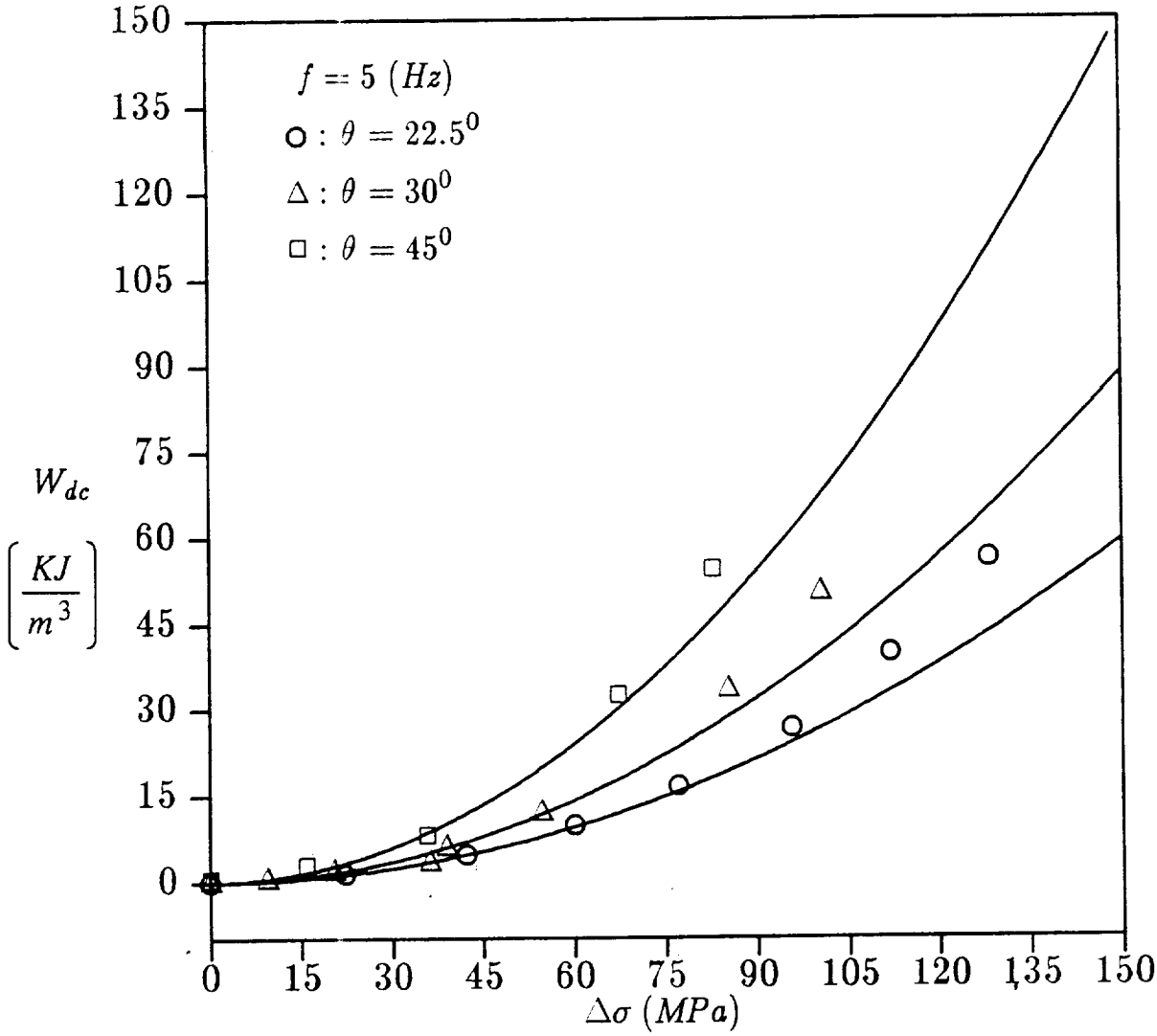

Fig. 47 Dissipated mechanical work per cycle vs.
stress amplitude(solid curve: prediction by master curve).

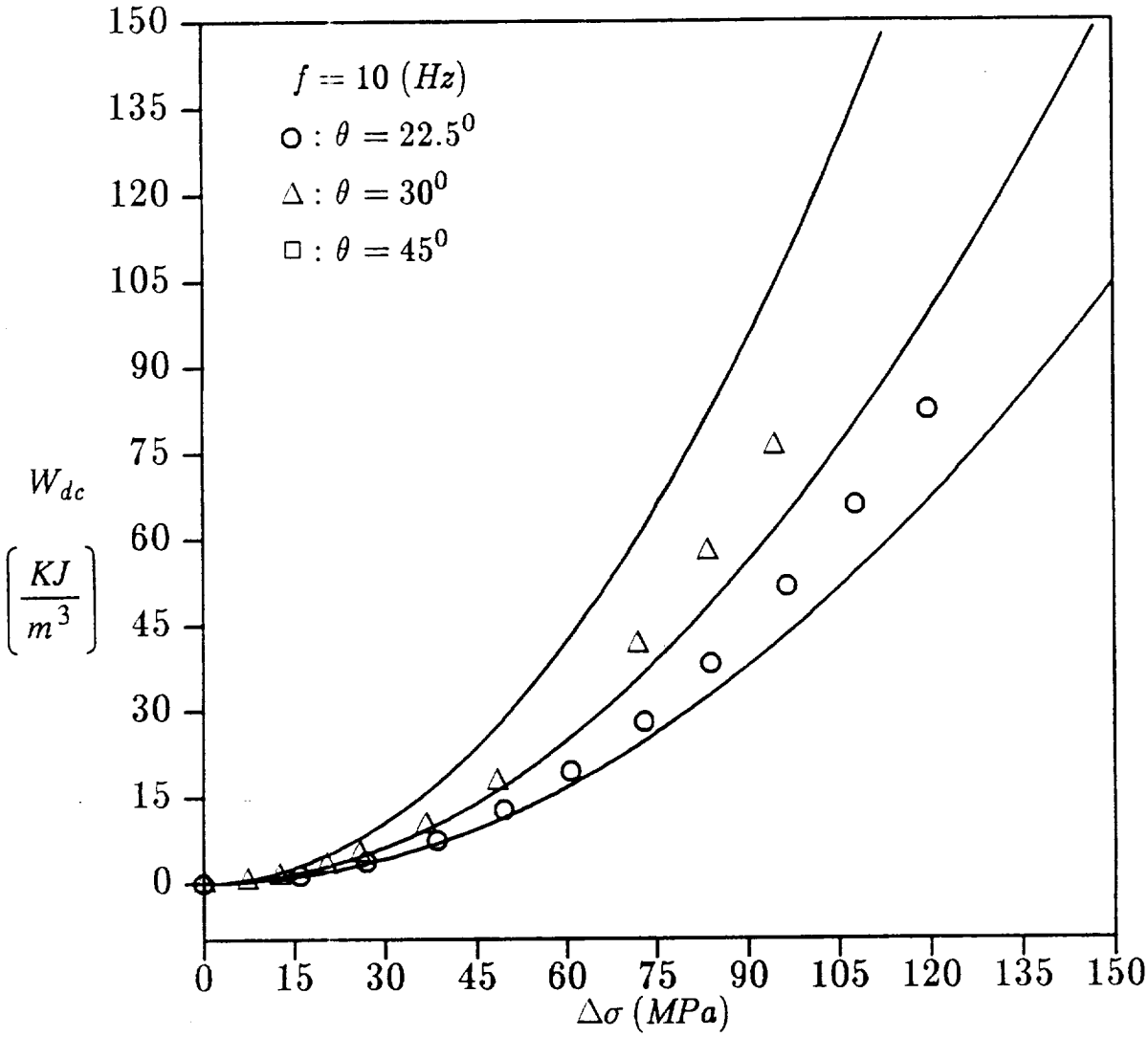

Fig. 48 Dissipated mechanical work per cycle vs.
stress amplitude(solid curve: prediction by master curve).

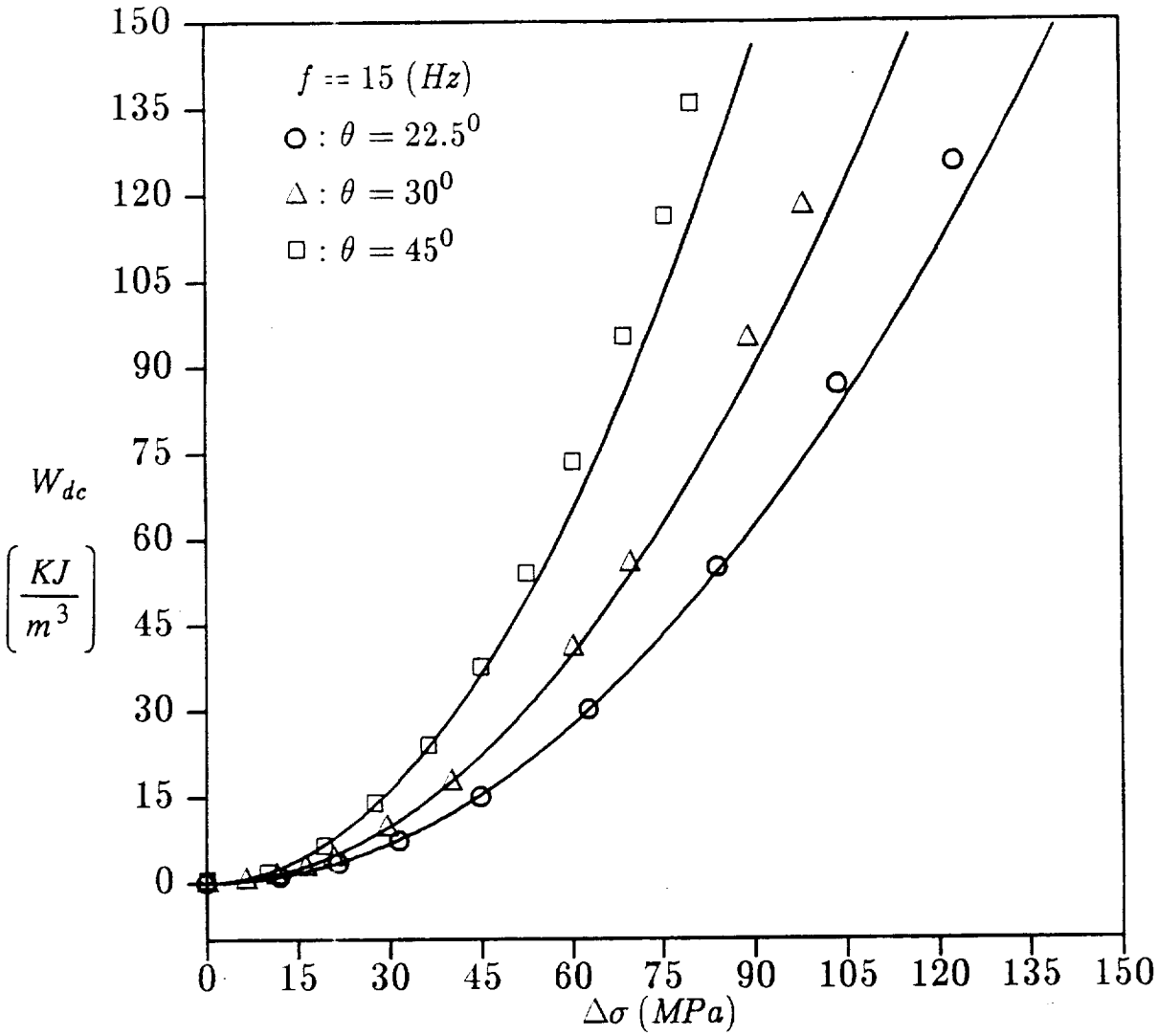

Fig. 49 Dissipated mechanical work per cycle vs. stress amplitude(solid curve: prediction by master curve).

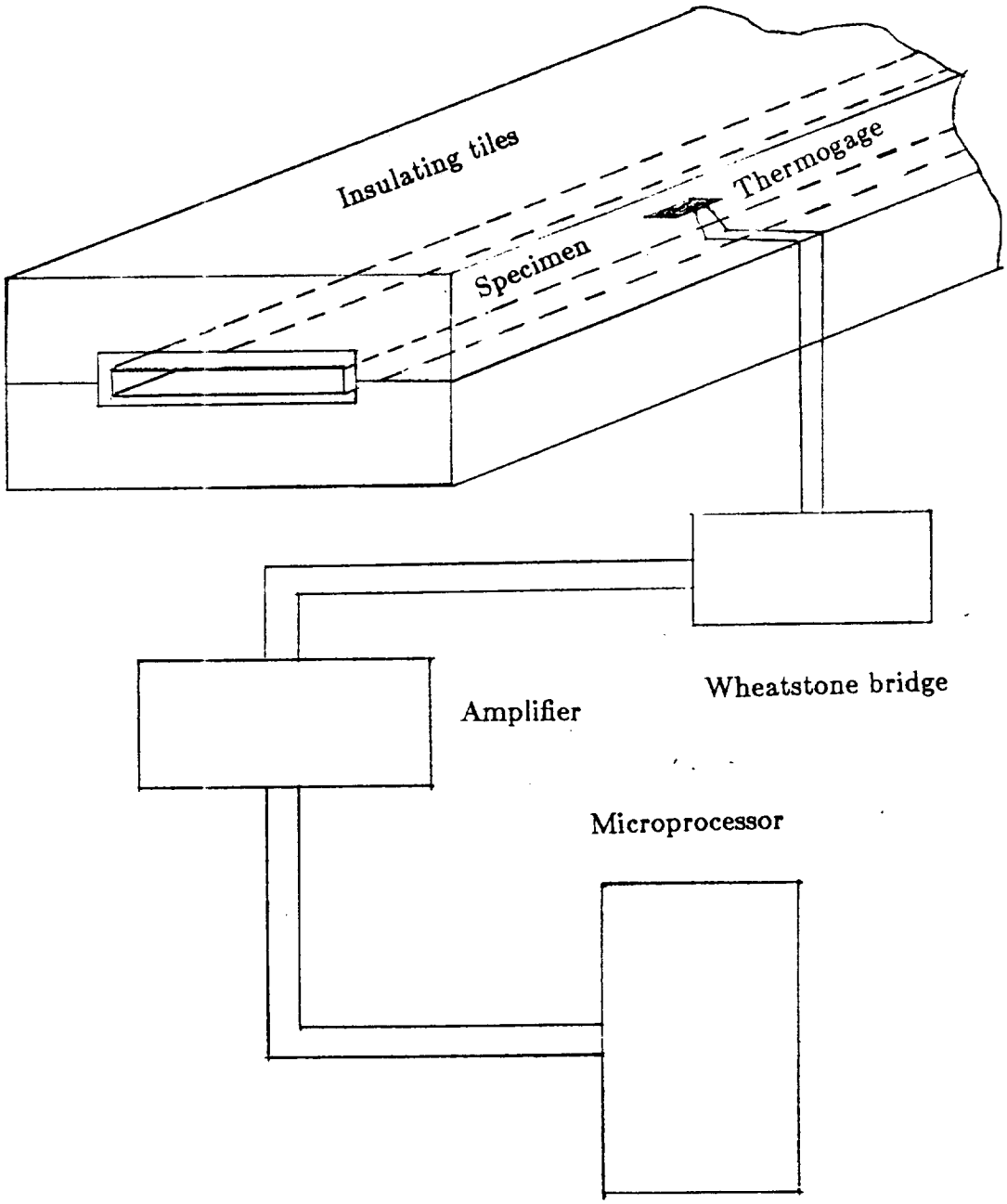

Fig. 50 Insulated specimen and experimental configuration used to measure temperature rise.

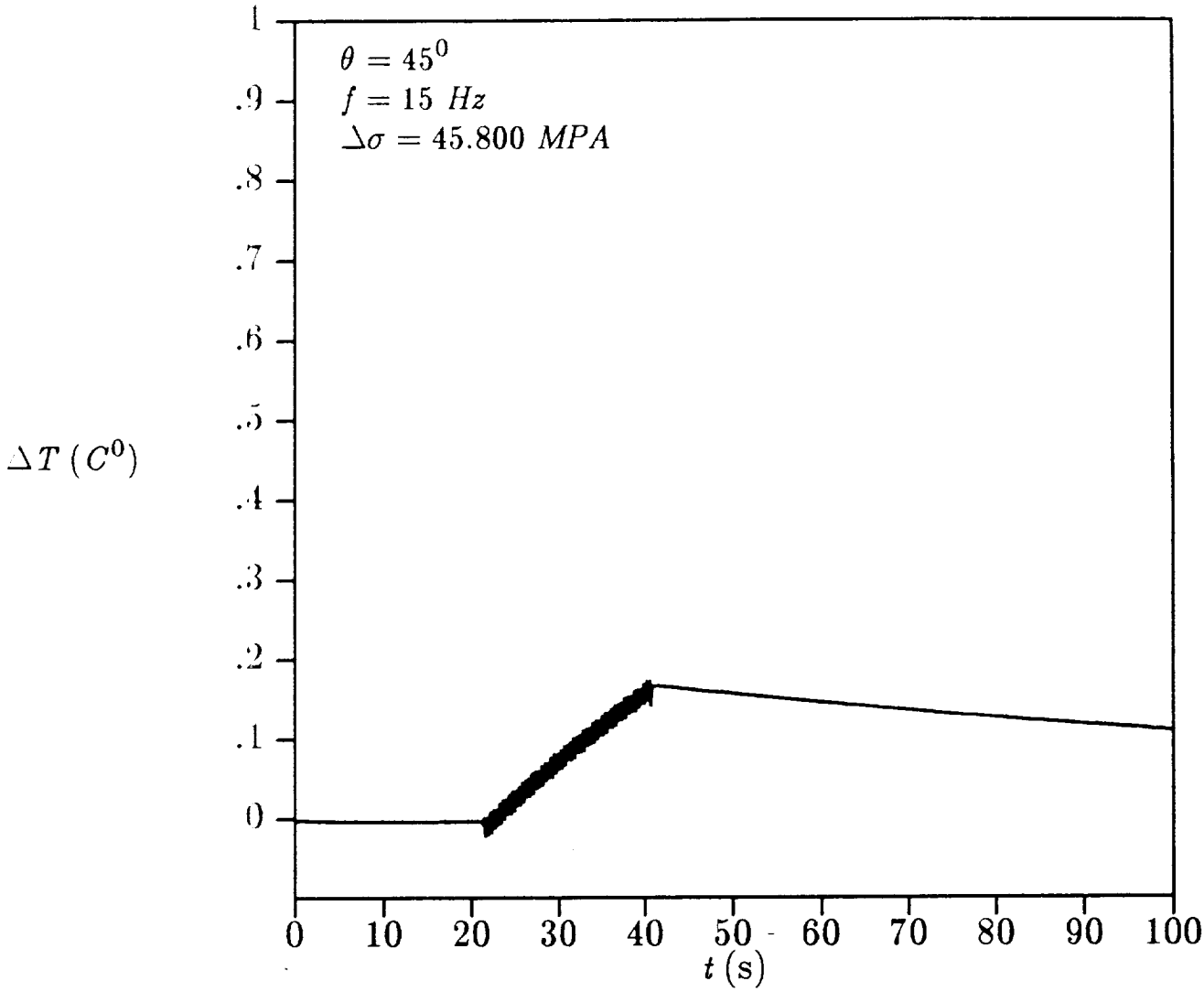

Fig. 51 Temperature rise vs. time(sinusoidal stress).

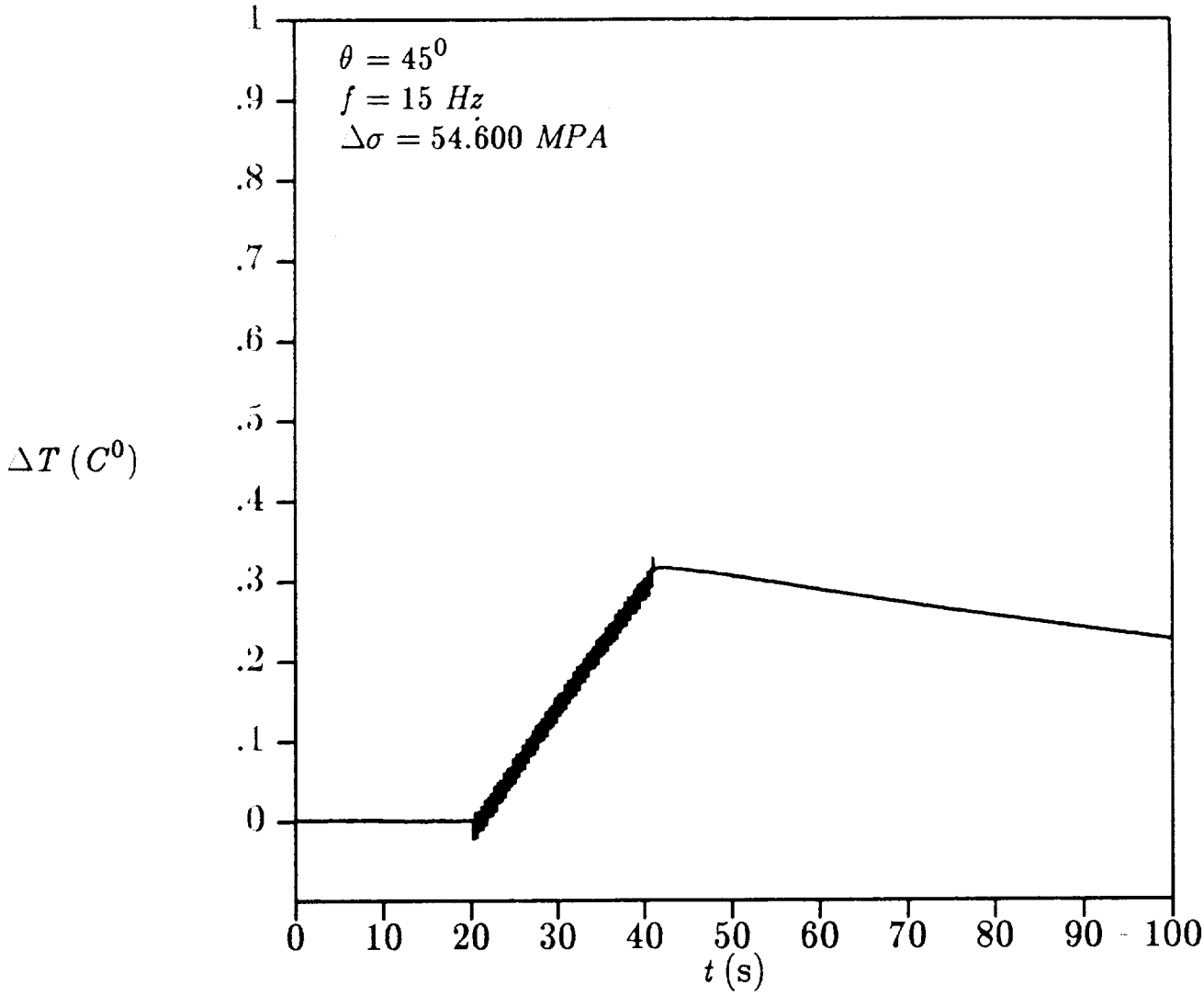

Fig. 52 Temperature rise vs. time(sinusoidal stress).

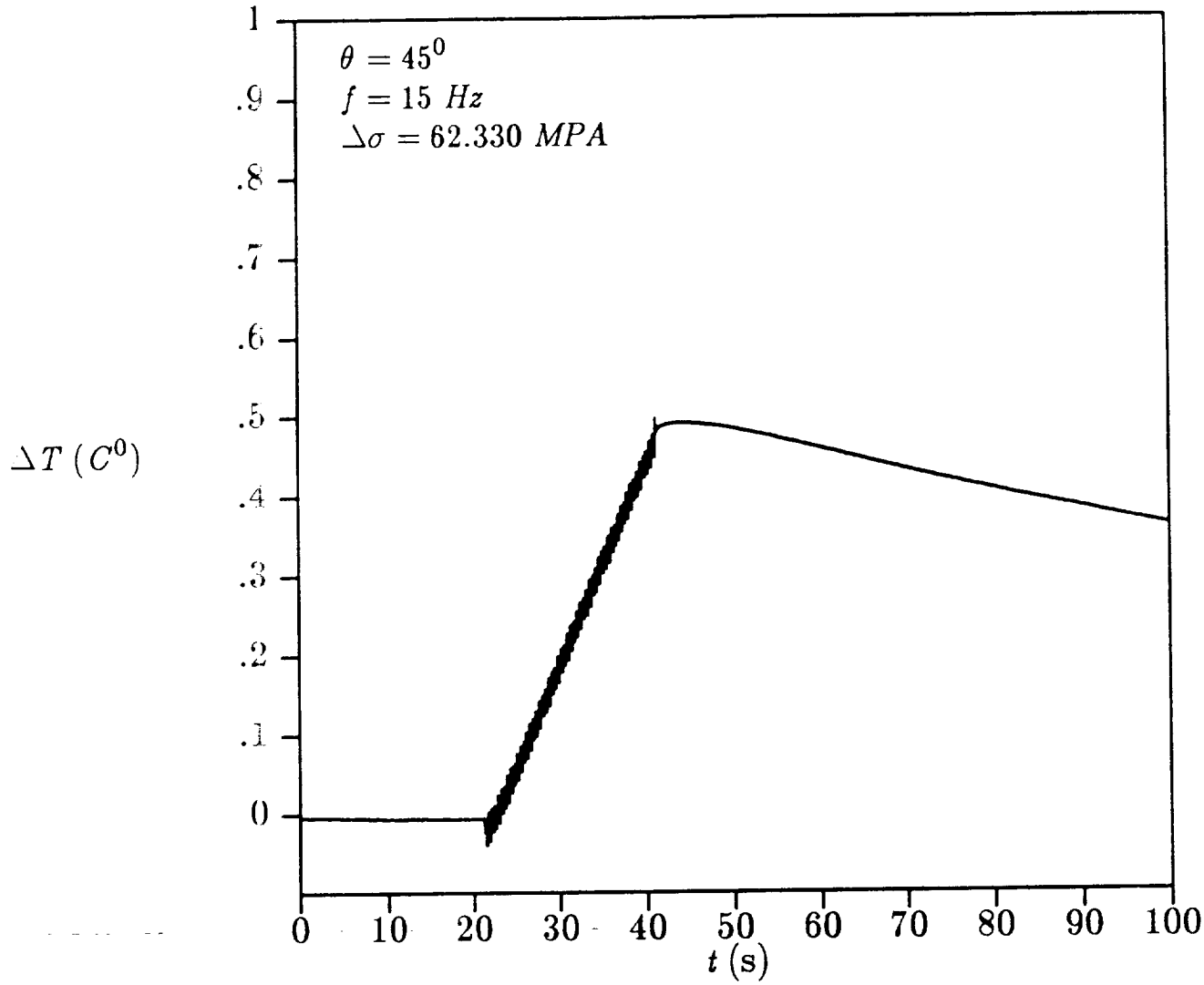

Fig. 53 Temperature rise vs. time(sinusoidal stress).

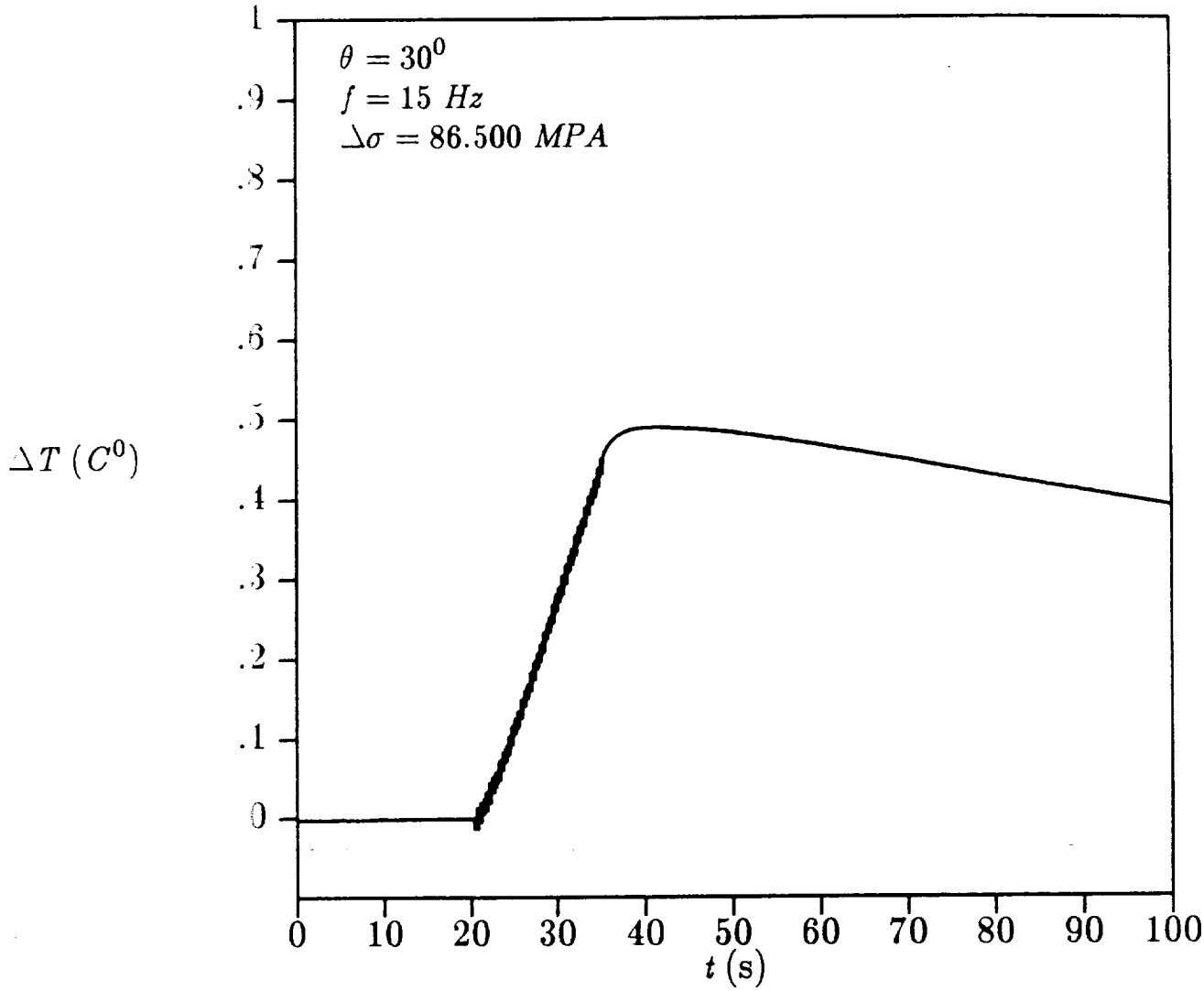

Fig. 54 Temperature rise vs. time(sinusoidal stress).

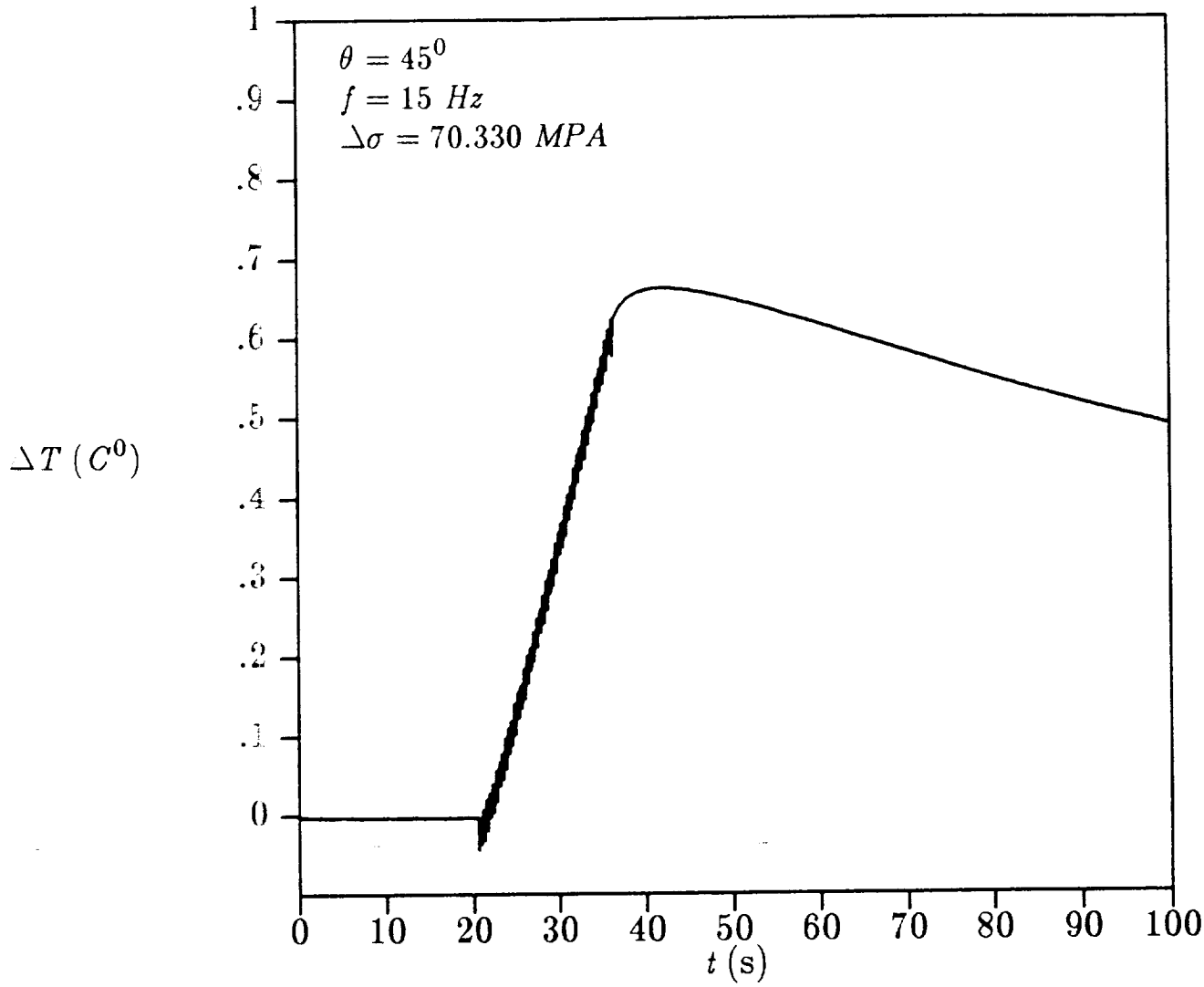

Fig. 55 Temperature rise vs. time(sinusoidal stress).

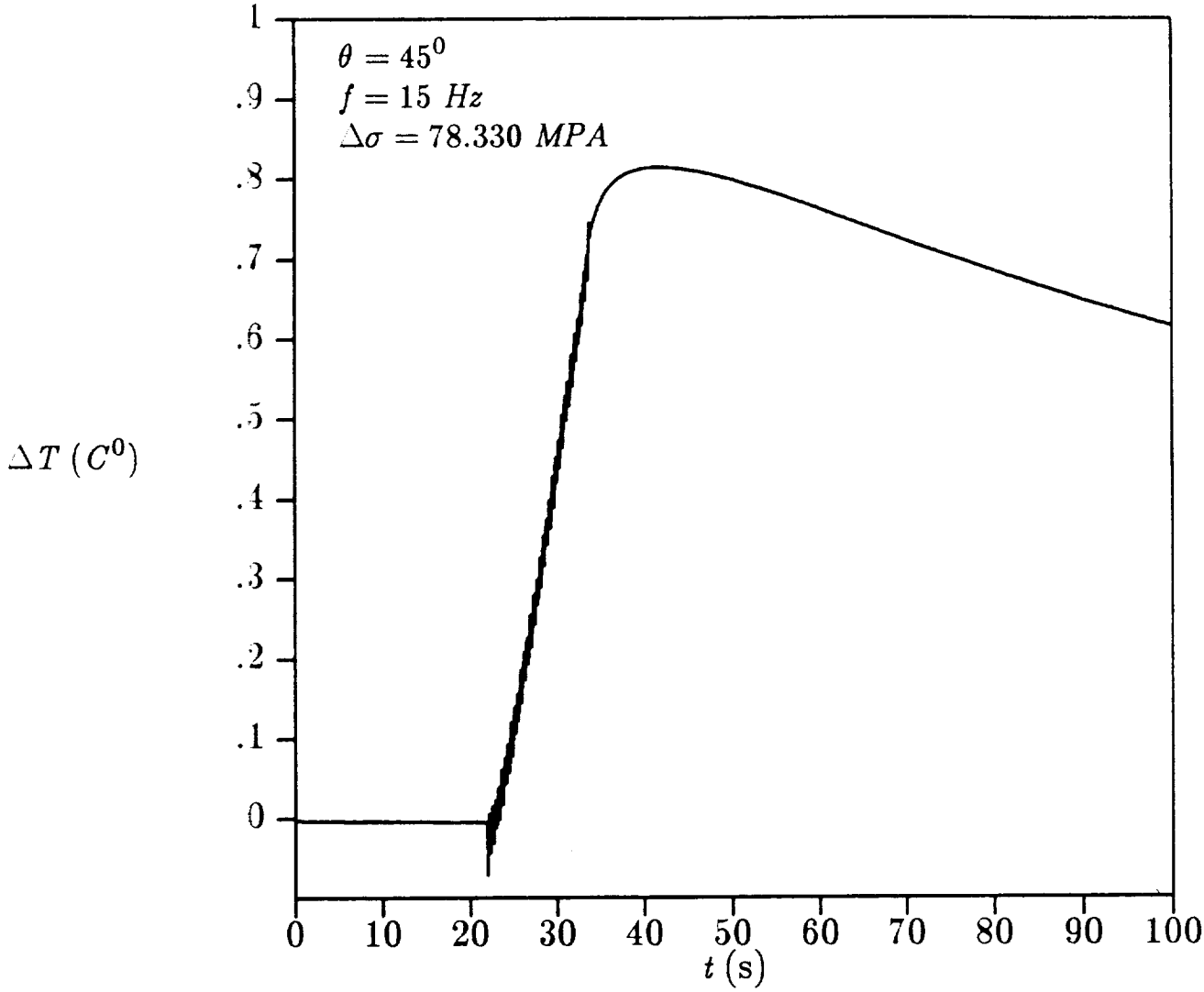

Fig. 56 Temperature rise vs. time(sinusoidal stress).

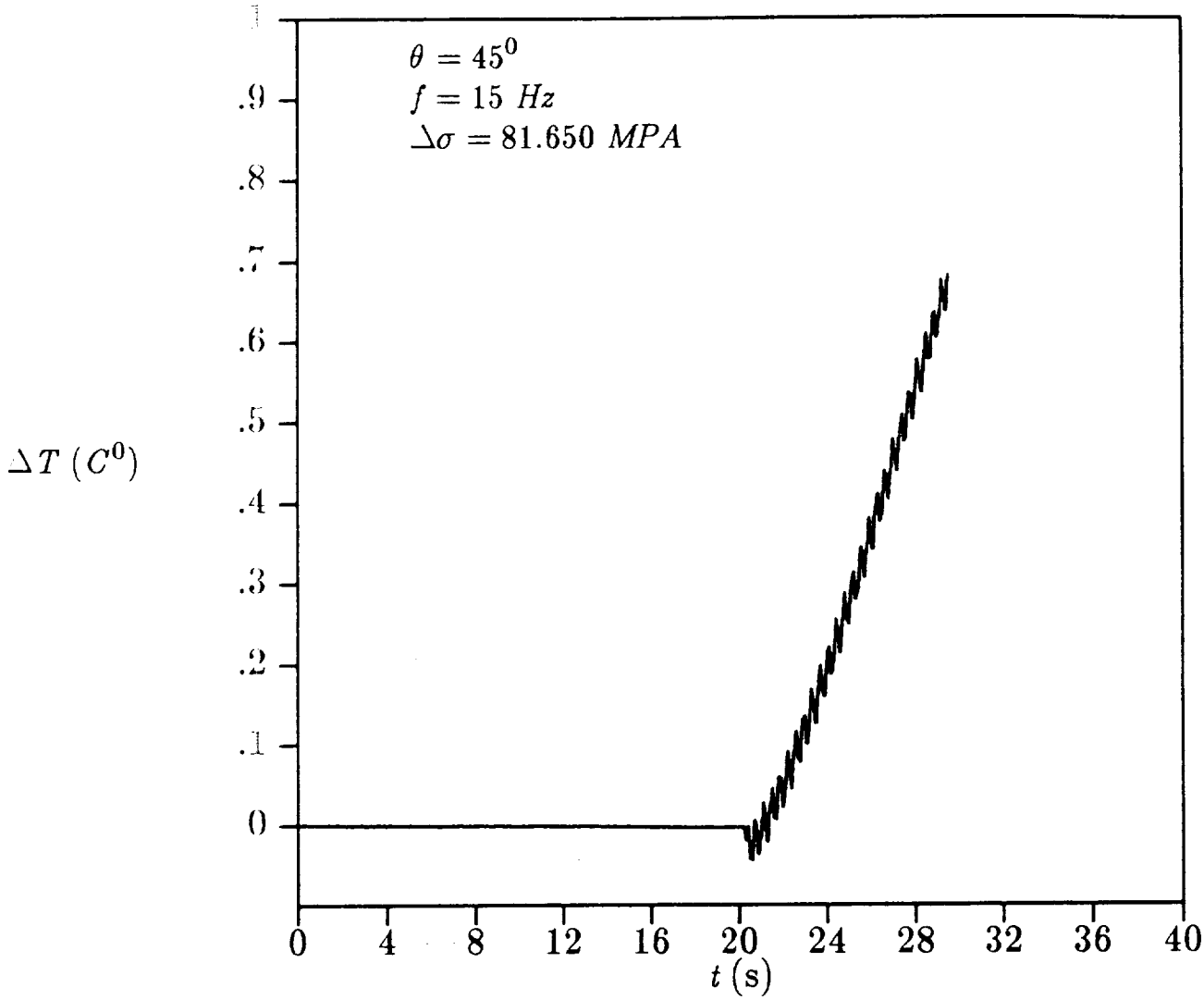

Fig. 57 Temperature rise vs. time(sinusoidal stress).

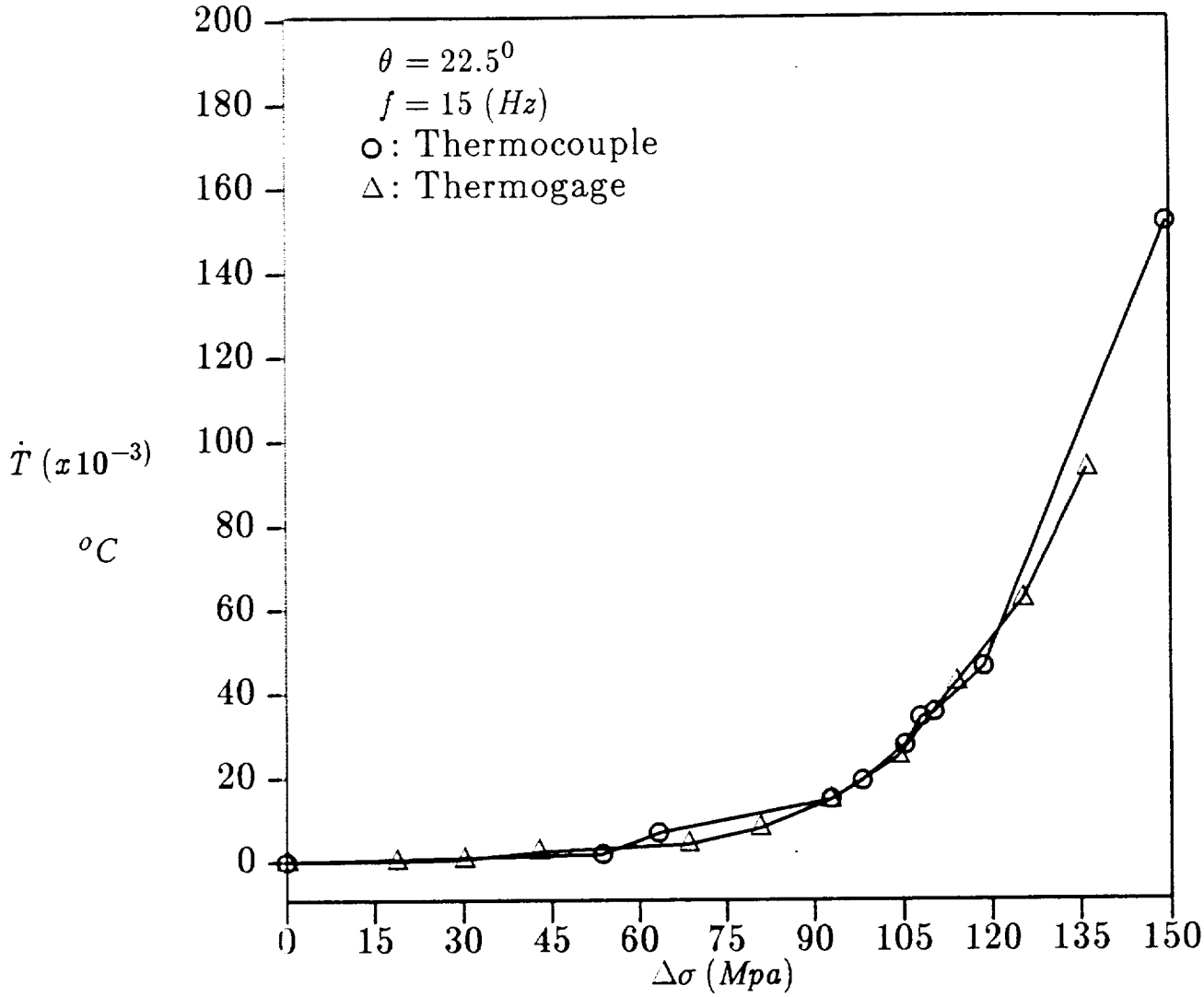

Fig. 58 Rate of temperature rise vs. stress amplitude
(solid curve: piecewise linear approximation).

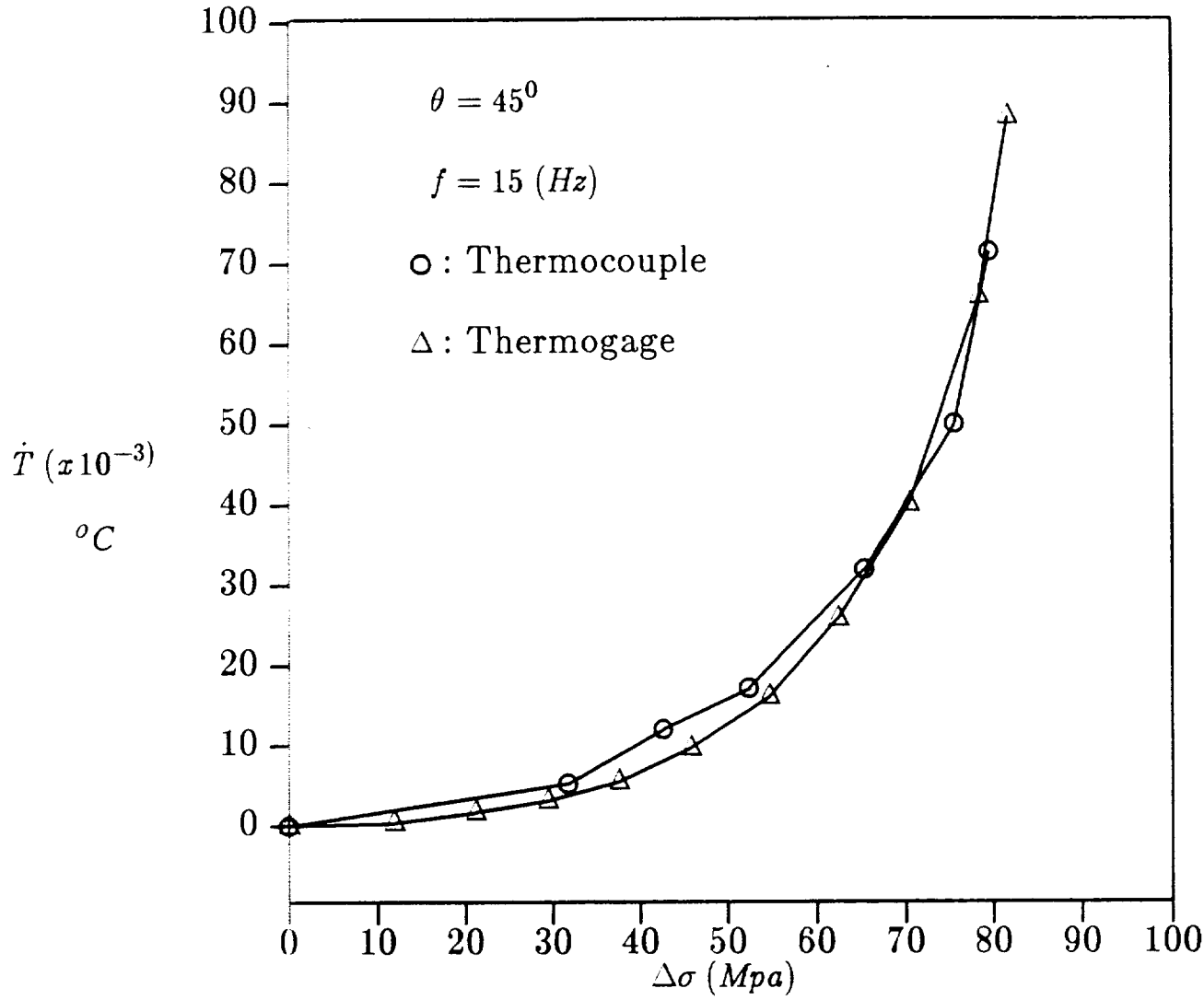

Fig. 59 Rate of temperature rise vs. stress amplitude
(solid curve: piecewise linear approximation).

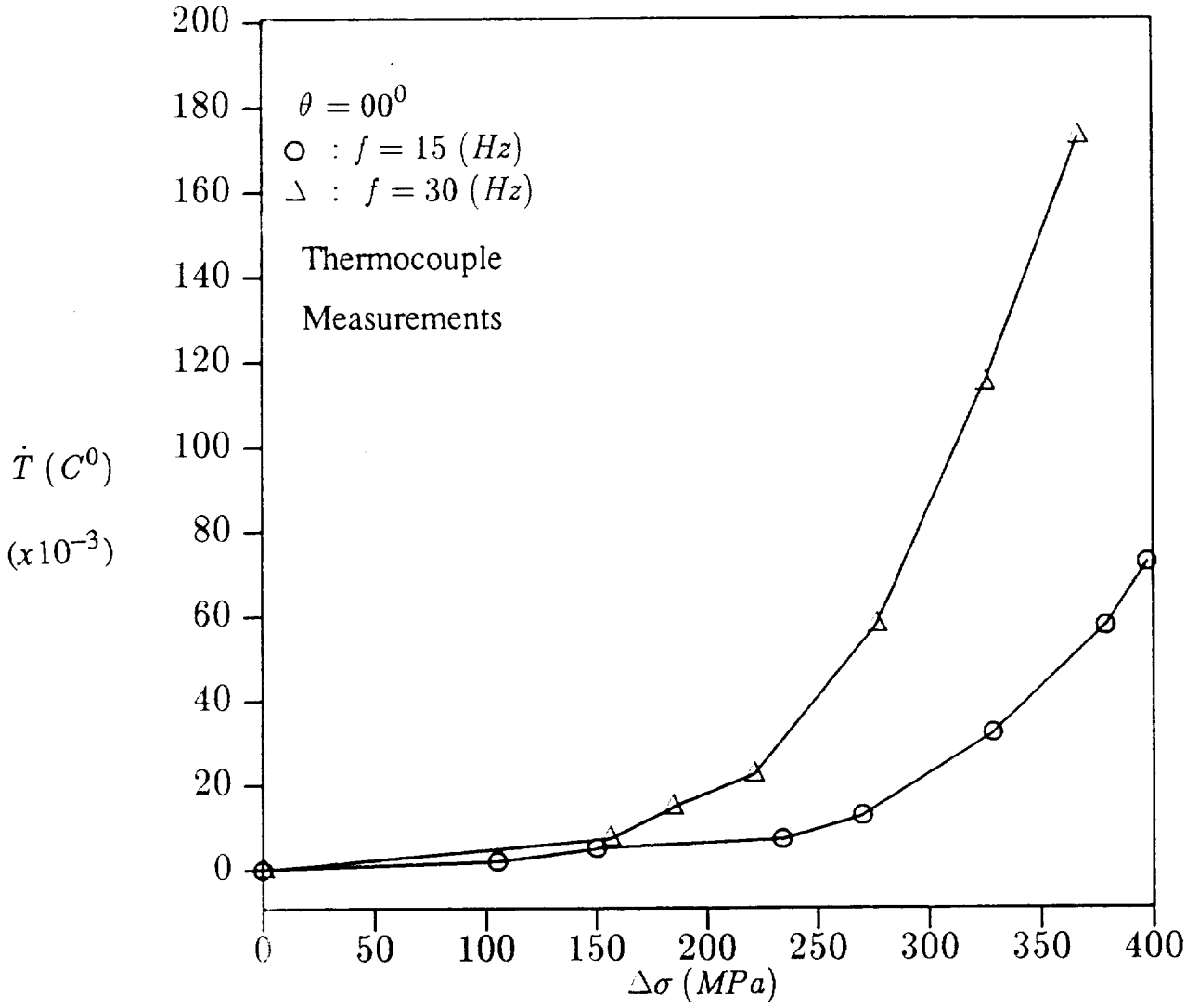

Fig. 60 Rate of temperature rise vs. stress amplitude
(solid curve: piecewise linear approximation).

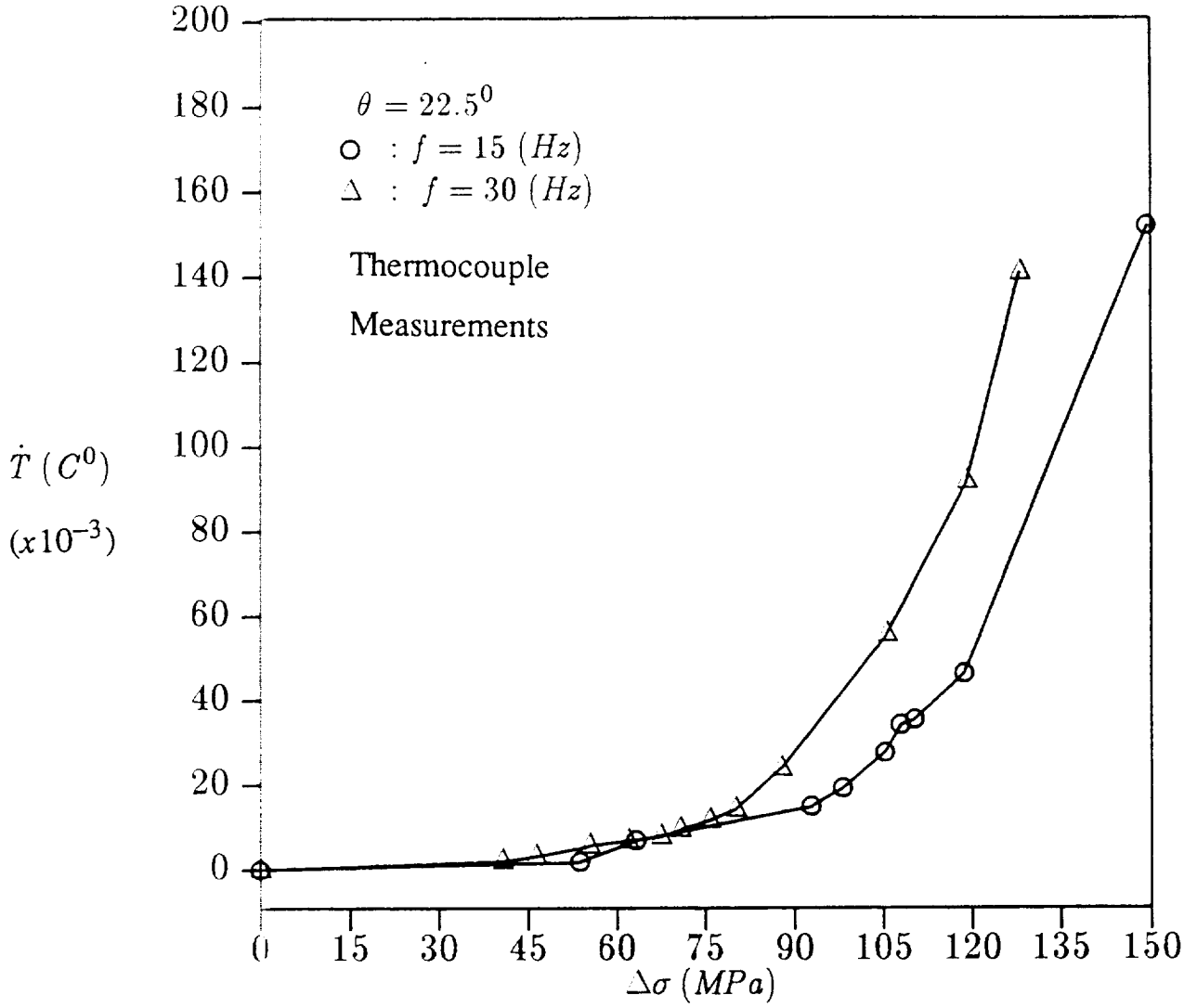

Fig. 61 Rate of temperature rise vs. stress amplitude (solid curve: piecewise linear approximation).

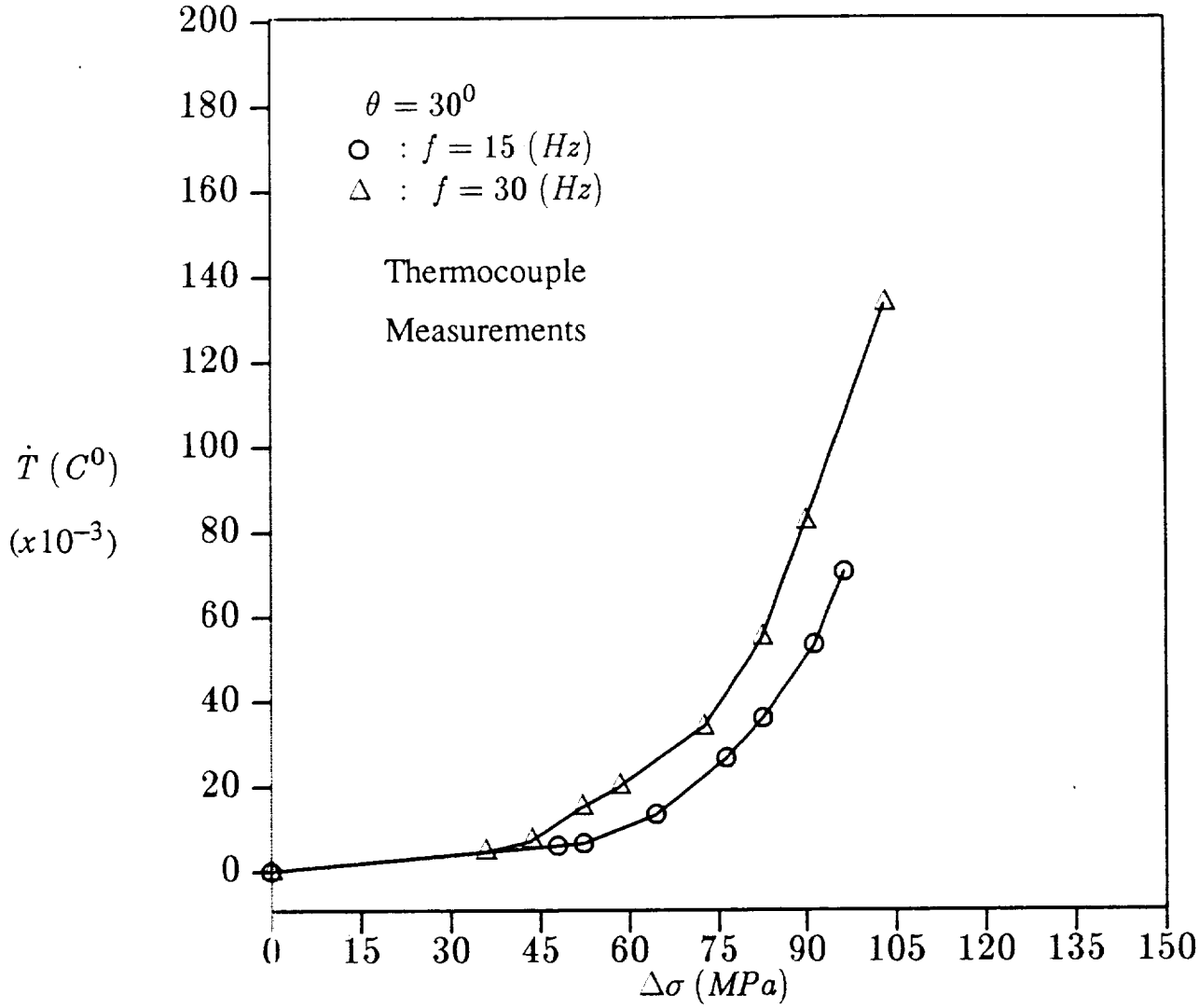

Fig. 62 Rate of temperature rise vs. stress amplitude
(solid curve: piecewise linear approximation).

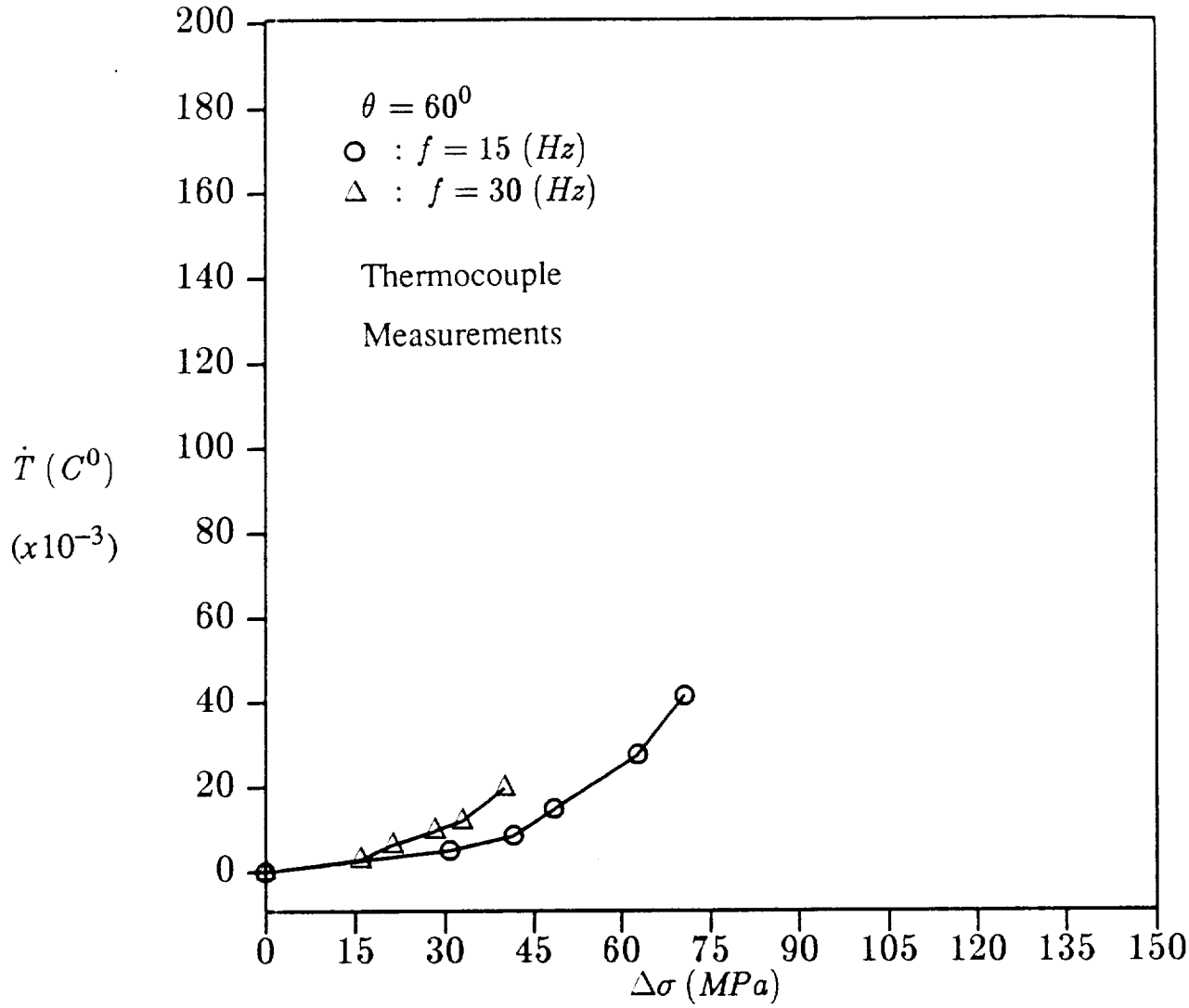

Fig. 63 Rate of temperature rise vs. stress amplitude
(solid curve: piecewise linear approximation).

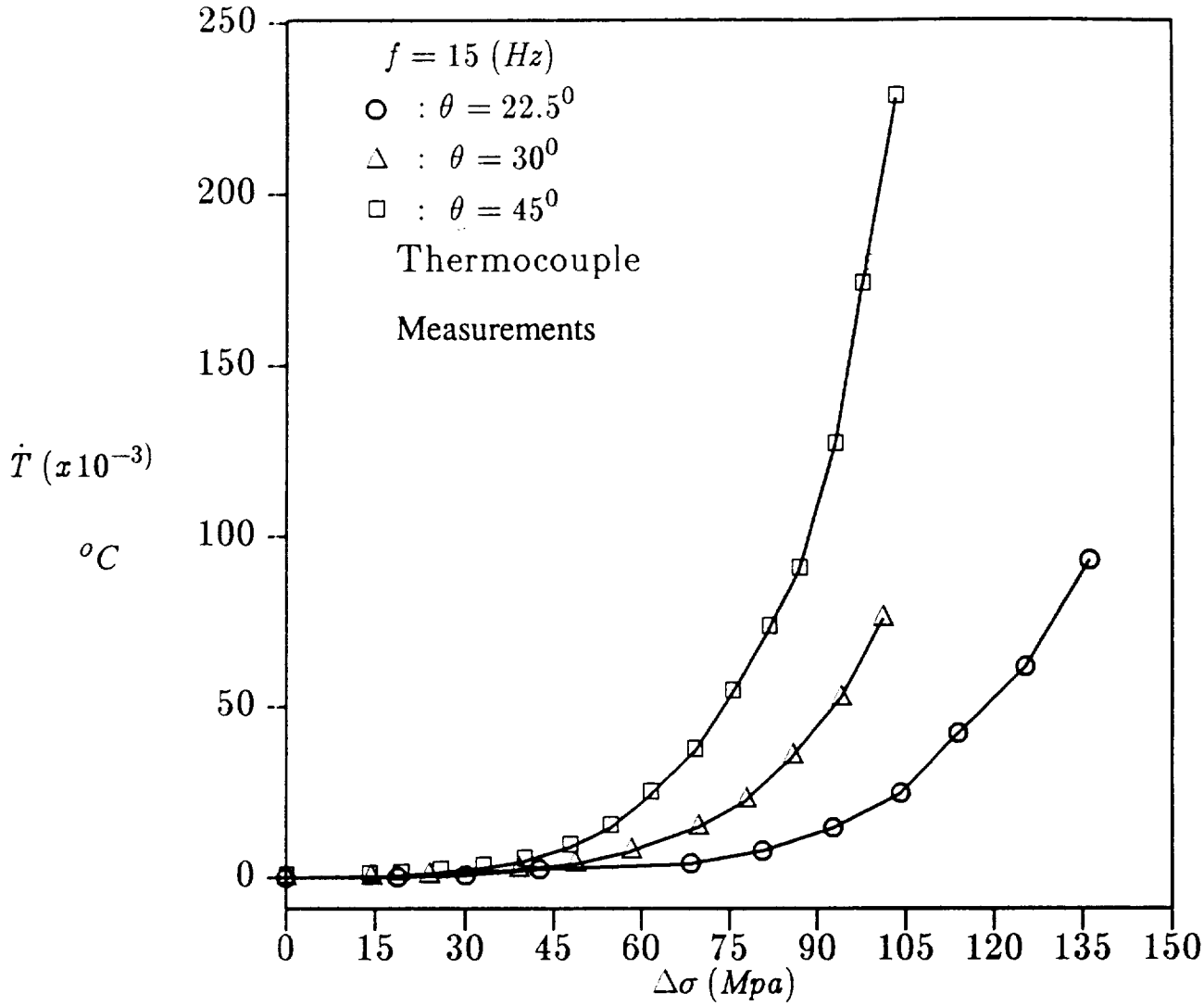

Fig. 64 Rate of temperature rise vs. stress amplitude
(solid curve: piecewise linear approximation).

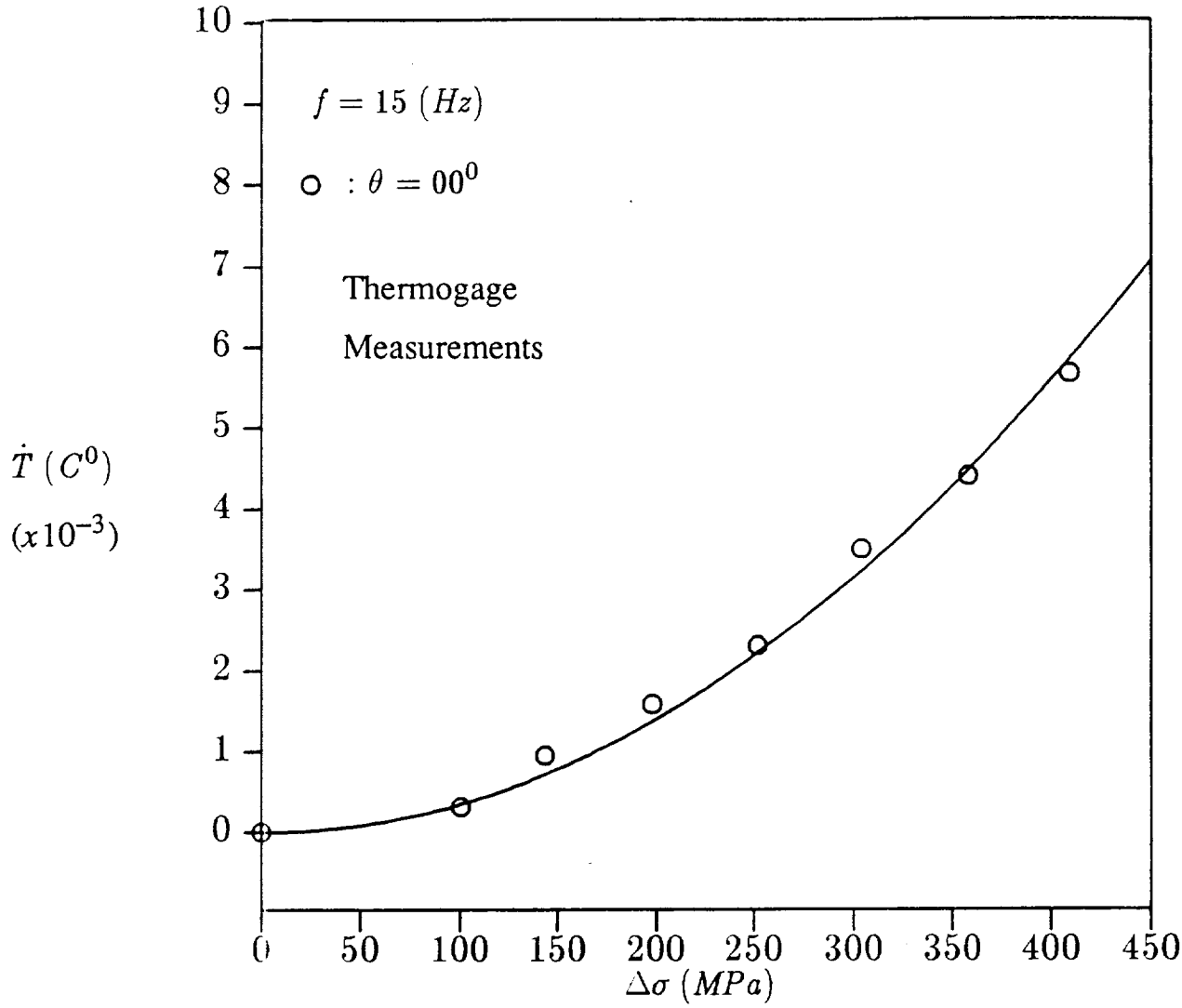

Fig. 65 Rate of temperature rise vs. stress amplitude (solid curve: best curve fit).

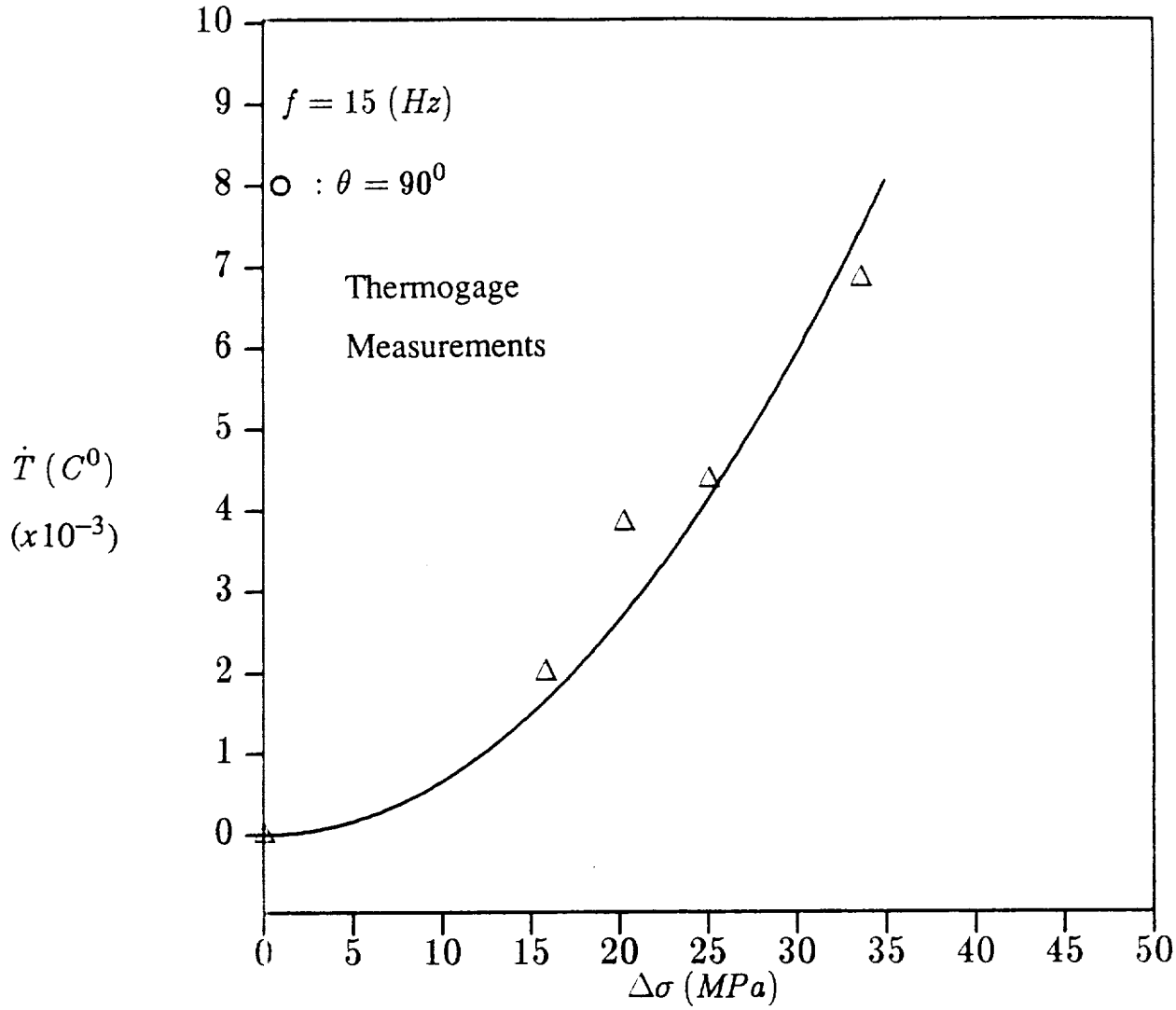

Fig. 66 Rate of temperature rise vs. stress amplitude (solid curve: best curve fit).

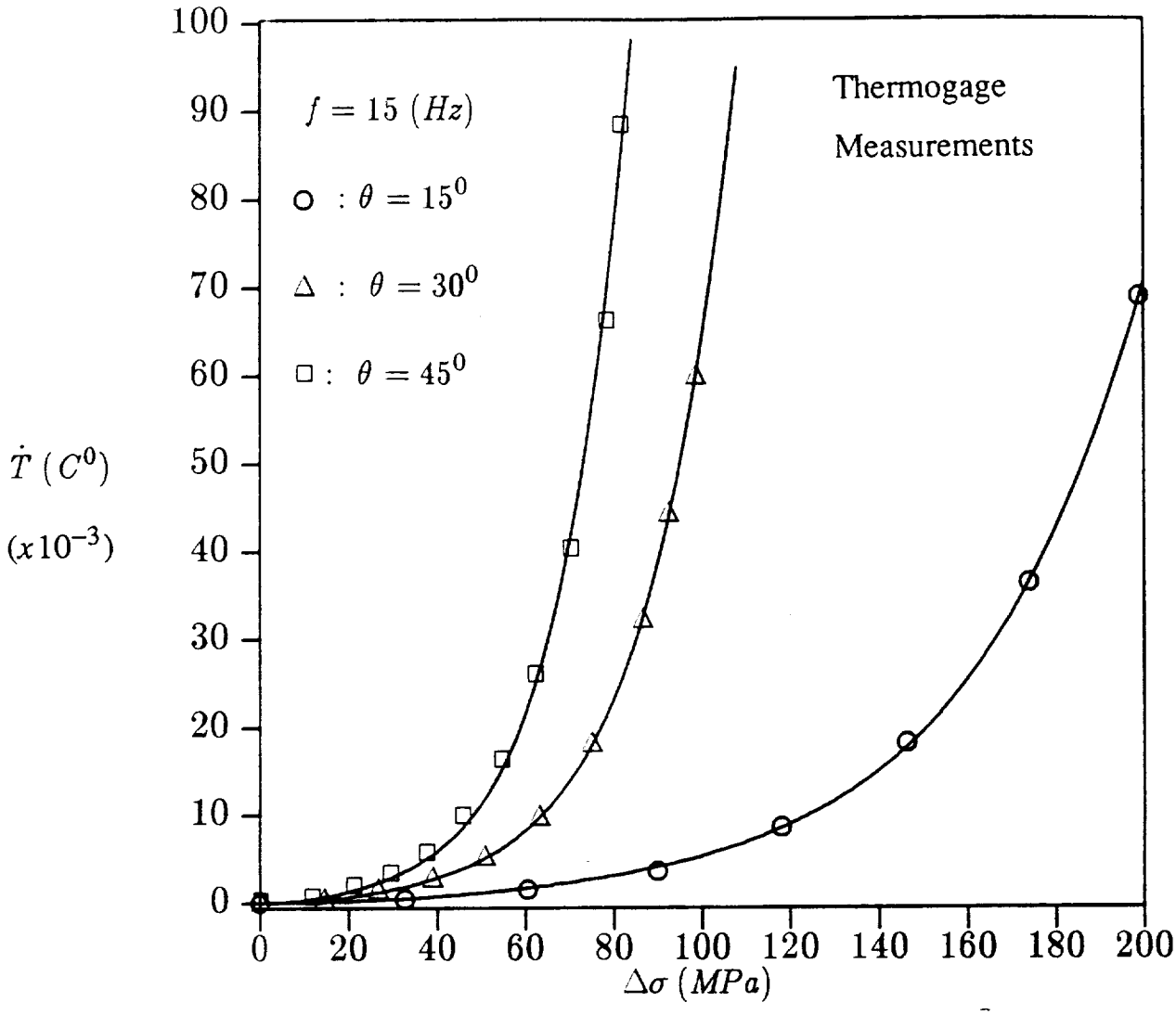

Fig. 67 Rate of temperature rise vs. stress amplitude
(solid curve: best curve fit).

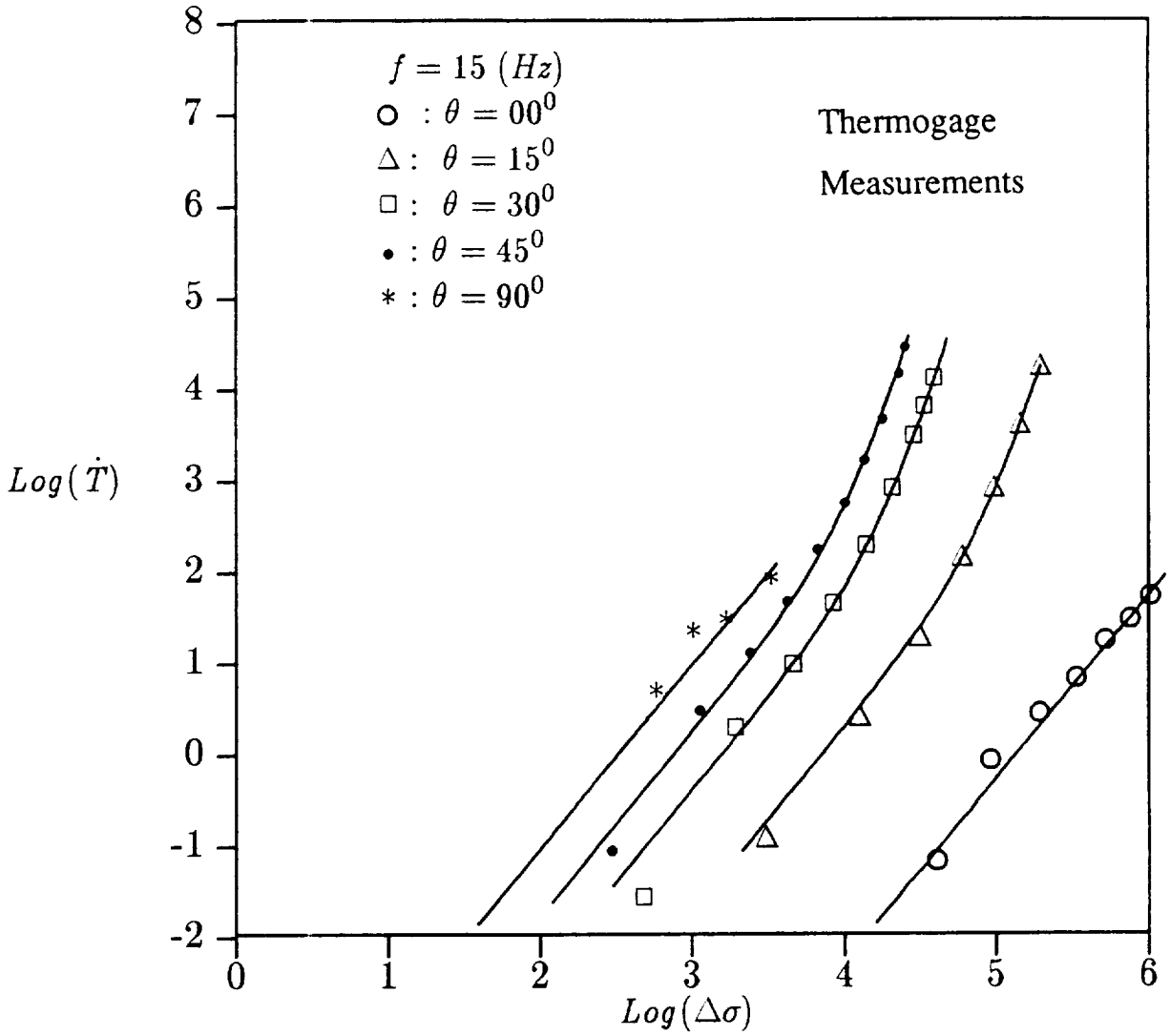

Fig. 68 Log($\Delta\dot{T}$) vs. Log($\Delta\dot{\sigma}$)